

University of Alberta

**Role of Betaine Homocysteine Methyltransferase in Regulating Lipid
Metabolism in McArdle RH7777 Cells**

by

Nusaibah Ab Aziz

A thesis submitted to the Faculty of Graduate Studies and Research
in partial fulfillment of the requirements for the degree of

Master of Science
in
Nutrition and Metabolism

Department of Agricultural, Food and Nutritional Science

©Nusaibah Ab Aziz
Fall 2013
Edmonton, Alberta

Permission is hereby granted to the University of Alberta Libraries to reproduce single copies of this thesis and to lend or sell such copies for private, scholarly or scientific research purposes only.

Where the thesis is converted to, or otherwise made available in digital form, the University of Alberta will advise potential users of the thesis of these terms.

The author reserves all other publication and other rights in association with the copyright in the thesis and, except as herein before provided, neither the thesis nor any substantial portion thereof may be printed or otherwise reproduced in any material form whatsoever without the author's prior written permission.

Abstract

Non-alcoholic fatty liver disease (NAFLD) is one of the most common chronic liver diseases worldwide. It is a clinical pathological state characterized by the accumulation of triacylglycerol (TG) in hepatocytes. It can progress to non-alcoholic steatohepatitis (NASH) and in some cases to fibrosis and cirrhosis. Previous studies have demonstrated that increased betaine homocysteine S-methyltransferase (BHMT) activity protects the liver from excess TG accumulation. BHMT is highly expressed in liver and is important for the synthesis of methionine, an intermediate of S-adenosylmethionine (SAM). The ability of BHMT to regulate hepatic lipid metabolism has been documented, but the precise mechanism is not completely clear. Here we show that expression of rat BHMT1 or BHMT2 in McArdle RH7777 rat hepatoma cells reduces intracellular TG content. Reduction in TG was associated with downregulation of key genes involved in *de novo* biosynthesis of TG, increased β -oxidation and possibly altered glucose metabolism. This thesis affirms the important role of BHMT in the regulation of hepatic lipid metabolism and provides potential mechanisms by which BHMT prevents hepatic TG accumulation and to our knowledge, this is the first report to show a potential metabolic role for BHMT2 with respect to lipid metabolism.

Acknowledgement

I would like to express my deepest appreciation to my supervisor, Dr. René Jacobs for the opportunity, guidance and motivation. Sincere thanks to my committee members, Dr. Richard Lehner and Dr. Donna Vine for their invaluable comments and immense knowledge. I am forever grateful to the members of the Jacobs' lab for all the help and support at different stages throughout the study: specifically, Randy Nelson (gene cloning and cell culture), Dr. Robin da Silva (enzyme assay and lipid analysis), Kelly-Ann Leonard (GC preparations) and Karen Kelly (gene expression). I also thank Dr. Desmond Pink for performing the confocal imaging of my cells. And not to mention, everyone who have directly and indirectly contributed to make this thesis possible. Last but not least, my utmost gratitude goes to my thoughtful husband, amazing parents and the rest of my family and friends. Thank you for the never-ending love, care and prayers.

Table of Contents

CHAPTER 1 INTRODUCTION	1
1.1 Rationale.....	2
1.1.1 Thesis Objectives	5
1.2 Literature review	8
1.2.1 Lipid metabolism.....	8
1.2.2 Non-alcoholic Fatty Liver Disease	11
1.2.3 One-Carbon Metabolism.....	15
1.2.4 Importance of SAM in Fatty Liver Disease	17
1.2.5 Betaine Homocysteine S-Methyltransferase (BHMT).....	22
1.2.6 Conclusion	28
CHAPTER 2 MATERIALS AND METHODS.....	30
2.1 Materials	31
2.1.1 Chemicals and Reagents.....	31
2.1.2 Plasmid	34
2.1.3 Antibodies	34
2.1.4 Primers	35
2.1.5 Buffers and solutions	37

2.2 Cloning of BHMT1 and BHMT2 cDNAs	39
2.2.1 Coding sequences of BHMT1 and BHMT2.....	39
2.2.2 Primer design.....	40
2.2.3 RNA isolation and DNase 1 treatment of RNA for RTPCR	41
2.2.4 cDNA generation from RNA by reverse transcription	41
2.2.5 BHMT1 and BHMT2 cDNAs amplification by PCR.....	42
2.2.6 High-fidelity amplification of BHMT1 and BHMT2 cDNAs	43
2.2.7 Restriction digestion	44
2.2.8 Transformation and purification of recombinant cDNA plasmid	45
2.2.9 Confirmation of insertion.....	46
2.2.10 Sequence analysis.....	47
2.3 Cell culture manipulation	49
2.3.1 Cell culture of McArdle cells	49
2.3.2 Stable transfection of McA cells.....	49
2.3.3 Freezing stable cell lines	50
2.4 Protein manipulation and analysis	51
2.4.1 Determination of protein concentration.....	51
2.4.2 SDS-PAGE	51
2.4.3 Western Blotting	52
2.5 BHMT1 enzyme activity assay.....	52

2.6 Lipid manipulation and analysis.....	53
2.6.1 Lipid extraction.....	53
2.6.2 Triacylglycerol assay	54
2.6.3 Lipid phosphorus assay.....	54
2.6.4 Preparation of Oleate Solution.....	55
2.6.5 Metabolic labeling of lipids.....	55
2.6.6 Thin layer chromatography	56
2.6.7 Fatty acid oxidation.....	57
2.7 Microscopy.....	57
2.7.1 Fixation and immunofluorescence staining of hepatocytes	57
2.8 Gene expression.....	58
2.9 Statistical analysis	59

CHAPTER 3 GENERATION OF STABLE McARDLE CELL LINES

EXPRESSING BHMT1 AND BHMT2	60
3.1 Amplification of BHMT1 and BHMT2 cDNA from rat liver RNA.....	61
3.2 Amplification of HA-tagged rat liver BHMT1 and BHMT2	61
3.3 High-fidelity amplification of HA-BHMT1 and HA-BHMT2	63
3.4 Restriction digestion and ligation of HA-BHMT1, HA-BHMT2 PCR fragments and pCI-Neo Vector.....	68

3.5 Transformation.....	69
3.6 Sequence analysis.....	69
3.7 Stable transfection of recombinant HA-BHMT1, HA-BHMT2 and pCI- Neo into McA cells.....	76

CHAPTER 4 ROLE OF BHMT1 AND BHMT2 IN HEPATIC LIPID

METABOLISM IN McARDLE CELLS	78
4.1 BHMT1 activity in stably transfected cell lines.....	79
4.2 Effect of rat BHMT1 and BHMT2 on TG metabolism.....	79
4.3 Effect of rat BHMT1 and BHMT2 on TG secretion	88
4.4 Effect of BHMT1 and BHMT2 on fatty acid oxidation	88
4.5 Effect of BHMT1 and BHMT2 on hepatic gene expression	93
4-6 Co-localization of BHMT1 or BHMT2 with LDs.....	103

CHAPTER 5 DISCUSSION, LIMITATIONS AND FUTURE DIRECTIONS107

5.1 Discussion.....	108
5.2 Limitations and Future directions	120
References.....	124

List of Tables

Table 2-1: Plasmid vector	34
Table 2-2: Primary antibodies	34
Table 2-3: Secondary antibodies	35
Table 2-4: Cloning primers used to amplify <i>bhmt1</i> and <i>bhmt2</i> gene	35
Table 2-5: Nucleotide sequencing primers	36
Table 2-6: List of common buffers used in this thesis.....	37
Table 4-1: Betaine homocysteine S-methyltransferase activity	80
Table 4-2: mRNA levels of genes involved in TG synthesis	96
Table 4-3: mRNA levels of genes involved in cholesterol and lipoprotein metabolism	97
Table 4-4: mRNA levels of genes involved in fatty acid oxidation	98
Table 4-5: mRNA levels of genes involved in fatty acid synthesis.....	99
Table 4-6: mRNA levels of genes involved in phospholipid metabolism ..	100
Table 4-7: mRNA levels of genes involved in glucose metabolism	101
Table 4-8: mRNA levels of key transcription factors involved in lipid metabolism	102

List of Figures

Figure 1-1: TG biosynthesis pathways	10
Figure 1-2: Two-hit model	14
Figure 1-3: One-carbon metabolism pathways	16
Figure 1-4: Sequence alignment of human BHMT1 and BHMT2	25
Figure 2-1: Coding sequence of rat BHMT1	39
Figure 2-2: Coding sequence of rat BHMT2	40
Figure 2-3: Schematic representation of recombinant DNA	48
Figure 3-1: Amplified coding sequence of BHMT1	64
Figure 3-2: Amplified coding sequence of BHMT2	64
Figure 3-3: Amplified coding sequence of HA-BHMT1	65
Figure 3-4: Amplified coding sequence of HA-BHMT2 and BHMT2-HA....	65
Figure 3-5: Amplified coding sequence of HA-BHMT1 using KAPA Hi-Fi DNA polymerase.....	66
Figure 3-6: Amplified coding sequence of HA-BHMT2 using KAPA Hi-Fi DNA polymerase.....	66
Figure 3-7: Amplified coding sequence of HA-BHMT2 using KAPA Hi-Fi DNA polymerase.....	67
Figure 3-8: PCR-restriction fragment length patterns for BHMT1.....	70
Figure 3-9: PCR-restriction fragment length patterns for BHMT2.....	71

Figure 3-10: Contig map of HA-BHMT1 and HA-BHMT2 sequencing.....	73
Figure 3-11: HA-BHMT1 nucleotide sequence	74
Figure 3-12: HA-BHMT2 nucleotide sequence	75
Figure 3-13: Sequence analysis of recombinant BHMT2	76
Figure 3-14: Immunoblot of expressed N-terminally tagged HA BHMT1 and BHMT2.....	77
Figure 4-1: Linearity with protein concentration and time for BHMT1 from rat liver	80
Figure 4-2: Effect of substrate availability on TG accumulation in McA cells expressing BHMT1 or BHMT2.....	82
Figure 4-3: Cellular label TG, PC, PE and PC:PE ratio	84
Figure 4-4: Cellular PC and PE mass	87
Figure 4-5: Media label TG, PC, PE and PC:PE ratio	89
Figure 4-6: β -oxidation.....	92
Figure 4-7: BHMT1 co-localization with LDs.....	104
Figure 4-8: BHMT2 co-localization with LDs.....	105
Figure 4-9: BHMT co-localization with LDs.....	106
Figure 5-1: Proposed model of BHMT action	116

List of Abbreviations

ABs	Antibodies
ACAT	Acyl-CoA:Cholesterol Acyltransferase
ACC	Acetyl-CoA Carboxylase
ACOX	Peroxisomal Acyl-CoA Oxidase
<i>ADRP</i>	Adipose Differentiation-Related Protein
AGPAT	Acylglycerol- <i>Sn</i> -3-Phosphate Acyltransferase
ALT	Alanine Transaminase
AMPK	AMP-Activated Protein Kinase
ApoB	Apolipoprotein B
BHMT	Betaine Homocysteine <i>S</i> -Methyltransferase
BSA	Bovine Serum Albumin
CD36	Fatty Acid Transport Protein
cDNA	Complementary Deoxyribonucleic Acid
CE	Cholesteryl Ester
CPT1	Liver Carnitine Palmitoyltransferase 1
CoA	Coenzyme A
DG	Diacylglycerol
DGAT	Diacylglycerol <i>O</i> -Acyltransferase
DMEM	Dulbecco's Modified Eagle Medium
DMG	Dimethylglycine
DNase	Deoxyribonuclease
dNTP	Deoxynucleotide Triphosphate

ECL	Enhanced Chemiluminescence
EDTA	Ethylene Diamine Tetra Acetic Acid
ER	Endoplasmic Reticulum
ERK	Extracellular Signal-Regulated Kinases
FA	Fatty Acid
FAS	Fatty Acid Synthase
FATP4	Fatty Acid Transport Protein 4
FFA	Free Fatty Acids
G-3-P	Glycerol-3-Phosphate
G6Pase	Glucose-6-Phosphatase
GPAT	Glycerol-3-Phosphate Acyltransferase
HA	Hemagglutinin
Hcy	Homocysteine
LCAD	Long Chain Acyl-CoA Dehydrogenase
LCFA	Long-Chain Fatty Acid
LDLR	Low-Density Lipoprotein Receptor
LXR	Liver X Receptor
MAT	Methionine Adenosyltransferase
McA	Mcardle RH777 Rat Hepatoma Cell Line
MCAD	Medium Chain Acyl-CoA Dehydrogenase
MCD	Malonyl-CoA Decarboxylase
MG	Monoacylglycerol
MGAT	Monoacylglycerol O- Acyltransferase

min	Minutes
mRNA	Messenger Ribonucleic Acid
MS	Methionine Synthase
MTHFR	Methylenetetrahydrofolate Reductase
NAFLD	Non-Alcoholic Fatty Liver Disease
NaOH	Sodium Hydroxide
NASH	Non-Alcoholic Steatohepatitis
OA	Oleic Acid
PA	Phosphatidic Acid
PAGE	Polyacrylamide Gel Electrophoresis
PBS	Phosphate Buffered Saline
PC	Phosphatidylcholine
PE	Phosphatidylethanolamine
PEMT	PE-Methyltransferase
PEPCK	Phosphoenolpyruvate-Carboxykinase
PL	Phospholipids
PL-C	Phospholipase C
PPARa	Peroxisome Proliferator-Activated Receptor Alpha
qPCR	Quantitative Polymerase Chain Reaction
SAH	S-Adenosylhomocysteine
SAM	S-Adenosylmethionine
SCD1	Stearoyl-Coenzyme A Desaturase 1
SDS	Sodium Dodecyl Sulfate

sec	Seconds
siRNA	Small Interfering RNA
SMM	S-Methylmethionine
SREBP	Sterol Regulatory Element Binding Protein
TBST	Tris Buffered Saline With Tween
TG	Triacylglycerol
TLC	Thin Layer Chromatography
VLCAD	Very Long Chain Acyl-CoA Dehydrogenase
VLDL	Very Low Density Lipoprotein

CHAPTER 1
INTRODUCTION

1.1 Rationale

Non-alcoholic fatty liver disease (NAFLD) has emerged as one of the most common causes of chronic liver diseases worldwide. Over the past 20 years, the prevalence of NAFLD has doubled in Western countries, affecting 20 - 30% of the United States population (Kim & Younossi, 2008) and has increased to a parallel extent in the Asia-pacific region (Farrell et al., 2013). The rapid increase in the prevalence of NAFLD corresponds to the global epidemic of metabolic abnormalities such as obesity and type 2 diabetes (Kotronen et al., 2010). Formerly dismissed as a benign condition, it is now evident that NAFLD can progressively develop into non-alcoholic steatohepatitis (NASH) and end stage liver failure (Charlton et al., 2001).

The pathogenesis of NAFLD is not very well understood and is likely a multifactorial process. Amongst the many factors that are implicated with NAFLD, impaired hepatic methionine metabolism, resulting in reduced S-adenosylmethionine (SAM) availability, has been associated with the disease development. SAM is the principal methyl donor in biological methylation reactions and is vital for the synthesis of hormones, lipids and proteins. SAM is synthesized from methionine and is an intermediate in the formation of homocysteine (Hcy), an amino acid which when elevated is linked to cardiovascular disease (Bellia et al., 2007). Homocysteine can be converted back to methionine via the transmethylation pathway. The liver expresses three enzymes that catalyze the remethylation of Hcy to methionine: betaine-dependent betaine homocysteine S-methyltransferase

1 (BHMT1) and cobalamin-dependent methionine synthase (MS). Another form of rodent and human cDNA sequence that encodes enzyme with 73% sequence similarity to BHMT1 called BHMT2 has also been identified (Chadwick et al., 2000). Compared to BHMT1, BHMT2 uses S-methylmethionine (SMM) to convert Hcy to methionine (Szegeedi et al., 2008). In liver, the conversion of Hcy to methionine is important for recycling of intracellular folates, the catabolism of betaine and choline and the maintenance of SAM.

Fatty liver disease is associated with impairment of hepatic methionine metabolism primarily due to reduced SAM availability (Barak et al., 1993). SAM deficiency has been shown to cause reduced phosphatidylethanolamine *N*-methyltransferase (PEMT)-mediated-phosphatidylcholine (PC) synthesis and consequently impaired very-low density lipoprotein (VLDL) secretion (Cano et al., 2011). Betaine supplementation, an important methyl donor for the remethylation of Hcy to methionine, not only stimulated BHMT activity but increased the generation of SAM and PC synthesis and as a result protected the liver from fat accumulation (Kwon et al., 2009 and Kharbanda et al., 2007). More recently, BHMT knockout mice were shown to develop a fatty liver, in part due to impaired PC-mediated VLDL secretion (Teng et al., 2011). This data further supports the potential role of BHMT as a determinant of fatty liver disease; however, the exact mechanism involved remains speculative.

A similar link between BHMT and VLDL secretion has been demonstrated in a cell culture model. Sowden et al. reported that ApoB expression and secretion were positively correlated with BHMT activity in rat hepatoma McArdle RH7777 (McA) cells (Sowden et al., 1999). Although this study supported a direct role for BHMT in regulating VLDL secretion, the process by which BHMT increases ApoB abundance was not established. It is important to note that McA cells lack endogenous PEMT activity (Cui et al., 1995). Since a similar relationship exists between BHMT and VLDL secretion in the absence of PEMT-mediated PC synthesis in McA cells, another pathway mechanism independent of PC biosynthesis is plausible. In addition, a recent finding from proteomic analysis of the compositions of cytosolic LDs that showed the presence of BHMT on LDs further strengthen the link between BHMT and lipid metabolism (Crunk et al., 2013).

As previously described, there are two isoforms of BHMT namely, BHMT1 and BHMT2. To our knowledge, no studies have investigated the link between BHMT2 and hepatic lipid metabolism. The creation of stable-cell lines that express BHMT, will allow us to determine, for the first time, whether BHMT1 and BHMT2 have different metabolic roles. Much of the focus of this thesis, therefore, investigates the role of BHMT1 and BHMT2 in regulating hepatic lipid metabolism.

1.1.1 Thesis Objectives

Thesis Objective 1

To investigate the role of BHMT1 and BHMT2 in regulating lipid metabolism in liver cells, we first created cell lines that stably express BHMT1, BHMT2 and pCI-Neo Control. The cell line chosen for this project is McArdle RH7777 (McA) rat hepatoma cells, which are easy to maintain and transfect. Similar to rat liver, McA cells are capable of secreting both apo B100 and apo B48 containing lipoproteins (Vance, 2002). McA cells do not express BHMT1 and BHMT2; therefore stable expression of these proteins in McA cells should be a good model for studying their potential role in regulating lipid metabolism. In Chapter 3, we employed various techniques, such as DNA cloning, polymerase chain reaction (PCR) and DNA sequencing to establish this model. Rat BHMT1 and BHMT2 cDNA were first engineered to express a 9 amino acid epitope tag from the influenza hemagglutinin antigen (HA) for BHMT1 and BHMT2 protein detection. The subsequent HA epitope tagged BHMT1 and BHMT2 cDNAs were cloned into the pCI-Neo vector and transformed into bacterial cells. The resulting constructs were then stably transfected into McA cells. Three stable cell lines expressing HA-BHMT1, HA-BHMT2 and pCI-Neo control were established and designated **BHMT1**, **BHMT2** and **pNeo** respectively.

Thesis Objective 2

Chapter 4 addresses the second objective, which is to determine the mechanism by which BHMT influence lipid metabolism in liver cells. Previous studies demonstrated that BHMT1 expression in McA cells correlates with increased ApoB mRNA expression and secretion (Sowden et al., 1999), suggesting a role for BHMT1 in regulating TG-rich VLDL secretion. We hypothesized that BHMT1 stimulates TG secretion and, as such, prevents TG accumulation in liver cells. Generally, the balance between TG input and TG output reflects hepatic fat accumulation (Musso et al., 2009). Therefore, we investigated the effects of BHMT expression on other factors that influence TG balance in liver cells including intracellular lipid levels, lipid turnover and fatty acid oxidation. It is hypothesized that BHMT1 expression in McA cells alter lipid turnover and influence lipid metabolism. To test these hypotheses, we utilized metabolic labeling of lipids, thin layer chromatography (TLC), and lipid assay to study lipid secretion and turnover. In an attempt to further clarify the possible mechanisms by which BHMT modulates hepatic lipid metabolism at molecular levels, we employed quantitative PCR to measure gene expression in real time. BHMT1 is highly regulated at the expression level (Park et al., 1997), we expect to see altered expression of key genes involved in hepatic *de novo* lipogenesis and TG biosynthesis following BHMT1 expression. The primary source of TG for VLDL assembly/secretion is the TG stored in lipid droplets (LD). Recent

evidence from a proteomic analysis of the cytosolic LDs fraction demonstrated an enrichment of BHMT1 on the purified LDs (Crunk et al., 2013). Since LD is involved in lipid storage and mobilization through lipolysis/reesterification (Beller et al., 2010), LD localization of BHMT1 provides further support for its proposed role in hepatic lipid metabolism. However, the study lack information on how much of BHMT is in the cytosol or on LD. We hypothesized that BHMT1 co-localizes with lipid droplets, and by doing so, it may be involved in the storage of neutral lipids and mobilization. To address whether BHMT1 or BHMT2 associated with LD, we examined intracellular localization using confocal microscopy. Based on the high sequence homology to BHMT1 and elevated protein expression in liver, it is hypothesized that BHMT2 expression in McA cells will result in similar metabolic changes as outlined for BHMT1.

1.2 Literature review

1.2.1 Lipid metabolism

Overview: The liver plays an important role in the regulation of lipid metabolism. The primary function of TG is to store excess energy consumed via the diet. Excessive TG storage has been implicated with clinical conditions (as discussed below). In the liver, free fatty acids (FFA) come from many different sources: diet, endogenous synthesis, and peripheral tissues. These FFAs are used for several different processes; they can be taken up by the mitochondria and metabolized for energy or ketone body production or converted to TG, phospholipids and other lipid classes. Hepatic TG, phospholipids, and cholesterol are stored in LDs until mobilized into ApoB-containing VLDL for secretion into the plasma or to the mitochondria for energy production. In principal, the balance between FFA and TG input and FFA and TG output reflects hepatic fat accumulation (Musso et al., 2009).

TG biosynthesis: TG synthesis occurs via two known major biosynthetic pathways, the glycerol-3-phosphate or Kennedy pathway, which functions in most cell types, and the monoacylglycerol (MG) pathway, which is most prominent in the intestine (Yen et al., 2002). The Kennedy pathway consists of four enzymatic steps. The first and committed step is the acylation of backbone glycerol-3-phosphate by fatty acyl-CoA at the *sn*-1 position. This reaction is catalyzed by glycerol-3-phosphate acyltransferase (GPAT)

results in the formation of lysophosphatidic acid (lysoPA), which is acylated by the enzyme acyl-CoA:1-acylglycerol-*sn*-3-phosphate acyltransferase (AGPAT) at the *sn*-2 position forming phosphatidic acid (PA). PA is dephosphorylated by enzyme PAP or lipin producing diacylglycerol (DG), which is a precursor for phospholipid synthesis (PC and PE). The final step of TG synthesis is the acylation of DG to form TG by the action diacylglycerol acyltransferase (DGAT). It is generally accepted that DGAT is the rate-limiting enzyme in TG biosynthesis, which actually accounts for more than 50% of very low-density lipoprotein (VLDL) TG (Liu et al., 2008). The MG pathway converts *sn*-2-MG and FA derived from hydrolysis of dietary TG to resynthesized TG for CM production. This is catalyzed by monoacylglycerol acyltransferase (MGAT) and DGAT via a stepwise acylation processes (**Figure 1-1**).

VLDL assembly and secretion: VLDL facilitates TG export from the liver to the circulation and protects the liver from excess accumulation of TG (Mason, 1998). VLDL assembly initiates in the endoplasmic reticulum (ER) and is proposed to occur in two steps: the first-step involves the formation of poorly-lipidated ApoB particles, followed by the addition of lipids in the second-step to generate mature secretion-competent VLDL (Borén et al., 1994). ApoB is an essential structural component for VLDL assembly and secretion. There are two forms of ApoB which are derived from the differen-

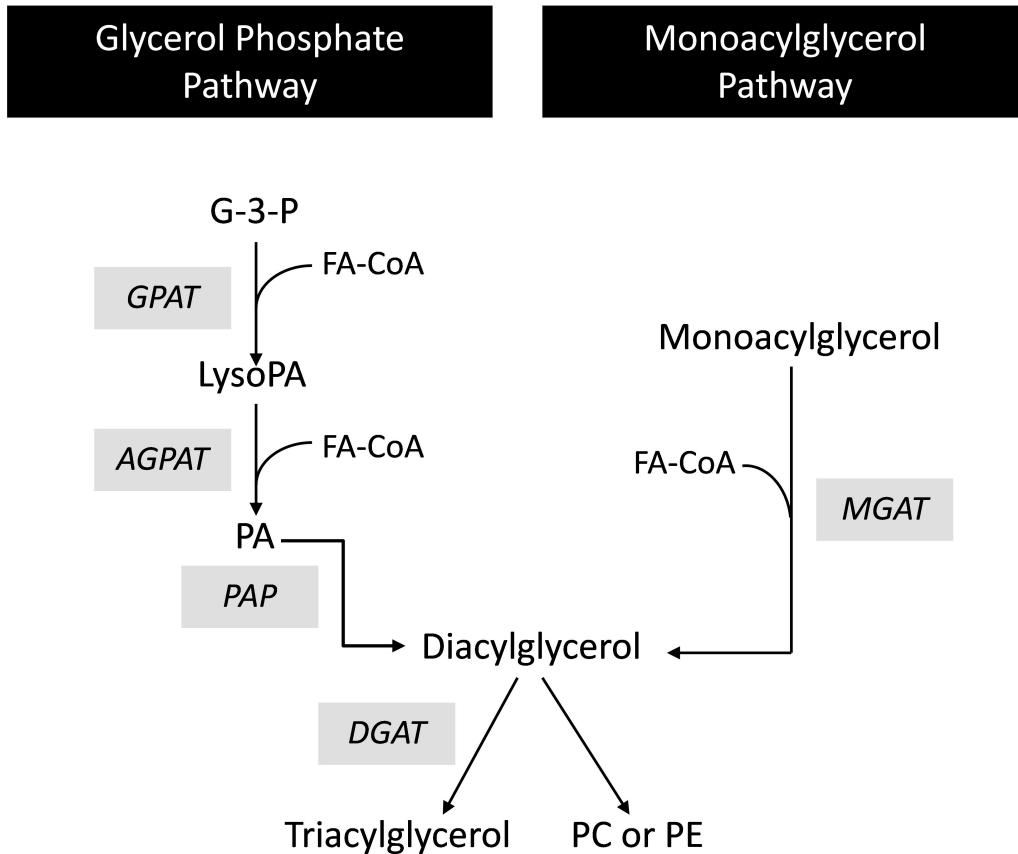


Figure 1-1 Two major TG biosynthesis pathways. The monoacylglycerol pathway begins with the acylation of MG with FA-CoA catalyzed by enzyme MGAT. The glycerol-3-phosphate pathway begins with the acylation of G-3-P with FA-CoA by GPAT, forming lysoPA. This is followed by sequential acylation by AGPAT and dephosphorylation by PAP, producing DG. DGAT catalyzed the final conversion of DG to TG. DG also serves as substrate for the synthesis of PC and PE. Abbreviation: G-3-P, glycerol 3-phosphate; LysoPA, lysophosphatidic acid; PA, phosphatidic acid, MGAT, monoacylglycerol acyltransferase2; DGAT, diacylglycerol acyltransferase; AGPAT, 1-acylglycerol-3-phosphate acyltransferase; PAP, phosphatidic acid phosphatase; FA-CoA, fatty acyl-CoA; PC, phosphatidylcholine; PE, phosphatidylethanolamine.

tial RNA editing of the same gene (Chen et al., 1987): ApoB100 and ApoB48. The availability of lipids, mainly TG, is considered rate-limiting for VLDL assembly (Dixon & Ginsberg, 1993). In the case of limited supply of TG, ApoB is degraded and VLDL secretion is reduced (Shelness & Sellers, 2001). Another requirement for VLDL assembly and secretion is the availability of PC, which is the major phospholipid on the surface monolayer of VLDL (Yao & Vance, 1988). Impaired PC synthesis has been shown to reduce VLDL secretion (Yao & Vance, 1988). Mouse models with deletion of genes needed for PC biosynthesis (CT α , PEMT or BHMT) have impaired VLDL secretion and increased accumulation of hepatic TG (Jacobs et al., 2004; Teng et al., 2011; Zhu et al., 2003). Cells supplemented with FA such as oleic acid (OA) have been shown to stimulate TG and PL synthesis and hence enhance the secretion of ApoB-containing VLDL particles. On the other hand, inhibition of TG synthesis using inhibitor of FA synthesis prevents OA-induced secretion (Dixon & Ginsberg, 1993).

1.2.2 Non-alcoholic Fatty Liver Disease

Introduction: Non-alcoholic fatty liver disease (NAFLD) is characterized by hepatic fat accumulation in people who do not consume excess alcohol. A person is considered to have a fatty liver when at least 5-10% of TG accumulated in the liver cells (Ahmed et al., 2009). Once considered a benign condition, there is now increasing evidence that NAFLD is one of the major causes of liver injury worldwide. NAFLD can progress from

simple liver steatosis to cirrhosis and hepatocellular carcinoma through the intermediate stage steatohepatitis (NASH) (Duvnjak et al., 2007). To date, the prevalence of NAFLD accounts for 30% of the general population, reaching 60-95% and 28-55% in obese and diabetic patients, respectively (Mazza et al., 2012). According to a study presented at the International Liver Congress in 2011, the occurrence of NAFLD is projected to increase by 50% in 2030 if the progressive epidemics of obesity and diabetes follow the current trends (Younossi et al., 2011). Also, it is estimated that NAFLD/NASH will directly or indirectly increase 5-year medical costs by 26%, increasing the global burden of liver disease (Abbas et al., 2012).

Diagnosis: NAFLD may progress silently without any clear clinical manifestations or symptoms. Most people with NAFLD are diagnosed with the detection of modest elevation of liver alanine aminotransferase (ALT) enzyme (Schreuder et al., 2008). However, studies have shown that 78% of fatty liver patients have normal plasma levels of liver enzymes (Browning et al., 2004), thus liver enzyme tests are not sensitive enough to establish diagnosis of NAFLD. Currently, liver biopsy though perceived as an invasive procedure, remains the most accurate diagnostic tool in the evaluation and management of fatty liver disease (Carey & Carey, 2010).

Pathogenesis: Although it is known that the progression of NAFLD is influenced by metabolic abnormalities, the etiology remains speculative. NAFLD can progress to NASH, a more severe form of fatty liver, which is associated with hepatic inflammation, and in some cases to fibrosis and cirrhosis. The progression from simple steatosis to NASH is proposed to follow the “two-hits” hypothesis (**Figure 1-2**), a frequently used model that describes the first ‘hits’ as increase in liver sensitivity from hepatic TG accumulation and the second ‘hits’ as mediators of liver inflammation and liver injury (Day, 2002). As TG accumulation increases, the liver becomes vulnerable to the second hits such as inflammatory cytokines, adipokines, oxidative stress and mitochondrial dysfunction (Day, 2002). These inflammatory responses could further lead to the progression of NASH, fibrosis and cirrhosis (Duvnjak et al., 2007). Over an extended period of time, as the liver damage continues, cirrhosis can ultimately progress to hepatocellular carcinoma, the most common type of liver cancer (Matteoni et al., 1999). However, NAFLD may also pose as an independent risk factor for the development of liver cancer in the absence of NASH or cirrhosis (Page & Harrison, 2009). Clearly, the pathogenesis of NAFLD is governed by a complex interplay between features of the metabolic syndrome, inflammatory markers, and genetic predisposition, many of which overlap with the onset of liver cancer (Dowman et al., 2013). This complexity creates a challenge in the search for effective therapies.

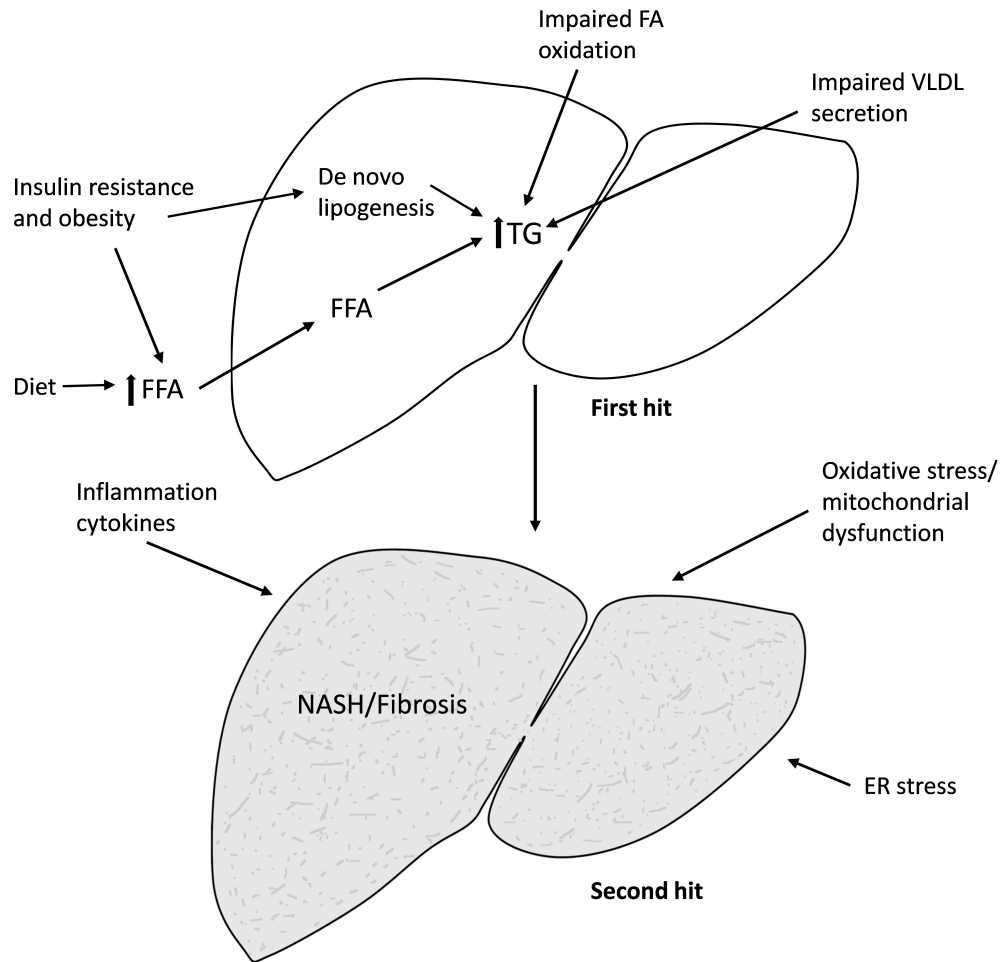


Figure 1-2 Two-hit model. The progression from simple steatosis to NASH is proposed to follow the “two-hits” hypothesis, a frequently used model that describes the first ‘hits’ as increase in liver sensitivity from hepatic TG accumulation and the second ‘hits’ as mediators to liver inflammation and liver injury mediated by inflammatory cytokines, oxidative stress, and mitochondrial dysfunction resulting in NASH and fibrosis.

1.2.3 One-Carbon Metabolism

Description of Pathway: The progression of NAFLD has been associated with impairment of the one-carbon metabolism. One-carbon metabolism consists of the cytosolic and mitochondrial folate cycle and the methionine cycle. Methionine is primarily metabolized in the liver (**Figure 1-3**). It is the precursor of S-adenosylmethionine (SAM), the principal methyl donor in various biological methylation reactions such as DNA methylation and is also vital for the synthesis of lipids, hormones, and proteins. The product of these methylation reactions, SAH is converted to Hcy and adenosine in a reversible reaction. Homocysteine has several possible fates: (1) it may be remethylated to methionine by transmethylation; (2) it may enter the transsulfuration pathway, a source of glutathione; or (3) it may be exported to the plasma. The liver expresses three enzymes that catalyze the remethylation of Hcy to methionine: the betaine-dependent betaine:homocysteine S-methyltransferase (BHMT1), S-methylmethionine-dependent BHMT2 and the cobalamin-dependent methionine synthase (MS). MS requires both 5-methyltetrahydrofolate as the methyl donor and vitamin B-12 as a cofactor for enzymatic activity. In the liver and kidney, BHMT1 catalyzes the transfer of a methyl group from betaine to Hcy to form dimethylglycine and methionine. The removal of Hcy from the methionine cycle occurs via the enzymes of the transsulfuration pathway; cystathionine- β -synthase (CBS) and cystathionine- γ -lyase (C γ L), which require vitamin B6 as a cofactor. Clearly, betaine, folate, vitamin B6 and cobalamin availability are key regulators in methionine and Hcy metabolism

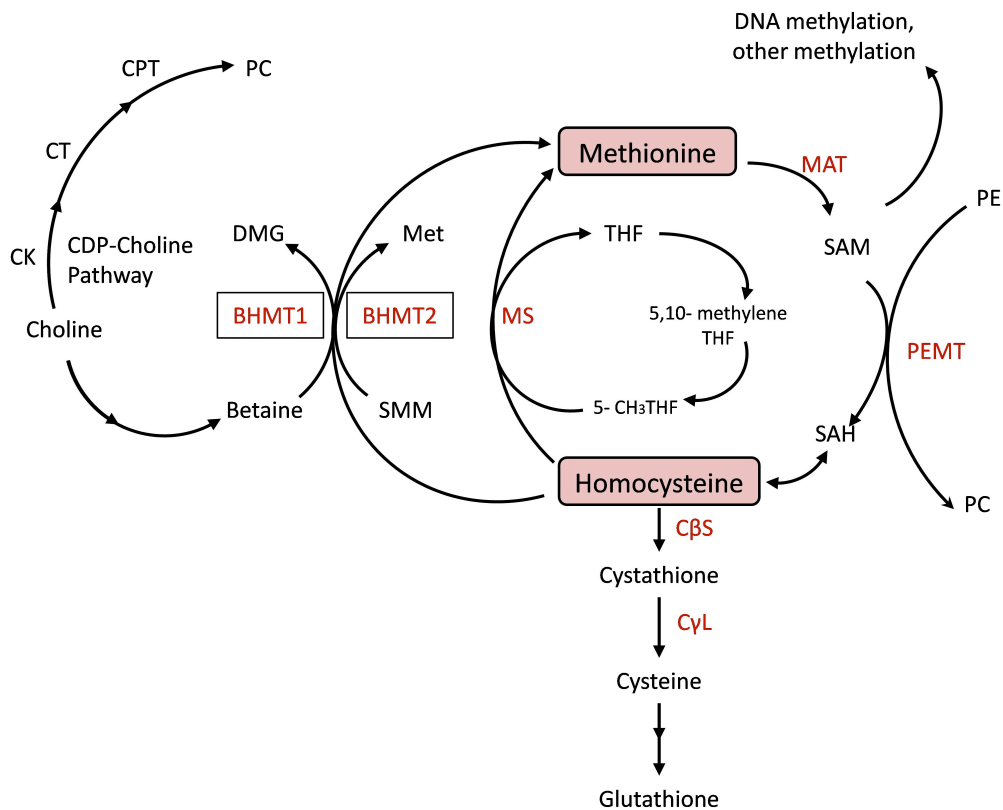


Figure 1-3 One-carbon metabolism pathways. The location of BHMT1 and BHMT2 are shown in box. Methionine is adenylated via MAT to form SAM. The products of these methyltransferase reactions are a methylated product and SAH, which is subsequently hydrolyzed to form homocysteine. Homocysteine may enter the transsulfuration pathway, thus removing sulfur from the methionine conservation cycle and forming other products, such as cysteine and glutathione or it may be remethylated to methionine via MS, BHMT1 or BHMT2. Abbreviations: MAT, methionine adenosyltransferase; MS, methionine synthase; BHMT1, betaine-homocysteine S-methyltransferase 1; BHMT2, betaine-homocysteine S-methyltransferase 2; CBS, cystathionine β -synthase; CyL, cystathionine- γ -lyase; MTHFR, methyl-THF reductase (MTHFR); PEMT, phosphatidylethanolamine; CK, choline kinase; DMG, dimethylglycine.

. Thus, it is not surprising that perturbation in one-carbon metabolism as a result of vitamin and/or metabolite deficiency or genetic polymorphisms are associated with many disease outcomes including cardiovascular disease, cancer and NAFLD (Frosst et al., 1995; Suzuki et al., 2008; Teng et al., 2011).

1.2.4 Importance of SAM in Fatty Liver Disease

SAM: A number of studies in both animal models and human patients have established a relationship between SAM (also known as AdoMet or SAdMe) deficiency and the pathogenesis of fatty liver disease. For example, in his earlier works, Barak et al. demonstrated that ethanol-induced fatty liver in rats have reduced hepatic SAM levels and altered hepatic methylation reactions (Barak et al., 1997; Barak et al., 1996; Barak et al., 1987). In 2003, Song et al. reported similar observations, whereby mice models subjected to acute alcohol administration had reduced hepatic SAM levels and developed hepatosteatosis (Song et al., 2003). In this study, animals were administered a control, ethanol treatment or SAM/ethanol treatment. The SAM/ethanol diet group received 5 mg/kg BW of SAM daily for three days prior to ethanol administrations. SAM treatment significantly attenuated liver damage and lipid peroxidation, improved liver enzymes, and prevented the depletion of hepatic SAM and glutathione levels caused by acute ethanol exposure (Song et al., 2003). A considerable amount of literature has been published on the role of oxidative stress in the

pathogenesis of fatty liver disease (Kurose et al., 1997; Nordmann, 1994; Wieland & Lauterburg, 1995). Glutathione is an important antioxidant that scavenges free radicals and maintains redox balance to protect the cells against oxidative stress (Marí et al., 2009). Therefore, restoration of glutathione may serve as one of the potential mechanisms for the observed hepatoprotective effects of SAM supplementation. A major report that clearly established the importance of SAM in liver health came from the *Mat1a* knockout (KO) mice (Lu et al., 2001). The absence of *Mat1a* gene encoding methionine adenosyltransferases (MATs), enzymes that catalyze the formation of SAM from methionine, resulted in chronic hepatic SAM deficiency. At 3 months, *Mat1a* KO mice develop hepatic hyperplasia and were more predisposed to fatty liver when consuming a choline-deficient diet, and by 8 months, these KO mice spontaneously develop macrovesicular steatosis (Lu et al., 2001). By 18 months of age, this condition was exacerbated whereby *Mat1a* KO mice develop hepatocellular carcinoma despite being fed a normal diet (Martínez-Chantar et al., 2002). Recently the interactions between SAM deficiency and fatty liver disease were investigated in human patients with biopsy-proven NASH. Kalhan et al (2011) administered L-[1-¹³C]methionine and L-[C²H₃]methionine tracers to measure the whole body flux of methionine, and its rate of transmethylation and transsulfuration. The rate of transmethylation of methionine was significantly reduced in the NASH subjects compared with controls, suggesting that patients with NASH suffer from SAM deficiency (Kalhan et

al., 2011). Putting the above into perspective, almost 50% of methionine metabolism and 85% of transmethylation occur in the liver making it the main organ for SAM production (Finkelstein, 1990; Mudd & Poole, 1975). Thus, it should not be surprising that balanced and sufficient supply of hepatic SAM is crucial for maintaining normal function and integrity of the liver.

Folate: Decreased plasma concentration of folate is another clinical feature associated with both alcoholic and non-alcoholic liver disease. Folate in a form of methyltetrahydrofolate acts as a methyl donor in the remethylation of Hcy to methionine in a reaction catalyzed by enzyme MS. MS and BHMT1 contributes equally to Hcy remethylation in the liver (Finkelstein, 1990). As a consequence, folate deficiency can impair hepatic methionine metabolism by reducing methionine and SAM synthesis and causing hyperhomocysteinemia (Pajares et al., 1992). This was clearly seen in micropigs fed a folate-deficient diet combined with ethanol. The onset of steatohepatitis was apparent after 3 months of ethanol feeding in folate-deficient (Halsted et al., 2002) as compared to 12 months in the folate-sufficient micropigs (Halsted et al., 1996). The development of hepatic steatosis in folate-deficient subjects was accompanied by an abnormal hepatic methionine metabolism including significant elevation of plasma Hcy, SAH and plasma ALT levels. Further, hepatic SAM and glutathione concentrations were decreased significantly in folate-deficient group

(Halsted et al., 2002). In agreement with these studies, Hirsch et al. (2005) found a negative correlation between folate status and the severity of NAFLD in human (Hirsch et al., 2005). In an attempt to identify the etiologic role of folate deficiency in the development of fatty liver, another study using liver samples from folate-deficient micropigs revealed that elevated plasma levels of Hcy and SAH are associated with increased cytochrome P-450 2E1 (CYP2E1) activity, ER stress signals, as well as lipogenic enzymes (Esfandiari et al., 2005). They showed that increased CYP2E1 activity by folate deficiency is mediated by the activation of sterol regulatory binding protein (SREBP), a central transcription factor in lipogenesis. CYP2E1 has been shown to be highly expressed in the liver and its activation promotes the generation of reactive oxygen species and oxidative stress (Cederbaum et al., 2001). Therefore, Hcy induced CYP2E1 activation may provide a mechanism by which folate-deficiency could cause steatosis and apoptosis.

Choline/phosphatidylcholine: In addition to the complex biochemical reactions previously discussed, the liver is also an important organ for the metabolism of choline. Choline can be oxidized to produce betaine, an alternative source of methyl group for the BHMT-dependent methionine synthesis from Hcy besides folate-dependent MS. Therefore, similar to folate, choline status in the liver impacts hepatic levels of SAM. Indeed, increasing evidence from experimental and human studies established that

choline deficiency plays an important mechanistic role in the development of fatty liver (Lombardi et al., 1968; Yao & Vance, 1990; Zeisel et al., 1991). Choline can be obtained from the diet or synthesized endogenously from PC. In the liver, PC is synthesized via two pathways: 70% of the synthesis is achieved via the CDP-choline pathway, a reaction catalyzed by CTP:phosphocholine cytidyltransferase (CT), the remaining 30% from the sequential methylations of PE by the enzyme phosphatidylethanolamine-*N*-methyltransferase (PEMT) (DeLong et al., 1999). On a chow diet, female mice that lack *CT* α gene had lower PC pools in the liver and develop fatty liver. These findings are associated with impaired VLDL secretion (Jacobs et al., 2004). In a subsequent study, the same author demonstrated that adenoviral delivery of *CT* α to *CT* α knockout mice not only normalizes hepatic CT activity and PC levels but also plasma VLDL levels (Jacobs et al., 2008). PC is a requirement for the assembly and secretion of VLDL, which export TG from the liver to circulation (Yao & Vance, 1988). Thus, it could be that *CT* α KO mice develop fatty liver due to the lack of PC to export TG from the liver, suggestive of the importance of PC in regulating hepatic lipid and lipoprotein metabolism. As mentioned, PC can also be synthesized from the consecutive conversion of PE via the PEMT-catalyzed reactions using three methyl groups from SAM (Vance, 1990). *Pemt* gene KO mice have lower choline pools and develop fatty liver despite meeting the recommended dietary intake of choline (Zhu et al., 2003). These results suggest that choline supplied from the PEMT pathway is important for

normal liver function. In humans, a polymorphism that resulted in a loss of function mutation in *PEMT* gene is associated with NAFLD (Song et al., 2005). Taken together, it appears that the methyl-donation function of choline is important in the pathogenesis of NAFLD.

1.2.5 Betaine Homocysteine S-Methyltransferase (BHMT)

Overview: It was a major advancement when Garrow and colleagues successfully cloned a 45 kDa unit human protein named BHMT1 in 1996. In mammals, BHMT1 proteins are highly conserved, with more than 80% identity at nucleotide level and 90% identity at the amino acid level for the human, rat and pig liver proteins (Garrow, 1996). Sequence analysis demonstrated that BHMT1 (E.C 2.1.1.5) belongs to the thiol/selenol methyltransferases (Pfam 02574) family. Typically, a Pfam 02574 enzyme contains a zinc-binding domain consisting of a conserved motif that includes three cysteine residues (positions 217, 299 and 300 of human sequence). A mutation analysis study of BHMT1 revealed that mutants missing the conserved cysteine residues resulted in Zinc depletion and complete loss of activity, suggesting the essential role of Zinc molecule (Millian & Garrow, 1998). BHMT1 is one of the three enzymes that contribute to the regulation of Hcy metabolism. BHMT1 is a cytosolic enzyme that catalyzes the transfer of a methyl group from betaine to Hcy to form DMG and methionine. Almost 50% of hepatic Hcy methylation capacity is achieved by BHMT1 (Finkelstein & Martin, 2000). In mammals,

BHMT1 is detected since early embryonic development (after day 10 of gestation period) (Feng et al., 2011) and in adults (Garrow, 1996). The liver and kidney are the main organs for BHMT1 expression (Garrow, 1996) where it represents approximately 0.6-1.6% of total liver protein. It has been suggested that BHMT1 activity is mainly regulated at the expression level (Park et al., 1997). Betaine is one of the major osmolytes in many tissues and is metabolically removed by BHMT1 (Lever & Slow, 2010). Therefore, the high expression of BHMT1 in kidney may be explained by its ability to regulate tonicity. Under the state of methionine deprivation and high abundance betaine and/or choline, BHMT1 gene expression and activity is increased (Park & Garrow, 1999). Therefore, the two known functions of BHMT1 are the regulation of hepatic methionine metabolism and cell/tissue tonicity. Recently, Chadwick et al., (2000) reported a rodent and human cDNA sequence that encodes an amino acid with 73% sequence similarity to BHMT1 called BHMT2 (E.C 2.1.1.5) (**Figure 1-4**). As with BHMT1, BHMT2 is involved in the remethylation of Hcy to methionine. However, BHMT2 uses S-methylmethionine (SMM), not betaine, as its methyl donor (Szegedi et al., 2008). Human and rat BHMT2 has been mapped to chromosome 5 (5q13) adjacent to BHMT1, suggesting tandem duplicates. BHMT2 protein is slightly smaller with a size of 40kDa units due to the missing residues of the C-terminal (40 residues). While BHMT2 is also abundantly expressed in liver and kidney, little is known about its functional aspect other than Hcy metabolism.

BHMT1 and lipid metabolism: Betaine is known to have hepatoprotective effects against fatty liver. Nevertheless, the exact underlying mechanisms are not completely clear. One proposed mechanism is that betaine promotes the generation of SAM, which is used for PC synthesis and in turn enhances lipid secretion from the liver. In 1969 Best et al. first reported that dietary betaine alleviates liver cirrhosis in rodents (Best et al., 1969). In 1993 Barak et al. administered betaine to ethanol-fed rats for 4 weeks (Barak et al., 1993) and found that betaine administration attenuated steatosis and increased hepatic BHMT1 activity and SAM levels. This was the first study to link the curative effect of betaine in alcohol-induced fatty liver subjects to SAM levels (Barak et al., 1993). More recently, Kathirvel et al. performed a longer betaine intervention study using a mouse model of NAFLD. In agreement with the previous study, they detected a significant increase in SAM in the betaine-supplemented group compared to control group. Betaine supplementation also prevented hepatic steatosis when administered with a moderate high-fat diet and reversed steatosis when administered following the development of NAFLD (Kathirvel et al., 2010). Together, the data suggests that the hepatoprotective effects of betaine, through BHMT1 activity, on both alcoholic and non-alcoholic subjects are associated with the elevation of SAM concentration in the liver.

There is accumulating evidence that betaine supplementation can attenuate fatty liver by providing enough supply of methyl groups for PC synthesis. As previously described, *Pemt* gene knockout mice have no

```

hBHMT1  MPPVGGKKAKKGILERLNAGEIVIGDGGFVFALEKRGYVKAGPWTPEAAV  50
hBHMT2  MAPAGRPGAKKGILERLESGEVIVIGDGSFLITILEKRGYVKAGLWTPEAVI  50
.....

hBHMT1  EHPEAVRQLHREFLRAGSNVMQFTTFYASEDKLENRGNVLEKISGQEVN  100
hBHMT2  EHPDAVRQLHMEFLRAGSNVMQFTTFSASEDNMESK-----WEDVN  91
.....

hBHMT1  EAACDIARQVADEGDALVAGGVSQTSPSYLSCKSETEVKKVFLQQLEVFMK  150
hBHMT2  AAACDLAREVAGKGDALVAGGICQTSIYKYQKDEARIKKLFRQQLEVFAW  141
.....

hBHMT1  KNVDFLIAEYFEHVVEEAVWAVETLIASGKPVAAATMCIGPEGDLHGVPPE  200
hBHMT2  KNVDFLIAEYFEHVVEEAVWAVEVLKESDRPVAVTMCIGPEGDMHDITPGE  191
.....

hBHMT1  CAVRLVKAGASIIIGVNCHFDPTISLKTIVKLMKEGLEAARLKAHLMSQPLA  250
hBHMT2  CAVRLVKAGASIVGVNCRFGPDTSLKTMELMKEGLEWAGLKAHLMVQPLG  241
.....

hBHMT1  YHTPDCNKQGFIDLPEFPFGLPEPRVATRWDIQKYAREAYNLGVRYIGGCC  300
hBHMT2  FHAPDCGKEGFVDLPEYPFGLPEPRVATRWDIQKYAREAYNLGVRYIGGCC  291
.....

hBHMT1  GFEPYHIRAIAEELAPERGFPPASEKHGSWGSGGLDMHTKPWVRARARKE  350
hBHMT2  GFEPYHIRAIAEELAPERGFPPASEKHGSWGSGGLDMHTKPWIRARARRE  341
.....

hBHMT1  YWENLRIASGRPYNPMSKPDGWGVTKGTAEMLQQKEATTEQQLKELFEK  400
hBHMT2  YWENLLPASGRPFCSLSKPD-----F--  363
.....

hBHMT1  QKFKSQ  406
hBHMT2  -----  363
.....

```

Figure 1-4 Sequence alignment of human BHMT1 and BHMT2. Conserved amino acids sequences are shaded in grey. The accession numbers are rat BHMT1, NP_001704.2; and rat BHMT2, NP_060084.2. This multiple sequence alignment is generated with ClustalX 2.1.

PEMT activity and develop severe fatty liver (Jacobs et al., 2010; Zhu et al., 2003). Researchers have also showed that hepatic steatosis attributed to chronic ethanol consumption have reduced conversion of PE to PC (Kharbanda et al., 2007). Following betaine administrations, PEMT activity and PC synthesis was increased in ethanol-induced fatty liver rats (Kharbanda et al., 2007). It was suggested that the restoration of SAM:SAH ratio by betaine is responsible for the increase in PEMT-mediated PC synthesis. Furthermore, the same group showed that betaine supplementation to ethanol-induced fatty liver normalizes VLDL secretion by restoring PEMT activity and PC synthesis (Kharbanda et al., 2009). These data collectively suggest that hepatic PC supplied via the PEMT pathway is one of the important targets in the development of hepatosteatosis. Betaine, by virtue of its role as a methyl donor, promotes TG-rich VLDL secretion by facilitating PEMT-mediated PC synthesis, and as such protects the liver from excessive lipid accumulation.

As described earlier, ApoB is an important structural protein of VLDL. Previously, Sparks and colleagues reported a positive correlation between the expression of BHMT1 and ApoB in rat hepatoma McA cells (Sowden et al., 1999). They found that the effect of BHMT1 expression was specific for ApoB mRNA, as the expression of other apolipoprotein species was not changed between the control and BHMT1-expressing cell lines. To examine whether a similar relationship occurs *in vivo*, the same researchers fed rats a methionine-restricted betaine-supplemented diet

(Sparks et al., 2006). The authors observed that the methionine-restricted betaine supplemented rats had a 3-fold increase in hepatic BHMT1 and ApoB mRNA as compared to methionine restriction alone. These findings were correlated with an increase in VLDL secretion as well as a significant reduction of liver TG. In both studies by Sparks et al., phospholipid levels were not measured; therefore it is not clear whether increased ApoB-containing VLDL secretion in this study is attributed to PC synthesis. It should be noted that McArdle hepatoma cells lack endogenous PEMT activity (Cui et al., 1995). In addition, an animal study suggest that PC derived from the PEMT pathway is the important source for VLDL secretion (Noga et al., 2002). Thus, the strong relationship between BHMT1 and VLDL demonstrated in these two studies may only be partially due to PC synthesis. It is possible that other mechanisms are responsible for the effects of BHMT1 expression on ApoB-containing VLDL secretion.

BHMT knockout model: Teng et al., recently reported on the first BHMT knockout mouse model (Teng et al., 2011). Deletion of both genes encoding BHMT1 and BHMT2 resulted in the complete loss of hepatic BHMT activity. As expected, BHMT KO mice have impaired one-carbon metabolism with a 43% reduction in hepatic SAM level and a significant increase in hepatic SAH. Furthermore, BHMT KO mice have altered choline metabolites in various tissues. The most striking change was observed in the liver, where they showed a significant reduction in choline and PC by 82

and 72% respectively. The transsulfuration and MS pathways were not able to compensate for the loss of BHMT, thus resulted in the accumulation of betaine and Hcy in many tissues, suggesting a critical role of BHMT in Hcy homeostasis. Despite increased betaine concentrations, methylation by betaine is prevented by the absence of BHMT activity, indicating a vital role for BHMT in betaine function. In addition, BHMT KO mice have elevated plasma ALT activity and develop fatty liver at 5 weeks of age. The authors suggested that the development of fatty liver in these mice is the result of decreased synthesis of PC. However, as the results from the *in vitro* cell culture study suggest (as discussed above) (Sparks et al., 2006), this may not be the only explanation to this observation and hence warrant further investigations. The importance of BHMT was further strengthened by the observation that BHMT KO mice developed hepatocellular carcinomas after 52 weeks (Teng et al., 2011). It is therefore evident that BHMT activity is essential for normal lipid and lipoprotein metabolism.

1.2.6 Conclusion

Current researches have highlighted several possible targets in the etiology of NAFLD. During the past 30 years much more information has become available on the important role of SAM in liver function. There are interrelations between folate, choline, betaine and methionine metabolism as all influence the production of SAM. Folate deprivation increases the use of choline and betaine for Hcy remethylation, and vice versa to maintain

normal level of Hcy (Schwahn et al., 2003). Two enzymes MS and BHMT1, which utilize folate and betaine as methyl donor respectively, govern these crucial reactions. In recent years, alteration of BHMT1 has been associated with liver steatosis and injury. The use of betaine as a therapy for NAFLD seems promising but remains controversial. Our understanding of the mechanisms by which betaine/BHMT1 improves steatosis is not entirely clear but one area that has been intensely studied is the link between BHMT1 and 1-carbon metabolism. It is proposed that increased in BHMT1 activity by betaine supplementation enhanced the generation of SAM, which consequently protects the liver via two ways: prevents hepatic TG accumulation by promoting PC synthesis that enables transport of TG and, reduces cellular stress by enhancing antioxidant glutathione production that safeguards the liver from further damage.

CHAPTER 2

MATERIALS AND METHODS

2.1 Materials

2.1.1 Chemicals and Reagents

<u>CHEMICALS</u>	<u>SOURCE</u>
[1- ¹⁴ C]Oleic acid	Perkin Elmer
[9,10- ³ H]Oleic Acid (5 mCi)	Perkin Elmer
[¹⁴ C] Betaine (50 μCi)	ARC, Inc.
100% Ethanol	Biochem Stores
2-propanol	Sigma Aldrich
40% Acrylamide/Bis solution 29:1 (3.3%)	Biorad
Acetic acid	Sigma Aldrich
AG 1-X4 Resin	Biorad
Agar	Invitrogen
Agarose	Invitrogen
Bovine serum albumin (BSA)	Sigma-Aldrich
Carbenicillin disodium	Sigma Aldrich
Chloroform	Fisher Scientific
Deoxynucleotides triphosphates (dNTPs)	Roche
Diisopropyl ether	Sigma Aldrich
Dimethyl sulfoxide (DMSO), cell culture grade	Sigma-Aldrich
DL-Homocysteine	Santa Cruz
DNase I	Invitrogen
Dnase/Rnase-free distilled water	Invitrogen
Dulbecco's Modified Eagle's Medium (DMEM)	Invitrogen

ECL immunoblotting reagents	GE Healthcare
Ethanol, 95%	Biochem Stores
Ethidium bromide	Sigma-Aldrich
Ethyl ether, anhydrous	Fischer Scientific
Ethylene-diaminetetra-acetic acid (EDTA)	Sigma Aldrich
Fetal bovine serum	Biochem Stores
Formaldehyde	Sigma Aldrich
G418 (Geneticin) Gibco	Biochem Stores
Glycerol	Sigma Aldrich
Hexane	Fischer Scientific
Hi-Fi polymerase	KAPA Biosystems
Horse serum	Invitrogen
Hydrochloric Acid	Fisher Scientific
Isopropanol	Fischer Scientific
Lipofectamine 2000	Invitrogen
Magic Marker XP Western protein standard	Invitrogen
Methanol	Biochem Stores
Mlu1 restriction enzyme	New England Bio.
Not1 restriction enzyme	New England Bio.
Oleic acid	Sigma-Aldrich
Oligo dT primers, 12-14	Biochem Stores
Opti-MEM	Biochem Stores
Perchloric acid	Sigma Aldrich

Phosphatase inhibitor cocktail	Sigma Aldrich
Phospholipase C (<i>Clostridium welchii</i>)	Sigma-Aldrich
Pierce Bicinchoninic Acid (BCA) protein kit	Thermo Scientific
Platinum® Taq DNA Polymerase	Biochem Stores
Precision Plus Protein All Blue standard	Biorad
Prolong Antifade kit	Invitrogen
Protease inhibitor cocktail	Sigma Aldrich
Sodium chloride	Sigma Aldrich
Sodium dodecyl sulfate (SDS)	Sigma Aldrich
Superscript™ II reverse transcriptase	Invitrogen
Sylon BFT (BSTFA + TMCS, 99:1)	Supelco (Sigma)
T4 DNA ligase	New England Bio.
TEMED	Sigma Aldrich
Triacylglycerol-SL	Fischer Scientific
Tris base	Sigma Aldrich
Trizol reagent	Invitrogen
Trypsin EDTA solution 0.25%	Invitrogen
Ultima Gold XR scintillation fluid	Perkin Elmer
Betaine	Sigma Aldrich
S-methylmethionine	Sigma Aldrich
L- α -Phosphatidylethanolamine	Avanti Polar Lipids
L- α -Phosphatidylcholine	Avanti Polar Lipids

2.1.2 Plasmid

Table 2-1 Plasmid vector

Vector	Insert	Source	Comments
pCI-Neo mammalian expression vector	rat BHMT1 rat BHMT2	Promega	HA-tag cDNA was placed at the N-terminus of rat BHMT1 and BHMT2 prior to the start codon. Mlu1 and Not1 restriction enzyme sequences were placed at the forward and reverse primers.

2.1.3 Antibodies

The list of primary and secondary antibodies used in this thesis is listed in Table 2-2 and Table 2-3.

Table 2-2 Primary antibodies

Name	Species	Dilution (IB)	Dilution (IF)	Source
Adipohilin	guinea pig	N/A	1:100	Cedarlane (Fitzgerald Industry)
Anti-HA	mouse	1:5000	1:150	Sigma
B-actin	rabbit	1:100	N/A	Fischer

Table 2-3 Secondary antibodies

Name	Source
Alexa Fluor 488- conjugated goat anti- Guinea Pig IgG	Invitrogen Molecular Probe
Horseradish peroxidase-conjugated goat- anti-rabbit IgG	Fischer Scientific
Horseradish peroxidase-conjugated goat- anti-mouse IgG	Fischer Scientific
Texas Red-X-conjugated goat-anti-mouse IgG	Invitrogen Molecular Probe

*All secondary antibodies were used at 1: 5000 dilutions for IB and 1:200 for IF.

2.1.4 Primers

The oligonucleotide primers used for PCR cloning and nucleotide sequencing are listed in Table 3-4 and Table 3-5.

Table 2-4 Cloning primers used to amplify *bhmt1* and *bhmt2* gene.

Name	Sequence	Direction	Notes/Source
PCR Primer BHMT1 a	5'- GCA CCG ATT GCC AAG AAG GCC A -3'	forward	Integrated DNA Technologies
PCR Primer BHMT1 b	5'- CTA CTG TGC GGA TTT GAA TTT TTG -3'	reverse	Integrated DNA Technologies
PCR Primer BHMT2 a	5'- GCA CCA GCC GGA GGC CCA CGA -3'	forward	Integrated DNA Technologies

PCR Primer BHMT2 b	5'- TCA AGC ATC TGG CTT TGA TAG G -3'	reverse	Integrated DNA Technologies
PCR Cloning Primer BHMT1 a	5'- AGA GAG ACG CGT CCA CCA TGT ACC CAT ACG ATG TTC CAG ATT ACG CTA TGG CAC CGA TTG CCG GCA AGA AGG CCA -3'	forward	HA tag, Mlu1 Restriction site. Integrated DNA Technologies
PCR Cloning Primer BHMT1 b	5'- GAG AGA GCG GCC GCC TAC TGT GCG GAT TTG AAT TTT TG -3'	reverse	Not1 restriction site. Integrated DNA Technologies
PCR Cloning Primer BHMT2 a	5'- AGA GAG ACG CGT CCA CCA TGT ACC CAT ACG ATG TTC CAG ATT ACG CTG CAC CAG CAG CCG GAG GCC CAC GA -3'	forward	HA tag, Mlu1 Restriction site. Integrated DNA Technologies
PCR Cloning Primer BHMT2 b	5'- GAG AGA GCG GCC GCT CAA GCA TCT GGC TTT GAT AGG -3'	reverse	Not1 restriction site. Integrated DNA Technologies

Table 2-5. Nucleotide sequencing primers. T7EE7 promoter and T3 terminator primers are vector-specific sequencing primers whereas BHMT1-387F – BHMT2-849R are gene-specific primers.

Name	Sequence	Direction	Notes/Source
T7EE7 Promoter	5'- AAG GCT AGA GTA CTT AAT ACG A -3'	forward	
T3	5'- CAT TAA CCC TCA CTA AAG GG -3'	reverse	

BHMT1-387F	5'- CAG CTG CAA GAG TGA GAC GGA AGT -3'	forward	Integrated DNA Technolog
BHMT1-761F	5'- CTG ACT GTG GCA AAC AGG GAT TTA -3'	forward	Integrated DNA Technologies
BHMT1-761R	5'- TAA ATC CCT GTT TGC CAC AGT CAG -3'	reverse	Integrated DNA Technologies
BHMT1-386R	5'- CTT CCG TCT CAC TCT TGC AGC TGA -3'	reverse	Integrated DNA Technologies
BHMT2-400F	5'- CTA CAG CTA GGT GTT TTT GCC AGG -3'	forward	Integrated DNA Technologies
BHMT2-767F	5'- GCT CCA GGC CGA AAG GAT ATT CAG -3'	forward	Integrated DNA Technologies
BHMT2-397R	5'- GGC AAA AAC ACC TAG CTG TAG TCG -3'	reverse	Integrated DNA Technologies
BHMT2-849R	5'- CAG CAG CCG CCA ATG TAC CTG ACC -3'	reverse	Integrated DNA Technologies

2.1.5 Buffers and solutions

Table 2-6 listed all the common buffers and solution used this thesis.

Name	Composition
50xTAE	242 g Tris base, 57.1 ml glacial acetic acid dissolved in 100 ml of 0.5 mM EDTA (pH 8.0)
1x PBS	137 mM NaCl, 2.7 mM Kcl, 10 mM Na ₂ HPO ₄ , 2 mM KH ₂ PO ₄ , pH 7.4
1x TBS	20 mM Tris-HCl, pH 7.4, 150 mM NaCl
1x TBST	50 mMTris-HCl, 150 mM NaCl, 0.1% Tween 20

1x resolving gel buffer	1.5 M Tris base, pH concentration with HCl to 8.8, 0.4% (w/v) SDS
10x running buffer	250 mM Tris base, 1.92 M Glycine, 1% SDS, bring to 2L, store at room temperature
1x transfer buffer	25 mM Tris base, 192 mM glycine, 20% methanol, bring to 2L, store at 4°C
1x TE buffer	10 mM Tris base, 1 mM EDTA, pH 8.0
6x Loading dye	4g sucrose, 0.5 M EDTA pH 8.0, 1.0% bromophenol blue, bring to 10 ml
1x Lysis buffer	20 mM Tris-HCl, pH 7.4, 50 mM NaCl, 50 mM NaFl, 5 mM NaPP, 0.25 M Sucrose

2.2 Cloning of BHMT1 and BHMT2 cDNAs

2.2.1 Coding sequences of BHMT1 and BHMT2

The coding sequences of BHMT1 (**Figure 2.1**) and BHMT2 (**Figure 2.2**) were retrieved online from the GenBank database of the National Center for Biotechnology Information (NCBI).

```
ATGGCACCGATTGCCGGCAAGAAGGCCAAGAGGGGAATCTTAGAACGCTTA
AATGCTGGCGAAGTCGTGATCGGAGATGGGGGATTTGTCTTTGCACTGGAAA
AGAGGGGCTACGTAAAGGCTGGACCCTGGACCCAGAGGCTGCGGTGGAG
CACCCCGAGGCAGTTCGGCAGCTTCATCGGGAGTTCCTCAGAGCTGGATCG
AACGTCATGCAGACCTTCACTTTCTATGCAAGTGAGGACAAGCTGGAAAACC
GAGGGAACACTACGTGGCAGAGAAGATATCTGGGCAGAAGGTCAATGAAGCTG
CTTGTGACATTGCACGGCAAGTTGCTGACGAAGGGGATGCATTGGTTGCAGG
AGGTGTGAGTCAGACACCTTCCCTACCTCAGCTGCAAGAGTGAGACGGAAGTT
AAAAAGATATTTACCAACAGCTTGAGGTCTTCATGAAGAAGAATGTGGACTT
CCTCATTGCAGAGTATTTTGAACATGTTGAAGAAGCCGTGTGGGCAGTCGAG
GCCTTAAAAACATCCGGGAAGCCTATAGCGGCTACCATGTGCATCGGACCTG
AAGGAGATCTACATGGCGTGTCTCCTGGAGAGTGCGCAGTGCGTTTGGTAAA
AGCAGGTGCCGCCATTGTCCGGTGTGAACTGCCACTTCGACCCAGCACCAG
CTTGCAGACAATAAAGCTCATGAAGGAGGGTCTGGAAGCAGCTCGGCTGAA
GGCTTACTTGATGAGCCACGCCCTGGCCTACCACACCCCTGACTGTGGCAAA
CAGGGATTTATTGATCTCCCAGAATTCCCCTTTGGATTGGAACCCAGAGTTGC
CACCAGATGGGATATTCAAAAATACGCCAGAGAGGCCTACAACCTGGGGGTC
AGGTACATTGGCGGCTGCTGCGGATTTGAGCCCTACCACATCAGGGCCATTG
CAGAGGAGCTCGCCCCAGAAAGGGGATTTTTACCACCAGCTTCAGAAAAACA
TGGCAGCTGGGGAAGTGGTTTGGACATGCACACCAAACCCTGGATCAGGGC
AAGGGCCAGGAAAGAATACTGGCAGAATCTTCGAATAGCTTCGGGCAGACC
GTACAATCCTTCGATGTCCAAGCCGGATGCTTGGGGAGTGACGAAAGGGGC
AGCAGAGCTGATGCAGCAGAAGGAAGCCACCACTGAGCAGCAGCTGAGAGC
GCTCTTCGAAAAACAAAATTCAAATCCGCACAGTAG
```

Figure 2-1 Coding sequence of rat BHMT1. The coding sequence begins with the ATG start codon and ends with the TAG stop codon, which represents nucleotides 71-1294, Genbank accession number NM_030850.1.

ATGGCACCAGCCGGAGGCCACGAGTCAAGAAGGGTATCTTGGAGCGTCTG
GACAGCGGGGAGGTTGTGGTTGGGGACGGCGGCTTTCTCTTCACTCTGGAA
AAGAGAGGCTTTGTGAAGGCAGGACTTTGGACTCCAGAAGCAGTGGTAGAGT
ATCCAAGTGCAGTTCGTCAGCTTCACACAGAATTCTTGAGAGCGGGAGCCGA
TGTCTTGCAGACATTCACCTTTTCGGCTGCTGAAGACAGAATGGAAAGCAAG
TGGGAAGCTGTGAATGCAGCTGCCTGTGACCTGGCCCAGGAGGTGGCTGAT
GGAGGGGCTGCTTTGGTGGCAGGGGGCATCTGCCAGACATCACTGTACAAG
TACCACAAGGATGAAACTAGAATTA AAAACATTTTCCGACTACAGCTAGGTGT
TTTTGCCAGGAAAAATGTGGACTTCTTGATTGCAGAGTATTTTGAGCATGTGG
AAGAAGCCGTGTGGGCTGTGGAAGTCTTGAGAGAGGTGGGGGCACCTGTGG
CTGTGACCATGTGCATCGGCCAGAGGGGGACATGCACGGCGTGACACCGG
GAGAGTGTGCGGTGAGACTGTCTCGTGCAGGGGGCGAACATCATTGGGGTAA
ACTGCCGTTTGGGCCCTGGACCAGCTTACAGACCATGAAGCTCATGAAGGA
GGGCCTCAGGGATGCCGGCCTACAAGCTCACCTTATGGTCCAGTGCTTGGG
TTTCCACACACCGGACTGTGGCAAGGGAGGGTTTGTGGACCTTCTGAATAT
CCTTTCCGGCCTGGAGCCAAGAGTTGCCACCAGATGGGATATTCAAAAATACG
CCAGAGAGGCCTACAACCTGGGGGTGAGGTACATTGGCGGCTGCTGCGGAT
TTGAGCCCTACCACATCAGGGCCATTGCAGAGGAGCTCGCCCCAGAAAGGG
GATTTTTGCCACCAGCTTCAGAAAAACATGGCATCTGGGGAAGTGGTTTGGGA
CATGCACACCAAACCCTGGATCAGAGCAAGGGCTAGACGGGAATACTGGGA
AACTCTGTTGCCAGCTTCGGGAAGACCTTTCTGTCTTCCCTATCAAAGCCAG
ATGCTTGA

Figure 2-2 Coding sequence of rat BHMT2. The coding sequence begins with the ATG start codon and ends with the TGA stop codon, which represents nucleotides 24-1115, Genbank accession number NM_001014256.2.

2.2.2 Primer design

The primers used in this project were designed using the Oligo Primer Analysis Software (version 6.7) as per the developer's instruction. For the cloning of BHMT1 and BHMT2, primer sequences for the start and end of the coding sequences were selected, tested for duplex features, then modified with the addition of an HA epitope tag, restriction enzyme sites, and spacer sequences. The selected primers were BLAST searched to confirm the specificity of the primers to BHMT1 or BHMT2. See Table 2-4

and Table 2-5 for the list of cloning and sequencing primers used in this thesis.

2.2.3 RNA isolation and DNase 1 treatment of RNA for RTPCR

Total RNA from rat (Sprague Dawley) liver was isolated using Trizol® reagent according to the manufacturer's instructions. RNA samples were treated with DNase 1 (amplification grade, Invitrogen) to degrade any genomic DNA contamination. The calculated volume needed for 2 µg RNA (2.1µg/µl) was added to a microcentrifuge tube and brought to a volume of 8 µl with DEPC-treated water. In a separate tube, DNase 1 and DNase 1 buffer (10x, supplied) were added enough so that the equivalent of 1 µl each can be added to each RNA sample. Mix of DNase 1 and DNase 1 buffer (total of 2 µl) was added to each RNA sample and mixed by gentle pipetting, and incubated at room temperature for 15 min. 1 µl of 25 mM EDTA (Invitrogen) solution was added to each sample and kept on ice followed by a vortex and a quick spin for sample collection. Finally, the sample was set in a PCR machine to 65°C for 10 min to kill the enzyme and ready for reverse transcription protocol.

2.2.4 cDNA generation from RNA by reverse transcription

First strand cDNA synthesis from 2 µg of total RNA was performed using Superscript™ II reverse transcriptase primed by oligo (dT)₁₂₋₁₈ primers. 1 µl of oligo (dT) was added to each tube containing DNase 1-

treated RNA sample and set to 65°C for 10 min for denaturation step. The samples were then set on ice for 5 min. A master mix for n + 1 reactions was prepared so that the final concentration of each reaction would consist of 4µl 5X First Strand buffer (supplied), 25mM dNTPs, 50mM DTT (supplied), 0.6 µl DEPC water and 25 U/µl Superscript™ II. All components of the master mix except the Superscript™ II were mixed by a quick vortex. The Superscript™ II enzyme was added last and mixed by gentle pipetting. 8 µl of the prepared master mix was added to each sample tube and set in a PCR machine at 42°C for 50 min, then 94°C for 15 min and hold at 4°C. Synthesized cDNA was either used for PCR or stored at -20°C.

2.2.5 BHMT1 and BHMT2 cDNAs amplification by PCR

To check the suitability of rat liver mRNA as template for amplifying genes, BHMT1 and BHMT2 cDNA were amplified by PCR. Primers for the amplification of rat BHMT1 were forward 5'-GCACCGATTGCCGGCAAGAAGGCCA-3' and reverse 5'-CTACTGTGCGGATTTGAATTTTTG-3'. Primers for the amplification of rat BHMT2 were forward 5'-GCACCAGCCGGAGGCCACGA-3' and reverse 5'-TCAAGCATCTGGCTTTGATAGG-3'. BHMT1 and BHMT2 amplification from 0.1 µg total cDNA were performed using Tag Platinum polymerase. PCR reactions were performed in 25 µL reactions consisting of 1x PCR buffer, 25 mM dNTPs, 1.25 µL Mg²⁺ (2.5 mM), 1 µL of each primer (8 µM), 0.2 µL Tag Invitrogen Platinum polymerase (0.04 U/µL), and dH₂O to a total

volume of 25 μ L. PCR amplification of BHMT1 cDNA was performed using the following conditions: 95 $^{\circ}$ C for 3 min, 94 $^{\circ}$ C for 30 sec for denaturing step, 61 $^{\circ}$ C for 30 sec for annealing step, and 72 $^{\circ}$ C for 90 sec for elongation step. The denaturing step to the elongation step was repeated for 35 cycles, followed by a final elongation step at 72 $^{\circ}$ C for 5 min. The same conditions were employed for BHMT2 except, 58 $^{\circ}$ C was set in the annealing step.

2.2.6 High-fidelity amplification of BHMT1 and BHMT2 cDNAs

For cloning, modified primers with the addition of HA epitope tag, restriction enzyme sites and spacer sequences were used (Table 2-4). HA-epitope tag allows a feasible detection of BHMT1 and BHMT2 proteins in our recombinants using HA-tag specific antibody. Primers used were

BHMT1-forward: 5'-

AGAGAGACGCGTCCATGTACCCATACGATGTTCCAGATTACGCTATGG

CACCGATTGCCGGCAAGAAGGCCA-3', BHMT1-reverse: 5'-

GAGAGAGCGGCCGCTACTGTGCGGATTTGAATTTTTG-3', BHMT2-

forward:

5'AGAGAGACGCGTCCACCATGTACCCATACGATGTTCCAGATTACGCT

GCACCAGCCGGAGGCCACGA-3' and BHMT2-reverse: 5'-

GAGAGAGCGGCCGCTCAAGCATCTGGCTTTGATAGG-3'. CTA and TCA

are the stop codons for BHMT1 and BHMT2 respectively: ACGCGT is a

Mlu1 restriction enzyme site sequence; GCGGCCGC is a Not1 restriction

enzyme site sequence; TACCCATACGATGTTCCAGATTACGCT encodes the HA epitope tag. The cDNAs were amplified using KAPA Hi-Fi polymerase; this facilitates robust amplification of longer DNA fragments. PCR amplification of BHMT1 cDNA was performed using the following conditions: 95 °C for 5 min, 98 °C for 20 sec for denaturation step, 65 °C for 15 sec for annealing step, and 72 °C for 40 sec for elongation step, with repetitions of the denaturation to elongation steps for 35 cycles, followed by a final elongation step at 72 °C for 5 min. The same conditions were employed for BHMT2 except, 64 °C was set in the annealing step. The PCR products were immediately purified using QiaQuick PCR purification kit (Qiagen). The samples were measured on a spectrophotometer (BioSpec-1601) to determine the concentration and purity by 200nm - 350nm wave scan and ratio determination of A260/A280.

2.2.7 Restriction digestion

BHMT1 and BHMT2 sequences with additional Mlu1 and Not1 restriction sites and HA-epitope tag sequences were excised from the PCR fragments by digestion with Mlu1 and Not1 restriction enzymes. An empty pCI-Neo mammalian expression vector (Promega) was also excised using the same restriction enzymes for controls. Restriction digestions were performed in 40 µL reactions consisting of 1X buffer #3 (supplied), 1X BSA, dH₂O, 2 µg DNA (PCR fragments) or pCI-Neo vector and 1 µL of each restriction enzyme. A control with Mlu1 enzyme was also prepared to

linearize the vector. The reactions were then incubated at 37 °C for 3 hours in a PCR machine. Following incubation, restriction digested reactions were separated on a 1.5 % (w/v) agarose gel containing 1 µg/mL of ethidium bromide in 1X TAE buffer [prepared as 50x concentrated stock]. The separated bands of correct size were excised on a trans-illuminator. The excised DNA bands were then placed in individual eppendorf tubes and centrifuged at 13000 rpm for 1 minute. The excised DNA bands were then weighed on an analytical balance and purified using Qiagen QiaQuick Gel Purification Kit (Qiagen). Quantification of DNA yield was performed using a spectrophotometer. The digested inserts encoding BHMT1 or BHMT2 were then ligated into pCI-Neo vector that was digested with the same restriction enzymes Mlu1 and Not1. In brief, ligation reactions were performed in 40 µL reactions consisting of 1X T4 DNA ligase buffer, digested pCI-Neo vector, digested insert DNAs, dH₂O, and T4 DNA ligase. The reactions were incubated overnight at room temperature.

2.2.8 Transformation and purification of recombinant cDNA plasmid

The ligated HA-BHMT1 or BHMT2 was transformed into *Escherchia coli* strain DH5α competent cells. Briefly, 100 µL of competent cells and 10 µL of ligated sample were mixed in an eppendorf tube and chilled on ice for 30 min. Following incubation, the reaction was heat-shocked at 37 °C for 2 min and chilled on ice for 5 min. 1 mL of Luria-bertani (LB) broth was added

into the reaction and shaken at 200 rpm at 37 °C for 1 hour. The transformed bacterial cells were spread onto agar plates containing carbenicillin (100µg/ml) or without carbenicillin. These plates were incubated overnight at 37 °C. Colonies were randomly picked and cultured in LB broth with carbenicillin (100 µg/ml) in a 37 °C shaker at 200-250 rpm overnight. 100 µL of overnight cell culture was added into 900 µL freezing stock consisting of LB broth, 15% glycerol and 1X Carbenicillin and kept in -80 °C for future use. The remaining overnight cell culture was prepared for purification. Briefly, overnight cell culture was centrifuged for 5 min at maximum speed of 3000 rpm at room temperature. The supernatant was removed from the culture and the pellet was resuspended in 250 µL buffer PI (supplied). From this point, the plasmid was purified using a QiaQuick Miniprep kit (Qiagen) according to package instructions. Quantification of plasmid DNA yield was performed using a spectrophotometer (Biospec-1601).

2.2.9 Confirmation of insertion

To confirm that the correct restriction fragments from section 2.2.8 were present, restriction digestions were performed on the recombinant DNA. Restriction digestions were performed as described in section 2.2.7 and the DNA fragments were separated by gel electrophoresis with 1 kb ladder on 1.5 % (w/v) agarose gel. Briefly, 8 µL of loading dye (refer Table 2-6) was added into each tube containing 25 µL DNA samples. Of these, 25

μL of each samples were loaded into each well of the agarose gel and electrophoresed under constant voltage of 75 V for approximately 1.5 hours. The separated bands were visualized by ethidium bromide staining using a Gel-Doc system. Upon confirmation that the plasmid DNAs consists of the correct insert (HA-BHMT1 or HA-BHMT2) and plasmid size (pCI-Neo), DNAs were purified on a larger scale using the Maxi Prep DNA purification kit according to the manufacturer's instructions (Qiagen).

2.2.10 Sequence analysis

The BigDye sequencing was performed in a 20 μL reactions consisting of BigDye premix from Molecular Biology Service Unit (MBSU), ABI BigDye buffer (ABI, CN: 4336697), 50 ng plasmid DNA, 5 pmols primers (refer Table 2-5) and dH_2O . The PCR conditions for sequencing reactions were set as following: 95°C for 30 second, 50°C for 15 sec and 60°C for 2 min with repetitions for 25 cycles. 20 μL of these sequencing reactions was added into 2 μL of NaOAc/EDTA MBSU in a separate microfuge tube. The samples were vortexed and left on ice for 15 min followed by a centrifugation at 4°C for another 15 min. The supernatant was carefully removed by aspiration. The pellets from this step were washed with 500 μL of 70% EtOH and centrifuged for 5-10 min. The supernatant was carefully aspirated out with a 21-gauge 1.5 inch needle connected to a vacuum aspirator. The pellets were air-dried and stored in -20 °C or immediately delivered to MBSU, University of Alberta, for sequencing.

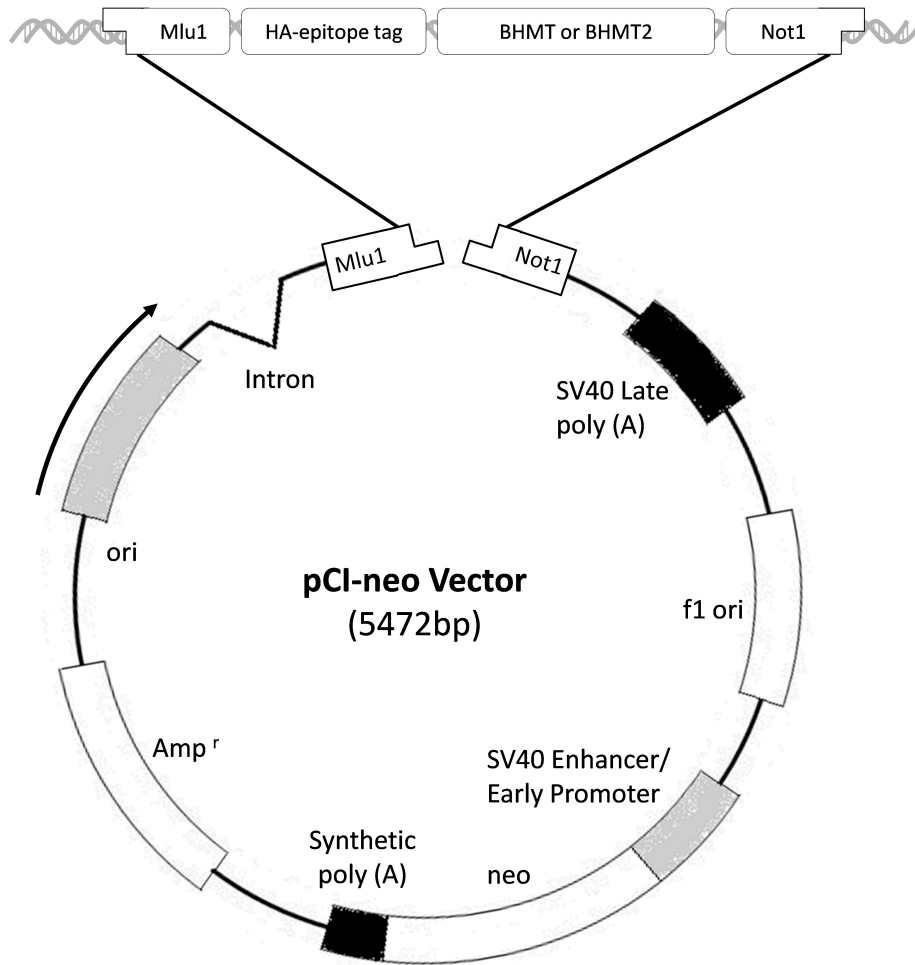


Figure 2-3 Schematic representation of recombinant BHMT DNA. BHMT1 or BHMT2 inserts amplified with modified primers containing HA epitope tag, restriction enzyme sites and spacer sequences was restriction digested with restriction enzymes Mlu1 and Not1 and ligated into pCI-neo vector that has been restriction digested with the same restriction enzymes Mlu1 and Not1. The resultant recombinant DNA was amplified and stably transfected into McA cells.

2.3 Cell culture manipulation

2.3.1 Cell culture of McArdle cells

McA cells obtained from Molecular Cell Biology of Lipids (MCBL) group stocks were cultured and maintained in DMEM containing 10% horse serum (HS) and 10% fetal bovine serum (FBS) at 37 °C in CO₂ incubator unless otherwise stated.

2.3.2 Stable transfection of McA cells

Twenty hours prior to transfection, 250,000 cells were added to 60 mm dish. Plasmid DNAs were introduced into cells via Lipofectamine 2000 as per the package instructions. Briefly, 4 µg of DNA in TE buffer (Tris-EDTA, pH 8.0) was diluted in 500 µL OptiMem and gently mixed. At the same time, 8 µL of Lipofectamine 2000 reagent was diluted in 500 µL OptiMem and incubated at room temperature for 5 min. After the 5 min incubation, the diluted DNA and diluted Lipofectamine 2000 were combined to a total volume of 1 ml. The combinations were gently mixed and incubated at room temperature for 20 min to allow DNA-Lipofectamine complex formation. Following incubation, 1 ml of the complexes was added into McArdle cells in each dish containing 4 ml DMEM + 10% heat-activated FBS. After 5-6 hours, the complexes were removed from the dish and the medium was replaced by complete DMEM (10% HS + 10% FBS) and incubated at 37 °C in CO₂ incubator. The following day, the cells in each dish were split into three 10 cm dishes. The next day, the stable cell lines

were selected by replacing the media in each dish with media containing 400 μ M Geneticin. The medium was changed with new media containing the same concentration of Geneticin every 2-3 days. Transfected cells were cultured in this condition for about 2 weeks until discrete colonies were evident due to massive cell death. Single colonies were then trypsinized off and carefully transferred using the 20- μ L pipette into a 6-well plate and cultured and checked for expression by Western blotting using anti-HA antibodies. The cells were maintained with 200 μ M Geneticin following initial selection.

2.3.3 Freezing stable cell lines

Before starting, tubes containing the complete growth medium or complete medium containing 20% DMSO were chilled on ice. Media from cells cultured in 10 cm dish was aspirated and the cells were washed with 2 ml Trypsin and quickly aspirated. The cells were then incubated in 1 ml Trypsin for 1 minute and 9 ml of complete media were added into each dish and the contents were transferred to a 15 ml tube and centrifuged at 1000 rpm for 5 min. The supernatant was carefully removed using a 1 ml pipette. The pelleted cells were resuspended in chilled media and an equal volume of chilled media plus 20% DMSO was added. The cells were transferred into freezing Cryovials and placed in a foam container before placing it in -80 °C. A day later, all samples were transferred to a liquid nitrogen tank.

2.4 Protein manipulation and analysis

2.4.1 Determination of protein concentration

Protein concentrations were determined by Bradford method using the Pierce BCA Protein Assay kit. Briefly, protein samples from cell culture homogenates were diluted at 1:10 ratio in 1X PBS solution (refer Table 2-6 for 1X PBS composition). The BSA standards were prepared to make up the following concentrations: 0, 0.05, 0.2, 0.5 and 1.0 mg/ml. In duplicate, 25 μ L of each standard and samples were added to a 96-well plate. Reagents A and B (supplied with the kit) were mixed at 50:1 ratio and 200 μ L was added into each well containing the standards and protein samples and thoroughly mixed by careful shaking. The 96-well plate was then incubated at 37 °C for 30 min. The absorbance of each sample was determined at 595 nm and the protein concentration of the homogenates was determined from the standard curve.

2.4.2 SDS-PAGE

Protein samples were mixed with 2X Laemmli buffer at 1:1 ratio to make up to final concentration of 2 μ g/ μ L and boiled for 5 minute to denature. Equal amount of protein was loaded into each well of 12.5 % polyacrylamide gel containing 0.1% SDS and 0.05% ammonium persulfate. Proteins were resolved against a molecular weight marker (MWM) Precision Plus All Blue Protein Standard (10 – 250 kDa) at constant volts (100 V) for approximately 20 min until the protein bands pass the stacking

gel. The voltage was increased to 130 V and run for approximately additional 90 min until the resolving gel runs through.

2.4.3 Western Blotting

Proteins resolved by SDS PAGE were transferred to nitrocellulose membranes (Immobilon) in 1X transfer buffer (refer Table 2-6 for composition) at 0.2 constant Amps and 100 V for 2 hours. Membranes were blocked with 5% skim milk in TBST, pH 7.5 at room temperature for 1.5 hour. After 1.5 hours, the membranes were washed 4 times for 15 min each with TBST. After a series of washings, the membranes were probed with primary antibodies diluted (Table 2-2 for dilution ratio) in 1% skim milk solution for 1 hour at room temperature or overnight at 4 °C. Following probing with primary antibodies, the membranes were again washed 6x for 10 minute each with TBST and probed for secondary antibody (Table 2-3 for dilution ratio) in 1% skim milk in TBST on a rocker at room temperature for 1 hour. The secondary antibodies were removed by a series of washings (6x 10 min) with TBST and final rinsed with 1x TBS. ECL solution was prepared as per manufacturer's instructions and 1 ml was used to cover the whole membrane and left to react for 5 min before chemiluminescent detection using a Typhoon Scanner.

2.5 BHMT1 enzyme activity assay

BHMT1 activity was measured as previously described by Garrow

(Garrow, 1996) with several modifications. The assay contained 5 mM DL-Hcy, 2 mM [¹⁴C]betaine (0.05-0.1 µCi), and 50 mM Tris-HCl (pH 7.5). The final reaction volume was 0.5 ml. To start the assay, tissue homogenate and other assay components were incubated at 37°C for 1 hour. Following the 1-hour incubation, 2.5 ml of ice-cold dH₂O was added and chilled on ice to halt the reaction. 2 ml of the solution was applied to a 2 ml bed volume of Dowex resin 1-x4 (OH⁻; 200-400 mesh) in a Poly-prep column (0.6 × 3.75 cm); the unreacted betaine and DMG were washed from the column with 3x 5 ml water. Methionine was eluted into scintillation vials with 3 ml 1.5M HCL. 5 ml Ultima Gold XR scintillation cocktail was added into each vial and radioactivity measured by a scintillation counter. The Dowex resin 1-x4 Chloride was changed to hydroxyl form prior to the incubation by washing the resin in dH₂O for 15 min and resuspended in 1M NaOH 2x for 10 min followed by water to excess NaOH until pH <9. Protein concentration (1.5 mg) and incubation time (1 hour) were selected according to the linear plot of time and protein concentration.

2.6 Lipid manipulation and analysis

2.6.1 Lipid extraction

Tissue homogenates were transferred into glass tubes and total lipids were extracted with chloroform/methanol (2:1, v/v). 4 ml of chloroform:methanol was added to each 0.75 ml tissue homogenates and mixed thoroughly by vortex for 15 sec and centrifuged at 2000 rpm for 5

min to separate lipid and aqueous phases. The lipid phase was transferred to a new tube using the double pipette technique. The samples were then evaporated under N₂. The lipid residues were dissolved in 100 µl chloroform for TLC or 100 µl 2-propanol for TG assay. For radioactive samples, 100 µg of liver homogenate was added into each sample before the addition of chloroform:methanol step.

2.6.2 Triacylglycerol assay

Lipids extracted in 100 µl 2-propanol from section 2.6.1 were thoroughly mixed by vortex for 15 sec. In duplicate, 20 µl of each sample was added into a 96-well plate followed by the addition of 150 µl Triacylglycerol-Stable Liquid (SL). Samples were carefully mixed by hand shaking the plate. The 96-well plate was then incubated at room temperature for 15 min. TG concentrations were determined by basic endpoint reading according to the standard curve plotted by measuring the absorbance of known concentrations (0 - 2.0 mg/ml) of glycerol stock at 505/660 wavelengths. All assays were performed in duplicate.

2.6.3 Lipid phosphorus assay

Lipids extracted and standards were placed into test tubes and the standards were dried in the heating block in the fume hood at 180 °C for 5 min. 450 µl of perchloric acid were added into each tube and heated at 180 °C for 60 min with tubes covered with marbles. Following the 60 min

heating, the tubes were let cooled before 2.5 ml water was added into each tube. 0.5 ml of 2.5% ammonium molybdate were added and immediately vortexed. 0.5 ml of 10% ascorbic acid were then added and immediately vortexed. Tubes were incubated in 95 °C water bath for 15 minutes, cooled and spinned at 2000 RPM for 5 min. Phospholipid concentrations were determined according to the standard curve plotted by reading the absorbance of known concentrations (0.01 – 2.0 mM) of sodium phosphate at 750nm wavelengths. All assays were performed in duplicate.

2.6.4 Preparation of Oleate Solution

Five g of FA-free BSA were dissolved in serum-free DMEM and the mixture was heated to above 53 °C. After that, 106 mg of OA was heated to 56 °C bath for 2 min. The heated BSA solution was added into OA and stirred vigorously for approximately 2 min until the solution changed from cloudy to relatively clear. The OA/BSA complex was filter-sterilized and stored in aliquots at -20 °C.

2.6.5 Metabolic labeling of lipids

McA cells were grown to 70% confluency in regular DMEM (10% HS + 10% FBS) prior to intracellular lipids labeling. After reaching 70% confluency, cells were incubated in serum-free DMEM containing 0.4 mM [9,10(n)-³H]-oleic acid complexed to 0.4% BSA for 4 hour (pulse). Following this incubation, media were removed by aspiration and cells were washed

with ice-cold PBS and harvested. If a chase study was performed, media was collected and replaced with serum-free DMEM and incubated for 8-16 hrs. Lipids were extracted as described in section 2.6.1. This experiment was performed in 4 replicates.

2.6.6 Thin layer chromatography

Sixty μL of lipids extracted in 100 μL chloroform from (2.6.1.) were spotted onto silica gel TLC plates (Sigma Aldrich). The samples were developed to $\frac{1}{2}$ the height of the plate with solution A (chloroform/ methanol/ acetic acid/ water, 50:30:8:4, v/v) to allow separation of phospholipids. Solution A was incubated in the glass tank for at 2 hours before the plates were added. Following separation, the samples were then developed in solution B (hexane/ diisopropylether/ acetic acid, 65:35:2 v/v) to separate the neutral lipids. The bands of lipid classes were visualized by exposure of TLC plates to iodine vapor and identified by comparing to the migration of lipid standards. For radioactive samples, identified bands were scraped off the plate and transferred into scintillation vials. The band residues were dissolved in 5 ml CytoScint scintillation fluid (ICN Biomedicals) and thoroughly mixed by vortex. Radioactivity incorporated into different lipid classes was counted with a scintillation counter (Beckman LS 6000TA).

2.6.7 Fatty acid oxidation

Cells were cultured in 25 cm² flasks with 20 ml DMEM to approximately ~75% confluency in regular DMEM. The medium was replaced with serum-free DMEM. To collect released ¹⁴CO₂, a filter paper (one-third of a 25-mm circle) was placed in a 1.5 ml eppendorf tube. The tube was then inserted into a rubber stopper, and the stopper was used to seal the flask with the tube facing outward. Using a 1 ml syringe and needle, 0.4 mM [1-¹⁴C]OA complexed to 0.4% BSA was injected into the media through the rubber stopper. The flasks were gently mixed and incubated for 4 hours at 37°C. At the end of the incubation period, the reaction was stopped by adding 1 ml of concentrated perchloric acid into the cells through the rubber stopper. Using a new set of syringe and needle, 1M KOH (0.4ml) was inserted into the filter paper-containing tube. The flasks were incubated for 1 hour, after which the filter paper and the remaining 1M KOH was collected and placed into scintillation vials for quantification. The vials were left overnight before the radioactivity was measured by scintillation counting with 5ml Gold Scintillation fluid.

2.7 Microscopy

2.7.1 Fixation and immunofluorescence staining of hepatocytes

Cells were grown to 70% confluency on a 12mm glass coverslips in a 24-well plate. For colocalization with LDs, cells were incubated with serum-free DMEM containing 0.4 mM OA/BSA complex for overnight. Cells were

washed 3x with ice-cold PBS. 1 ml of 3.7% paraformaldehyde in PBS was added into each well and the plate was incubated at room temperature in the dark for 20 min. At the end of incubation period, cells were again washed with ice-cold PBS and blocked with 1% BSA in 1X PBS at room temperature for 1 hour. Blocking solutions were rinsed off the cells followed by overnight incubation with primary antibodies (Table 2-2 for list of primary Abs) diluted in 1% BSA in PBS at 4°C. Following this incubation, the cells were washed 4x 10 min with PBS and incubated with the appropriate secondary antibody at room temperature for 1 hour (Table 2-3 for list of secondary Abs). Cells were then rinsed with 1X PBS and mounted onto frosted microscope slides using the Prolong Antifade reagent. The edges of the coverslips were sealed with clear nail polish after 4-5 hours of incubation in the dark at room temperature. The slides were sent to Dr. Desmond Pink at the Department of Oncology, University of Alberta for imaging using a confocal microscope.

2.8 Gene expression

Real-time reactions were carried out to analyze key genes regulating lipogenesis, lipid uptake, fatty acid oxidation, and phospholipid and glucose metabolism. Total RNA was isolated from tissue homogenate using Trizol and assessed for RNA quality with an Agilent 2100 bioanalyzer by using an RNA 6000 Nano kit. Samples were treated with DNase I to digest genomic DNA. The RNA was then reverse transcribed using Superscript™ II. Primer

sets and a corresponding probe for each gene of interest were designed using the Universal Probe Library (Roche) based on the NCBI reference nucleotide sequences for *Rattus norvegicus*. qPCR (StepOnePlus, Applied Biosystems) was used to test each primer pair and probe combination. Primer mixes for each gene were combined in a single assay that was used to preamplify the cDNA of the genes of interest in each sample. Preamplification was tested using a probe for cyclophilin by qPCR. Forty-eight gene assays and cDNA samples were loaded into separate wells on a 48-by-48 gene expression chip (Fluidigm) and the qPCR was run on the Biomark system (Fluidigm) for 40 cycles. Relative RNA expression for each gene in a sample was standardized to the endogenous housekeeping gene cyclophilin (*Ppia*) and calculated using the $\Delta\Delta C_T$ method. All assays were performed in triplicate

2.9 Statistical analysis

Statistical differences were determined by One-way ANOVA and Benferroni post test using GraphPad PRISM version 5.0. Data are reported as means \pm SD with $P < 0.05$ indicates significance.

CHAPTER 3

**GENERATION OF STABLE
McARDLE CELL LINES
EXPRESSING BHMT1 AND BHMT2**

3.1 Amplification of BHMT1 and BHMT2 cDNA from rat liver RNA

To check the suitability of rat liver mRNA as template for amplifying genes, BHMT1 and BHMT2 cDNA were generated from the extracted liver RNA by reverse transcription (section 2.2.4) and amplified by PCR (section 2.2.5). Analysis of agarose gel (1.5%) showed that only the PCR products of BHMT1 cDNA was successfully amplified with the expected band size of ~1200 bp (**Figure 3-1**). Although PCR reactions with annealing temperature of 61 °C successfully amplified the 1200 bp fragment, there were no detectable PCR products for BHMT2 with the expected band size of ~1090 bp fragment (**Figure 3-1**). Because the annealing temperature of 61 °C failed to amplify BHMT2 cDNA, another set of PCR reaction using a lower annealing temperature of 58 °C was performed. As **Figure 3-2** shows, there were strong bands of ~1090 bp fragment detected in both rat liver samples. Therein, the optimal annealing temperature for the amplification of BHMT2 cDNA using the designed forward and reverse primers is 58 °C.

3.2 Amplification of HA-tagged rat liver BHMT1 and BHMT2

Results from section 3.1 confirmed the suitability of rat liver mRNA as template for amplifying BHMT1 and BHMT2 genes. For cloning, a different set of primers were designed to include an HA epitope tag on the N-terminus just prior to the start codon of the forward primers of BHMT1

(HA-BHMT1). For BHMT2, the HA epitope was tagged on either the N-terminus (HA-BHMT2) prior to start codon or the C-terminus (BHMT2-HA) just prior to stop codon. HA-epitope tag allows a feasible detection of BHMT1 and BHMT2 proteins using HA-tag specific antibody. The cloning primers were also engineered to include Mlu1 and Not1 restriction enzyme sites sequence in the forward and reverse primer respectively (section 2.2.6). To test the sensitivity of HA-tagged primers, a low scale amplification of HA-BHMT1, HA-BHMT2, and BHMT2-HA were performed using Tag DNA polymerase and analyzed by agarose gel (1.5%) electrophoresis. As shown in **Figure 3-3**, it is apparent that the HA-BHMT1 primer pair successfully amplified HA-BHMT1 cDNA in both rat liver sample 1 and 2 but resulted in higher yield of HA-BHMT1 in rat liver sample 1. Since rat liver sample 1 had higher yield of amplified products, HA-BHMT2 and BHMT2-HA were only amplified from rat liver sample 1. **Figure 3-4** shows that both N-terminal HA and C-terminal HA tag primer pair successfully amplified BHMT2 cDNA.

To facilitate robust amplification of longer DNA fragments, HA-BHMT1, HA-BHMT2, BHMT2-HA cDNAs were amplified using high fidelity DNA polymerase. KAPA Hi-Fi DNA polymerase was chosen due to its high sensitivity. Before proceeding to a large-scale PCR reaction (100 μ L), optimal conditions were first determined using a small-scale PCR reaction (25 μ L). To determine the optimal annealing temperature for the hi-fidelity PCR reaction for HA-BHMT1, annealing temperature of 65 °C and 69 °C

were used as recommended by the manufacturer (KAPA Biosystem). As can be seen in **Figure 3-5**, it appears that the annealing temperature of 65 °C resulted in higher PCR amplification products.

3.3 High-fidelity amplification of HA-BHMT1 and HA-BHMT2

For the amplification of HA-BHMT2 and BHMT2-HA, several high-fidelity PCR reactions were conducted to obtain the optimal annealing temperature. The first trial using the annealing temperature of 65 °C resulted in very low yield of the expected band size (**Figure 3-6**). The second trial with annealing temperature of 68 °C failed to amplify both the N-terminal HA and C-terminal HA tagged BHMT2 cDNAs (data not shown). Therefore, another set of PCR reactions were performed with an annealing temperature in increments of 1 °C. It can be seen from **Figure 3-7** that annealing temperature of 69 °C successfully amplified the N-terminally labeled HA tag but there was no detectable band in the C-terminal HA BHMT2 lane. This is likely due to binding interference of HA epitope at the C-terminus. This experiment was repeated under the same condition and the result obtained confirmed our finding (data not shown). For cloning, large-scale hi-fi PCR reactions were then performed using optimal conditions determined in this section.

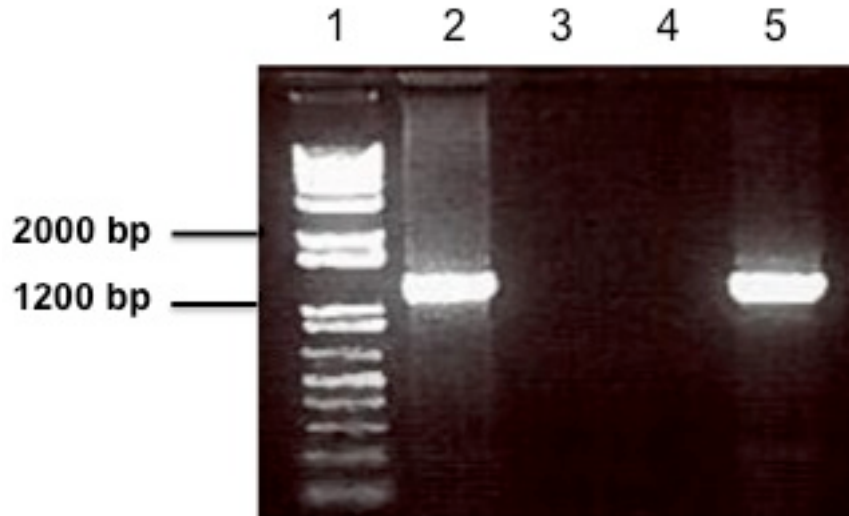


Figure 3-1 Amplified coding sequence of BHMT1 in rat liver sample 1 and 2. Lane 1 shows a 1 Kb DNA ladder. Lane 2 and 5 show cDNA (1217 bp) encoding the entire coding sequence of BHMT1 from rat liver sample 1 and 2 respectively. Lane 3 and 4 show non-detectable BHMT2 cDNA from rat liver sample 1 and 2.

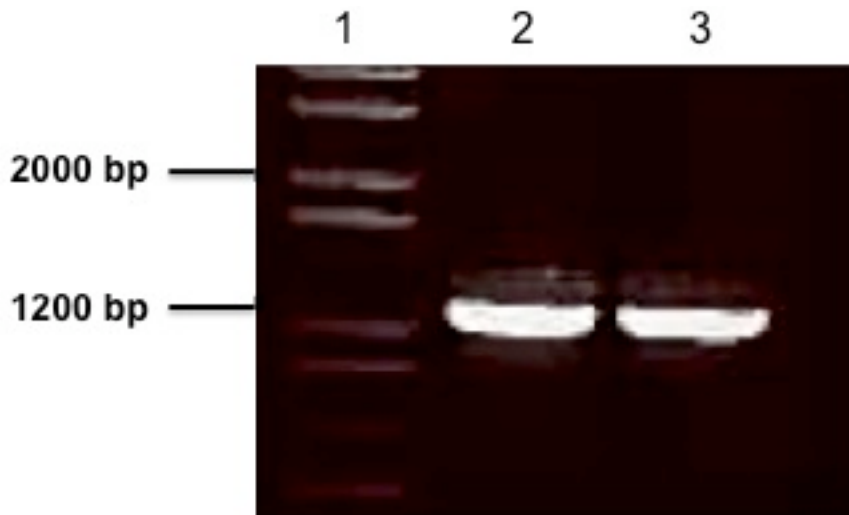


Figure 3-2 Amplified coding sequence of BHMT2 in rat liver sample 1 and 2. Lane 1 shows a 1 Kb DNA ladder. Lane 2 and 3 show cDNA (1091 bp) encoding the entire coding sequence of BHMT2 from rat liver sample 1 and 2 respectively.

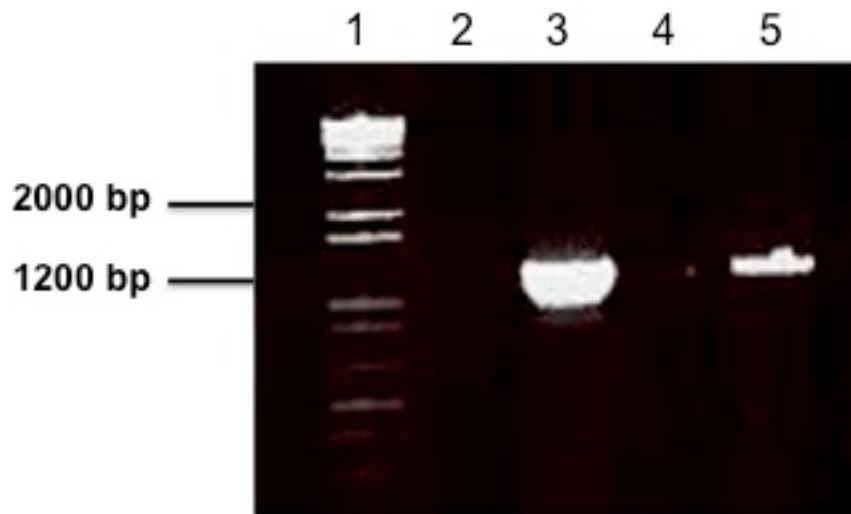


Figure 3-3 Amplified coding sequence of HA-BHMT1 in rat liver sample 1 and 2. Lane 1 shows a 1 Kb DNA ladder. Lane 2 and 4 show controls (without DNA). Lane 3 and 5 show HA-BHMT1 in rat liver sample 1 and 2 respectively.

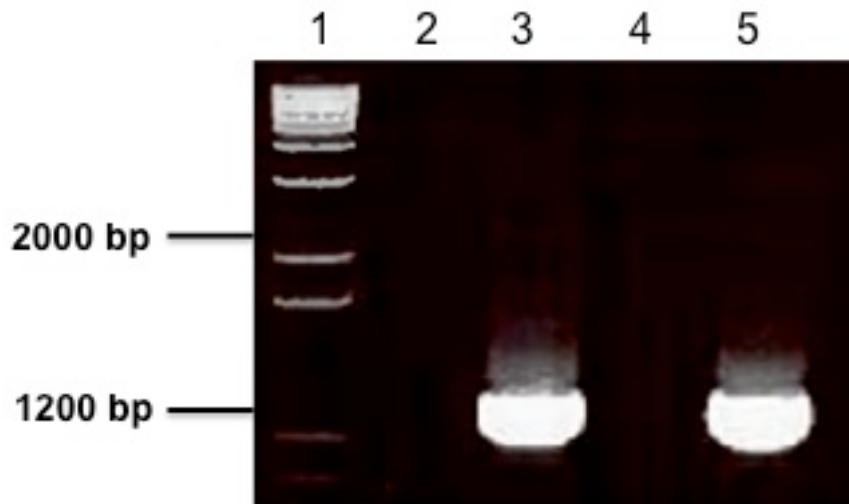


Figure 3-4 Amplified coding sequence of HA-BHMT2 and BHMT2-HA in rat liver sample 1. Lane 1 shows a 1 Kb DNA ladder. Lane 2 and 4 show controls (without DNA). Lane 3 and 5 show HA-BHMT2 and BHMT2-HA in rat liver sample 1 and 2 respectively.

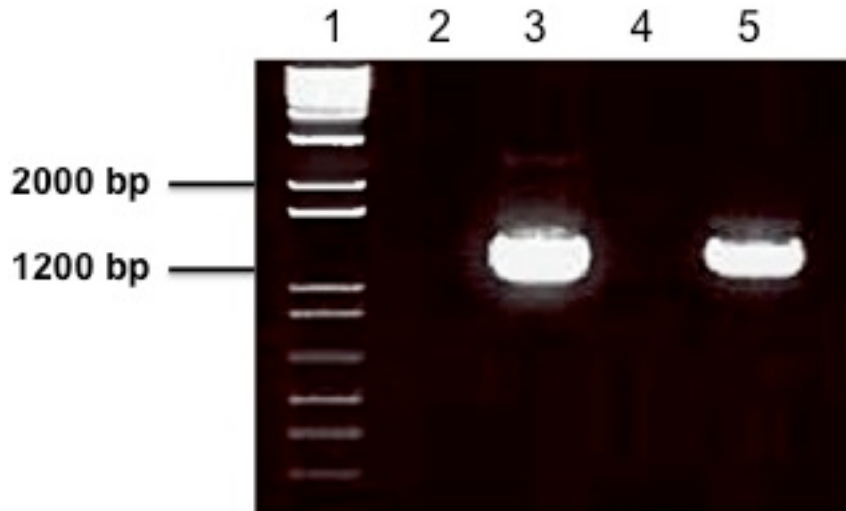


Figure 3-5 Amplified coding sequence of HA-BHMT1 using KAPA Hi-Fi DNA polymerase. Lane 1 shows a 1 Kb DNA ladder. Lane 2 and 4 show control (without DNA) amplified at 65 °C and 69 °C respectively. Lane 3 and 5 show HA-BHMT1 amplified at 65 °C and 69 °C respectively.

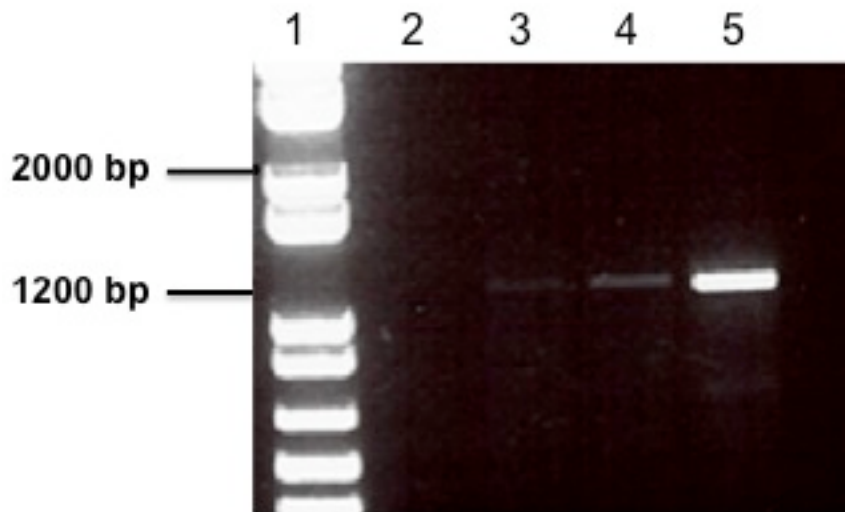


Figure 3-6 Amplified coding sequence of HA-BHMT2 using KAPA Hi-Fi DNA polymerase. Lane 1 shows a 1 Kb DNA ladder. Lane 3 and 4 show N-terminus HA and C-terminus HA BHMT2 amplified at 65 °C annealing temperature, respectively. Lane 5 shows the control BHMT2 without HA epitope tag.

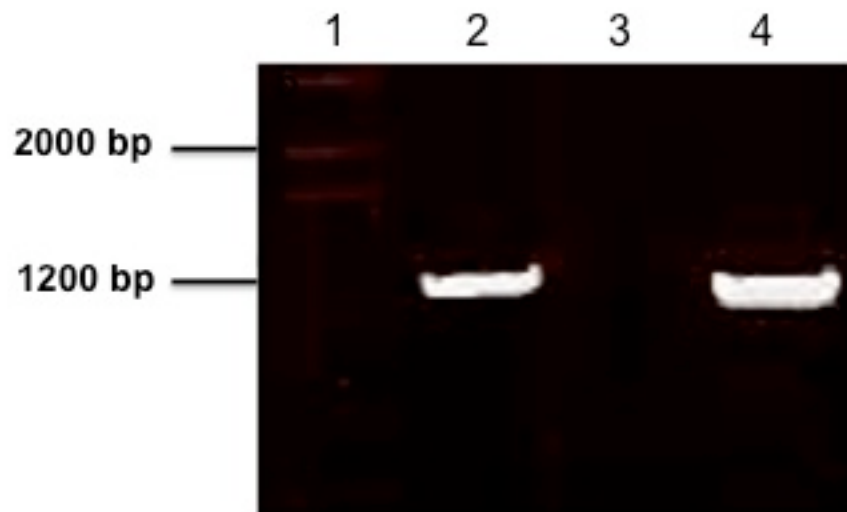


Figure 3-7 Amplified coding sequence of HA-BHMT2 using KAPA Hi-Fi DNA polymerase. Lane 1 shows a 1 Kb DNA ladder. Lane 2 shows N-terminus BHMT2. Lane 3 shows C-terminus HA BHMT2 and lane 4 is the control (BHMT2 without HA epitope tag). All samples were amplified at 69 °C annealing temperature.

3.4 Restriction digestion and ligation of HA-BHMT1, HA-BHMT2 PCR fragments and pCI-Neo Vector

Following the large-scale amplifications of HA-BHMT1 and HA-BHMT2 using KAPA Hi-Fi DNA polymerase, the amplified products were immediately purified using QiaQuick purification kit. Spectrophotometric analysis of quality and quantity of the purified DNA of HA-BHMT1 and HA-BHMT2 was performed as per the manufacturer's recommendation. The absorbance for A260/A280 (quality check) for HA-BHMT1 and HA-BHMT2 were 2.18 and 1.7 respectively and the concentration for HA-BHMT1 and HA-BHMT2 were 0.38 $\mu\text{g}/\mu\text{L}$ and 0.09 $\mu\text{g}/\mu\text{L}$ respectively. The purified products were excised from the PCR fragments by digestion with Mlu1 and Not1 restriction enzymes (section 2.2.7). A pCI-Neo mammalian expression vector was also excised using the same restriction enzymes. Restriction digested PCR fragments were separated by gel electrophoresis and the HA-BHMT1 band, HA-BHMT2 band and pCI-Neo vector band were excised from the gel and DNA purified using QiaQuick gel purification kit. The digested inserts encoding for HA-BHMT1 and HA-BHMT2 were ligated into pCI-Neo vector digested with the same enzymes Mlu1 and Not1. Ligation is an important step for the insertion of the digested HA-BHMT1 and HA-BHMT2 into the digested pCI-Neo vector (pCI-Neo: 5472 bp, HA-BHMT1: 1267 bp and HA-BHMT2: 1135 bp).

3.5 Transformation

Ligation products were transformed into *Escherichia coli* strain DH5 α competent cells (section 2.2.8). Four colonies were randomly picked and cultured overnight in LB broth containing carbenicillin and purified using QiaQuick Miniprep kit according to package instructions. To confirm successful ligation, the recombinant DNA from the 4 selected colonies were subjected to double digestion with *Mlu1* and *Not1* restriction enzymes (section 2.2.9) and analyzed by gel electrophoresis. Expected bands for undigested plasmids are 6739 bp for pCI-Neo (with insert HA-BHMT1) and 6607 bp for pCI-Neo (with insert HA-BHMT2). Restriction digestion of successful cloning by *Mlu1* and *Not1* is expected to produce two bands (pCI-Neo: 5472 bp and HA-BHMT1: 1267 bp or pCI-Neo: 5472 bp and HA-BHMT2: 1135 bp). All four colonies of recombinant HA-BHMT1 showed positive transformants (**Figure 3-8**). For recombinant HA-BHMT2, three out of four colonies screened contain the HA-BHMT2 inserts of expected band sizes (**Figure 3-9**). One positive colony from both recombinant HA-BHMT1 and HA-BHMT2 were purified and sent for sequencing.

3.6 Sequence analysis

Six different sequencing primers, which were strategically designed to sequence both strands of the DNA were used to sequence HA-BHMT1 and HA-BHMT2 (Table 2.5). **Figure 3-10** shows the sequencing map and the placement of corresponding contigs. The contigs were placed so that

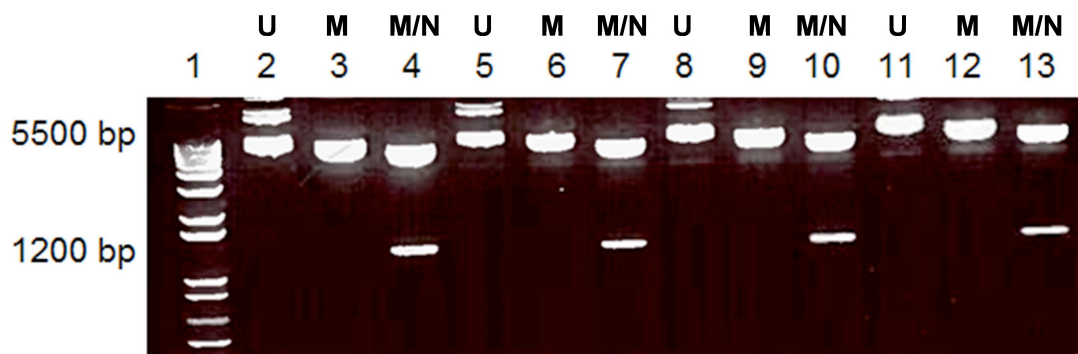


Figure 3-8 PCR-restriction fragment length patterns for BHMT1 obtained after digestion with Mlu1 and Not1. The restriction products were analyzed by 1.5 % agarose gel stained with ethidium bromide. Lane 1 shows a 1 Kb DNA ladder. U Lane 2, 3 and 4 show colonies 1. Lane 5, 6, and 7 show colonies 2. Lane 8, 9 and 10 show colonies 3. Lane 11, 12 and 13 show colonies 4. Three samples of colonies numbered 1-4 were either undigested, single digested (Mlu1) or double digested (Mlu1 and Not1) as labeled. U, undigested; M, Mlu1 digested and M/N; Mlu1 and Not1 double digested.

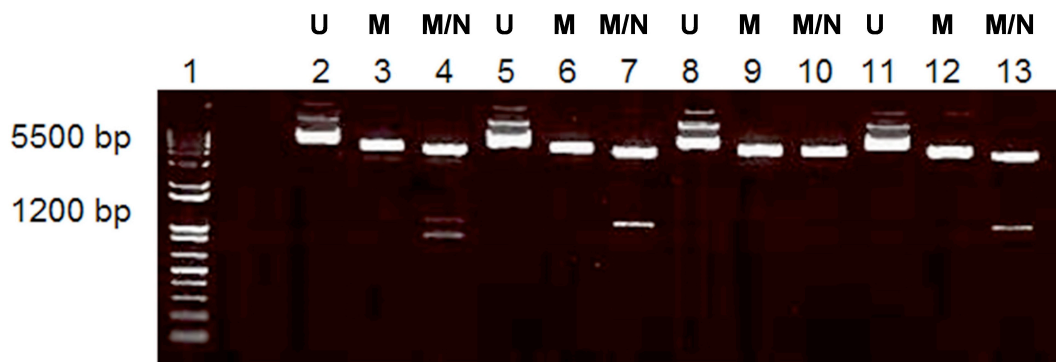


Figure 3-9 PCR-restriction fragment length patterns for BHMT2 obtained after digestion with Mlu1 and Not1. The restriction products were analyzed by 1.5 % agarose gel stained with ethidium bromide. Lane 1 shows a 1 Kb DNA ladder. Lane 2, 3 and 4 show colonies 1. Lane 5, 6, and 7 show colonies 2. Lane 8, 9 and 10 show colonies 3. Lane 11, 12 and 13 show colonies 4. Three samples of colonies numbered 1-4 were either undigested, single digested (Mlu1) or double digested (Mlu1 and Not1) as labeled. U, undigested; M, Mlu1 digested and M/N; Mlu1 and Not1 double digested.

each strand was sequenced in both directions several times throughout the entire length of the gene. The resulting nucleotide sequence is given in **Figure 3-11** and **Figure 3-12**. The results from the sequencing of BHMT1 and BHMT2 were then compared to the published sequence on Genbank sequence database. As shown in **Figure 3-11**, sequencing of BHMT1 resulted in sequence that is in agreement with the sequence published on Genbank database (Accession number: NM_030850.1). However, sequence alignment of our recombinant BHMT2 with the sequence published in Genbank database (Accession number: NM_001014256.2) revealed that there was a discrepancy at 734 base between the sequences obtained from the sequencing of BHMT2 and the Genbank data base (**Figure 3-12**). This sequence discrepancy would cause a proline to leucine substitution in the translated sequence (**Figure 3-13**). There is a possibility that there are several variations of BHMT2 sequence. To confirm, a BLAST search was performed around the nucleotide discrepancy and it was found that there were several nucleotide sequence submissions, either partial or complete for BHMT2 gene. However, the sequence discrepancy at 734 base found in our BHMT2 sequence did not match with any sequence variations available on Genbank database of the NCBI website.

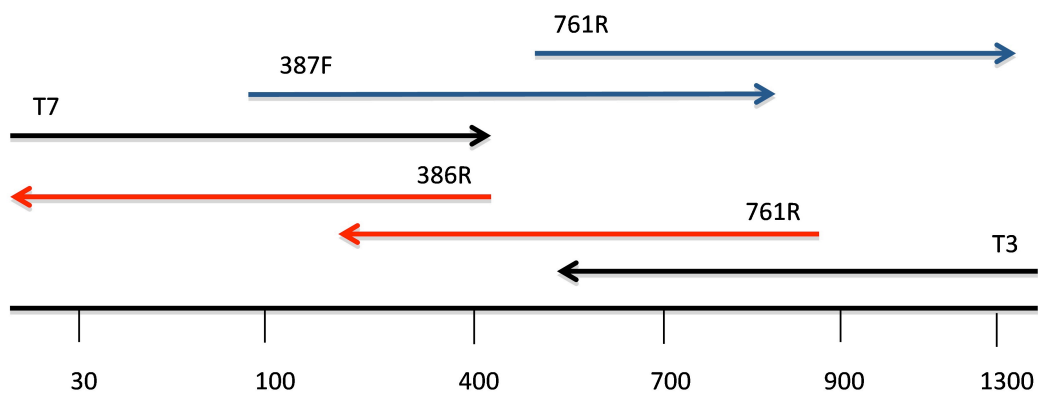


Figure 3-10 Contig map of HA-BHMT1 and HA-BHMT2 sequencing. T3 and T7 act as promoter and terminator sequence, respectively for sequencing towards extremes. The red and blue arrows show the lengths and directions of the sequencing reactions and are labeled according to the sequencing primers used. The length of the entire contig is given in the base pair along the bottom.

```

AGAGAGACGCGTCCACCATGTACCCATACGATGGCACCGATTGCCGGCAAGAAG
GCCAAGAGGGGAATCTTAGAACGCTTAAATGCTGGCGAAGTCGTGATCGGAGAT
GGGGGATTTGTCTTTGCACTGGAAAAGAGGGGCTACGTAAAGGCTGGACCCTGG
ACCCAGAGGCTGCGGTGGAGCACCCCGAGGCAGTTCGGCAGCTTCATCGGGA
GTTCTCAGAGCTGGATCGAACGTCATGCAGACCTTCACTTTCTATGCAAGTGAG
GACAAGCTGGAAAACCGAGGGAACTACGTGGCAGAGAAGATATCTGGGCAGAAG
GTCAATGAAGCTGCTTGTGACATTGCACGGCAAGTTGCTGACGAAGGGGATGCAT
TGGTTGCAGGAGGTGTGAGTCAGACACCTTCTACCTCAGCTGCAAGAGTGAGAC
GGAAGTTAAAAAGATATTTACCAACAGCTTGAGGTCTTCATGAAGAAGAATGTGG
ACTTCCTCATTGCAGAGTATTTTGAACATGTTGAAGAAGCCGTGTGGGCAGTCGA
GGCCTTAAAAACATCCGGGAAGCCTATAGCGGCTACCATGTGCATCGGACCTGAA
GGAGATCTACATGGCGTGTCTCCTGGAGAGTGCGCAGTGCGTTTGGTAAAAGCA
GGTGCCGCCATTGTCGGTGTGAACTGCCACTTCGACCCAGCACCAAGCTTGCAG
ACAATAAAGCTCATGAAGGAGGGTCTGGAAGCAGCTCGGCTGAAGGCTTACTTGA
TGAGCCACGCCCTGGCCTACCACACCCTGACTGTGGCAAACAGGGATTTATTGA
TCTCCAGAAATCCCTTTGGATTGGAACCCAGAGTTGCCACCAGATGGGATATT
CAAAAATACGCCAGAGAGGCCTACAACCTGGGGGTGAGGTACATTGGCGGCTGC
TGCGGATTTGAGCCCTACCACATCAGGGCCATTGCAGAGGAGCTCGCCCCAGAA
AGGGGATTTTTACCACCAGCTTCAGAAAAACATGGCAGCTGGGGAAGTGGTTTGG
ACATGCACACCAAACCCTGGATCAGGGCAAGGGCCAGGAAAGAATACTGGCAGA
ATCTTCGAATAGCTTCGGGCAGACCGTACAATCCTTCGATGTCCAAGCCGGATGC
TTGGGGAGTGACGAAAGGGGCAGCAGAGCTGATGCAGCAGAAGGAAGCCACCA
CTGAGCAGCAGCTGAGAGCGCTCTTCGAAAAACAAAATTCAAATCCGCACAGTA
GGGGGCCGCTCTCTC

```

Figure 3-11 HA-BHMT1 nucleotide sequence. The BHMT1 nucleotide sequence with N-terminal labeled HA epitope tag determined in this study. This sequence was obtained by sequencing both strands of the BHMT1 gene, which was subcloned into pCI-Neo vector. There are 1267 bases in the complete coding sequence including the HA epitope sequence. The start and stop codons are highlighted in yellow.

```
AGAGAGACGCGTCCACCATGTACCCATACGATGGCACCAGCCGGAGGCCACGA
GTCAAGAAGGGTATCTTGGAGCGTCTGGACAGCGGGGAGGTTGTGGTTGGGGAC
GGCGGCTTTCTCTTCACTCTGGAAAAGAGAGGCTTTGTGAAGGCAGGACTTTGGA
CTCCAGAAGCAGTGGTAGAGTATCCAAGTGCAGTTCGTCAGCTTCACACAGAATTC
TTGAGAGCGGGAGCCGATGTCTTGCAGACATTCACCTTTTCGGCTGCTGAAGACA
GAATGGAAAGCAAGTGGGAAGCTGTGAATGCAGCTGCCTGTGACCTGGCCCAGGA
GGTGGCTGATGGAGGGGCTGCTTTGGTGGCAGGGGGCATCTGCCAGACATCACT
GTACAAGTACCACAAGGATGAAACTAGAAATTAACATTTTCCGACTACAGCTAG
GTGTTTTTGGCAGGAAAAATGTGGACTTCTTGATTGCAGAGTATTTTGAGCATGTG
GAAGAAGCCGTGTGGGCTGTGGAAGTCTTGAGAGAGGTGGGGGCACCTGTGGCT
GTGACCATGTGCATCGGCCAGAGGGGGACATGCACGGCGTGACACCGGGAGAG
TGTGCGGTGAGACTGTCTCGTGCAGGGGGCAACATCATTGGGGTAAACTGCCGT
TTGGGCCCTGGACCAGCTTACAGACCATGAAGCTCATGAAGGAGGGCCTCAGGGA
TGCCGGCCTACAAGCTCACCATATGGTCCAGTGCTTGGGTTTCCACACACCGGAC
TGTGGCAAGGGAGGGTTTGTGGACCTTCTGAATATCCTTTCCGGCCTGGAGCCAA
GAGTTGCCACCAGATGGGATATTCAAAAATACGCCAGAGAGGCCTACAACCTGGG
GGTCAGGTACATTGGCGGCTGCTGCGGATTTGAGCCCTACCACATCAGGGCCATT
GCAGAGGAGCTCGCCCCAGAAAGGGGATTTTTGCCACCAGCTTCAGAAAAACATG
GCATCTGGGGAAGTGGTTTGGACATGCACACCAAACCCTGGATCAGAGCAAGGGC
TAGACGGGAATACTGGGAAACTCTGTTGCCAGCTTCGGGAAGACCTTTCTGTCCTT
CCCTATCAAAGCCAGATGCTTGAAGCGGCGCTCTCTC
```

Figure 3-12 HA-BHMT2 nucleotide sequence. The BHMT2 nucleotide sequence with N-terminally labeled HA epitope tag determined in this study. This sequence was obtained by sequencing both strands of the BHMT2 gene, which was subcloned into pCI-Neo vector. There are 1135 bases in the complete coding sequence including the HA epitope sequence. The start and stop codons are highlighted in yellow. The single nucleotide discrepancy at nucleotide 734 is highlighted in red.

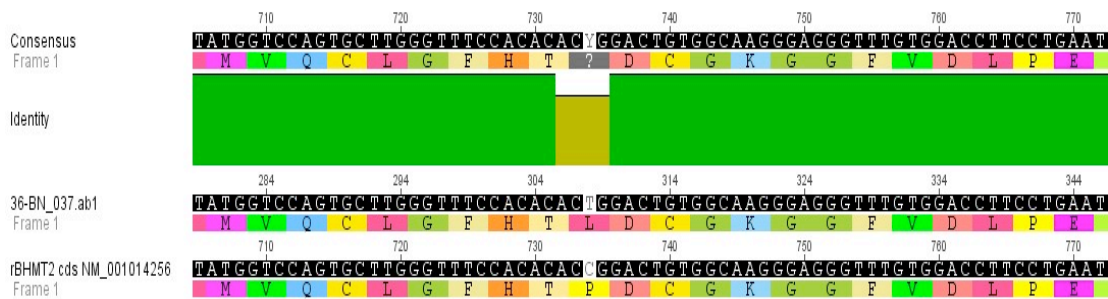


Figure 3-13 Sequence analysis of recombinant BHMT2. A discrepancy at 734 base was identified, which cause a substitution in translated amino acid from proline to leucine. This alignment sequence was generated by Geneious Pro Software.

3.7 Stable transfection of recombinant HA-BHMT1, HA-BHMT2 and pCI-Neo into McA cells

For BHMT1 expression, four McA clones were identified to express the expected band size of ~45 kDa (**Figure 3-14**). For BHMT2, all eight colonies had BHMT2 expression with varying degree of BHMT protein (**Figure 3-14**). One colony from BHMT1 and BHMT2 expressing cell lines were selected and used for the experiments throughout this project. BHMT1 cell colony 9 and BHMT2 cell colony 6 were selected, cultured and denoted cell line **BHMT1** and **BHMT2**, respectively. For the control group, empty vector pCI-Neo was stably transfected into McA and the resulting cell line was denoted **pNeo**.

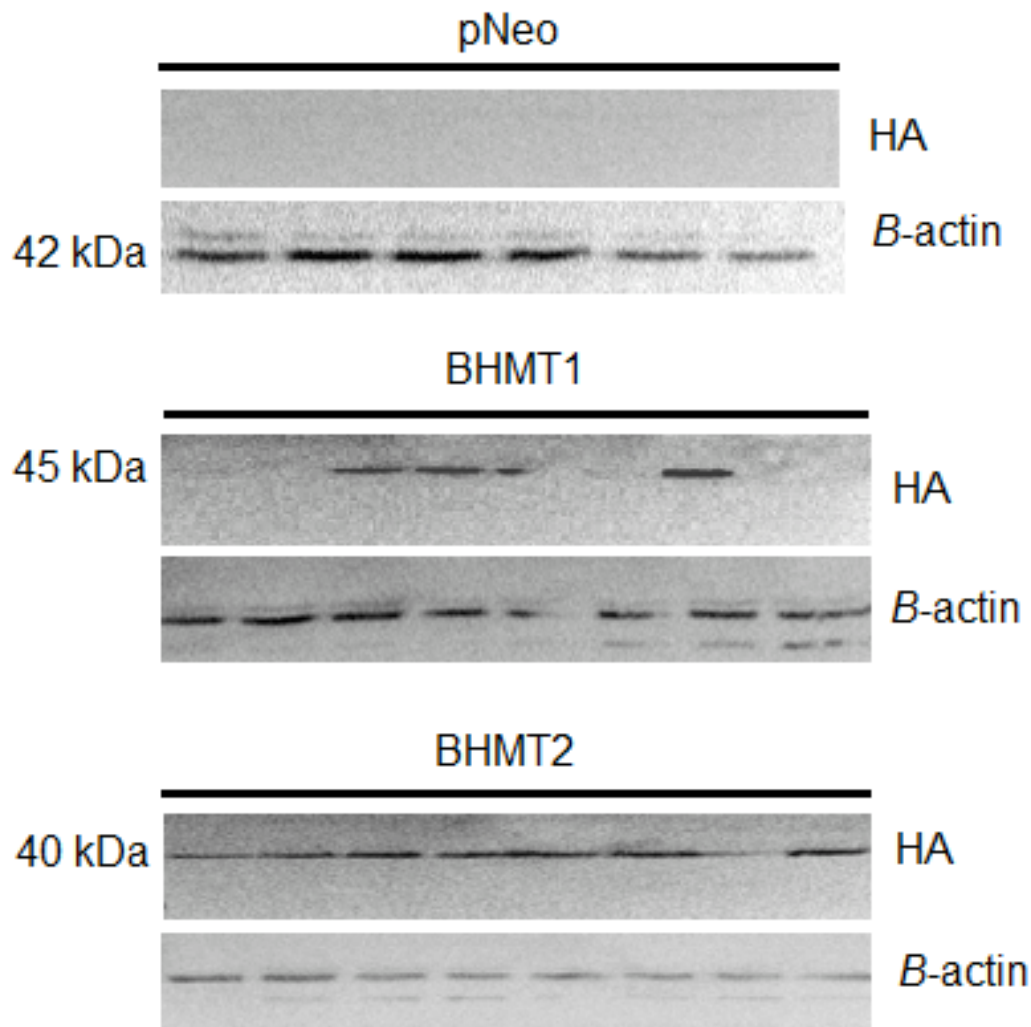


Figure 3-14 Immunoblot of expressed N-terminally tagged HA-BHMT1 and HA-BHMT2. pNeo are cells stably transfected with empty vector, BHMT1 and BHMT2 are cells stably transfected with BHMT1 and BHMT2 cDNA respectively. β -actin was used as the loading control. Out of nine colonies tested for expression only 4 colonies for BHMT1 and 9 colonies for BHMT2 had expression.

CHAPTER 4

ROLE OF BHMT1 AND BHMT2 IN HEPATIC LIPID METABOLISM IN McARDLE CELLS

4.1 BHMT1 activity in stably transfected cell lines

Before proceeding to lipid analysis experiments, BHMT1 cell lines were first tested for enzyme activity. To determine the presence of BHMT1 activity, an assay that utilizes ion-exchange resins was adopted (section 2.5). The enzyme assay was standardized with respect to time and protein concentration. It was determined that the BHMT1 assay was linear to at least 2 mg protein and 60 mins (**Figure 4.1**). On this basis, the time and the protein selected for measuring BHMT1 activity in McA cells were 1 hour and 1.5 mg protein, respectively. Table 4-1 shows that cell line BHMT1 exhibited BHMT1 activity that was absent in pNeo controls. This data shows that BHMT1 activity in homogenates from cultured cells is significantly lower than that present in samples from rat liver. BHMT2 activity in BHMT2 cell line was not tested due to the limited availability of labeled [¹⁴C] SMM.

4.2 Effect of BHMT1 and BHMT2 on TG metabolism in McA cells

To test the hypothesis that BHMT1 and BHMT2 modulate lipid metabolism, we first assessed the effect of substrate availability on TG accumulation in McA cells expressing BHMT1 or BHMT2. McA pNeo, BHMT1 and BHMT2 cells were incubated with 0.4 mM OA and corresponding substrates for 4 hours. The cells were collected for lipid analysis after the 4-hour incubation and lipids were extracted. The medium

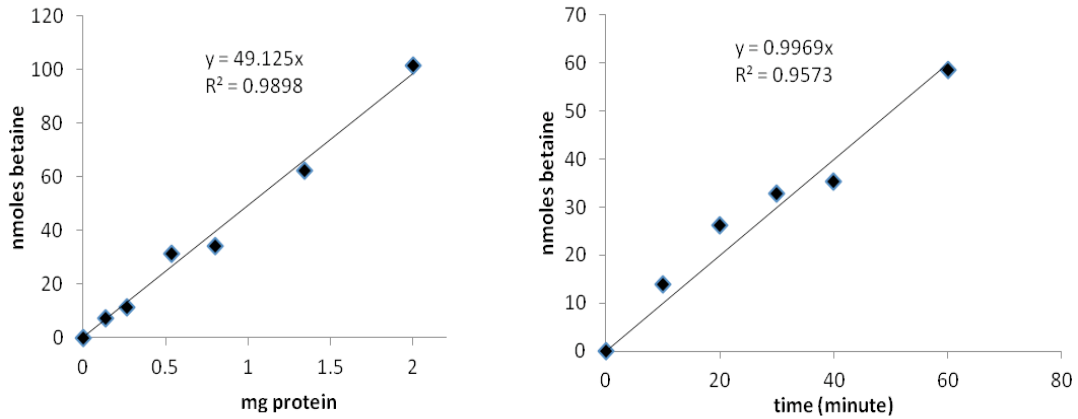


Figure 4-1 Linearity with protein concentration and time for BHMT1 enzyme activity from rat liver (Sprague Dawley) sample. The linear graph for protein concentration was obtained using a 1 hour incubation period. The linearity for time was determined using 1 mg protein.

Table 4-1 Betaine homocysteine S-methyltransferase activity in rat liver, BHMT1 expressing cells (BHMT1) and pNeo control (pNeo). BHMT1 activity in BHMT1 and pNeo was performed using 1.5 mg protein and 1 hour incubation time. Rat liver BHMT1 activity was demonstrated using 1 mg protein and 1 hour incubation time.

Sample	BHMT1 activity (pmoles/min/mg protein)
Rat liver	730
BHMT1	95
pNeo	4.0

(DMEM) used to culture the cells contained 0.03 mM choline chloride that could be oxidized to betaine, the substrate for BHMT1. After the 4-hour incubation with 0.4 mM OA, BHMT1 expressing cell lines accumulated approximately 50% less intracellular TG compared to controls pNeo (**Figure 4-2A**), which is consistent with the hypothesis that BHMT1 reduces hepatic TG accumulation. However, there was no further reduction in TG levels with increasing concentration of betaine supplemented to BHMT1 cells, suggesting that the effects of BHMT1 on TG metabolism in McA cells may not be dose-dependent (**Figure 4-2A**).

Due to high sequence homology with BHMT1, it is hypothesized that BHMT2 may also reduce hepatic TG accumulation. DMEM does not contain SMM, the substrate for BHMT2. Therefore, to determine if SMM treatment would increase BHMT2 activity and consequently alter TG metabolism, a concentration curve of SMM treatment to BHMT2 cell line and control was graphed. Interestingly, there was a trend for decreased cellular TG in response to increased concentration of SMM (2.5 mM) in BHMT2 cell lines compared to the non-treatment groups (**Figure 4-2B**). BHMT2 expressing cells accumulated approximately 14% ($p < 0.05$) less TG compared to controls in 2.5 mM SMM treatment group (**Figure 4-2B**). Since TG level was not altered in control pNeo cells by the inclusion of SMM, the data supports the idea that altered TG metabolism in BHMT2 cells is the result of BHMT2 expression. On this basis, 2.5 mM SMM was selected as the standard concentration supplemented to BHMT2 express-

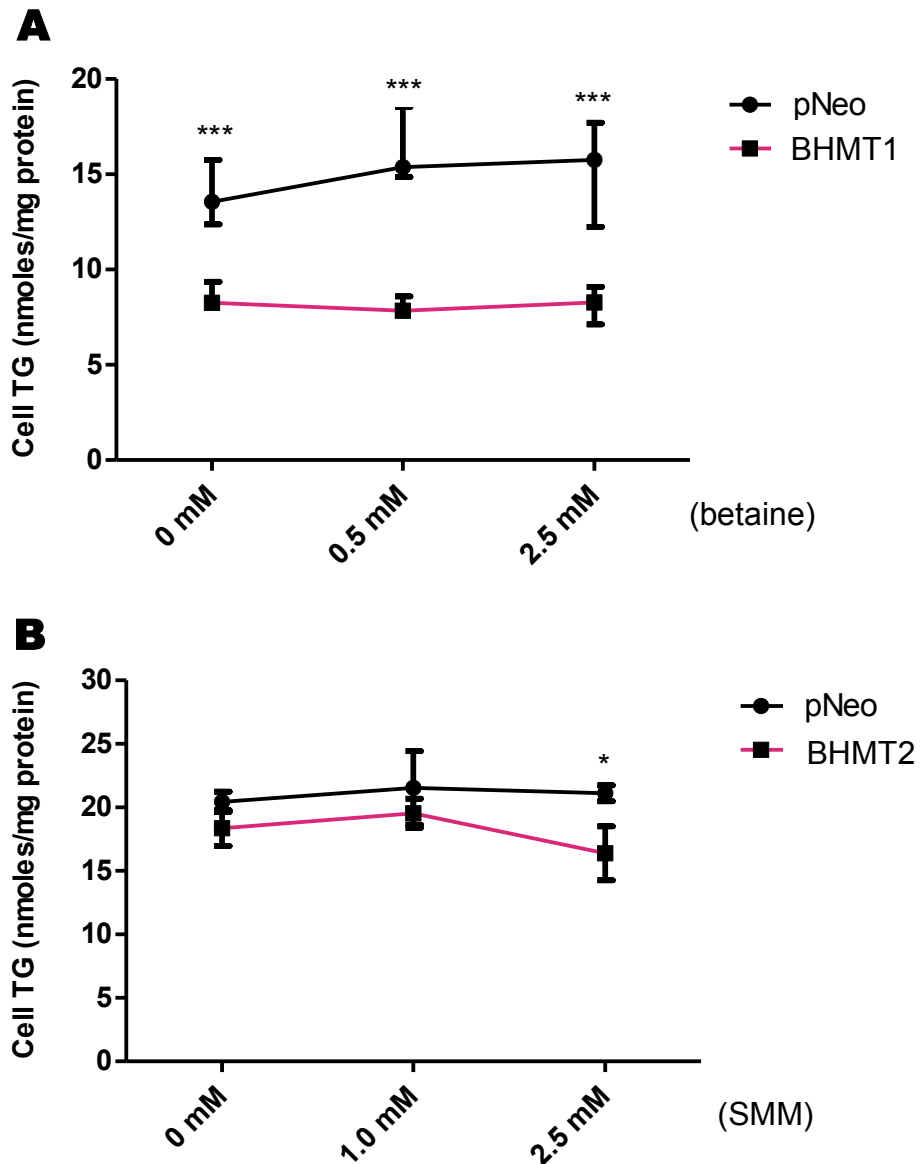


Figure 4-2 Effect of substrate availability on TG accumulation in McA cells expressing BHMT1 or BHMT2. Intracellular TG was measured after treatment increasing levels of betaine to cells expressing BHMT1 (A) or after treatment of increasing levels of SMM to cells expressing BHMT2 (B). Data shown are means \pm SD for $n=4$. * $p<0.05$, ** $p<0.01$, *** $p<0.001$.

ing cells throughout this thesis unless otherwise noted.

In agreement with the hypotheses, data in **Figure 4-2** suggests that expression of BHMT1 or BHMT2 can reduce TG accumulation in McA cells. To further address the effects of BHMT1 and BHMT2 on lipid turnover and secretion, radiolabeled OA pulse/chase experiments were undertaken. In these experiments, pNeo, BHMT1 and BHMT2 cells were incubated with 0.4 mM [³H]OA complexed to 0.4% BSA for 4 hours. Cells were either collected for lipid analysis after the 4-hour pulse with excess OA or incubated with OA-free DMEM for an additional 8-16 hour period (section 2.6.5). In agreement with data from **Figure 4-2A**, after the 4 hour pulse incubation with 0.4 mM [³H]OA, BHMT1 expressing cells accumulated approximately 48% less ($p < 0.001$) intracellular label TG. In contrast, BHMT2 had approximately 27% higher ($p < 0.05$) intracellular label TG relative to controls pNeo (**Figure 4-3A**). This data is the opposite of the mass data (**Figure 4-2B**) where we saw reduction in TG levels in BHMT2 upon treatment with 2.5 mM SMM. During the 8 hour chase period in the absence of exogenous OA, the rate of labeled TG turnover was similar between control and BHMT1 expressing cells, 75% in controls and 70% in BHMT1 expressing cells (**Figure 4-3A**). Furthermore, intracellular TG also decreased almost equally by 85% in control and BHMT1 cells during the 16 hour chase period (**Figure 4-3A**). This finding suggest that TG lowering effect of BHMT1 is only detected with newly synthesized TG, in the presence of exogenous OA but not with preformed TG, which is the stored

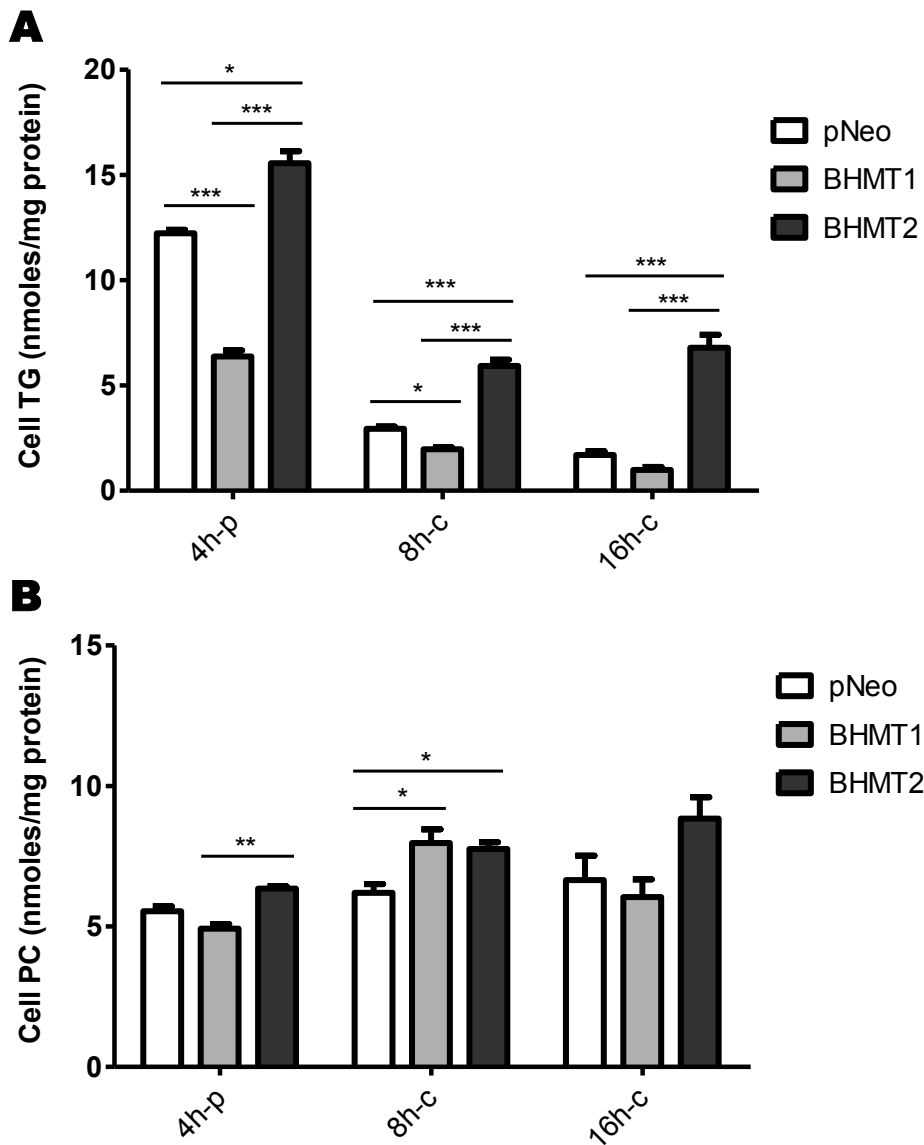


Figure 4-3 [³H]OA pulse-chase experiments in stably transfected McA cells. McA cells stably transfected with empty vector (pNeo), BHMT1 cDNA (BHMT1), and BHMT2 cDNA (BHMT2) were incubated with 0.4 mM [³H]OA/BSA for 4 h (pulse), followed by chase (absence of OA) for 8 and 16 h. Incorporation of [³H]OA into TG (A), PC (B). Data shown are means ± SD for n=3-4 from 3 different experiments. TG, triacylglycerol; PC, phosphatidylcholine. **p*<0.05, ***p*<0.01, ****p*<0.001.

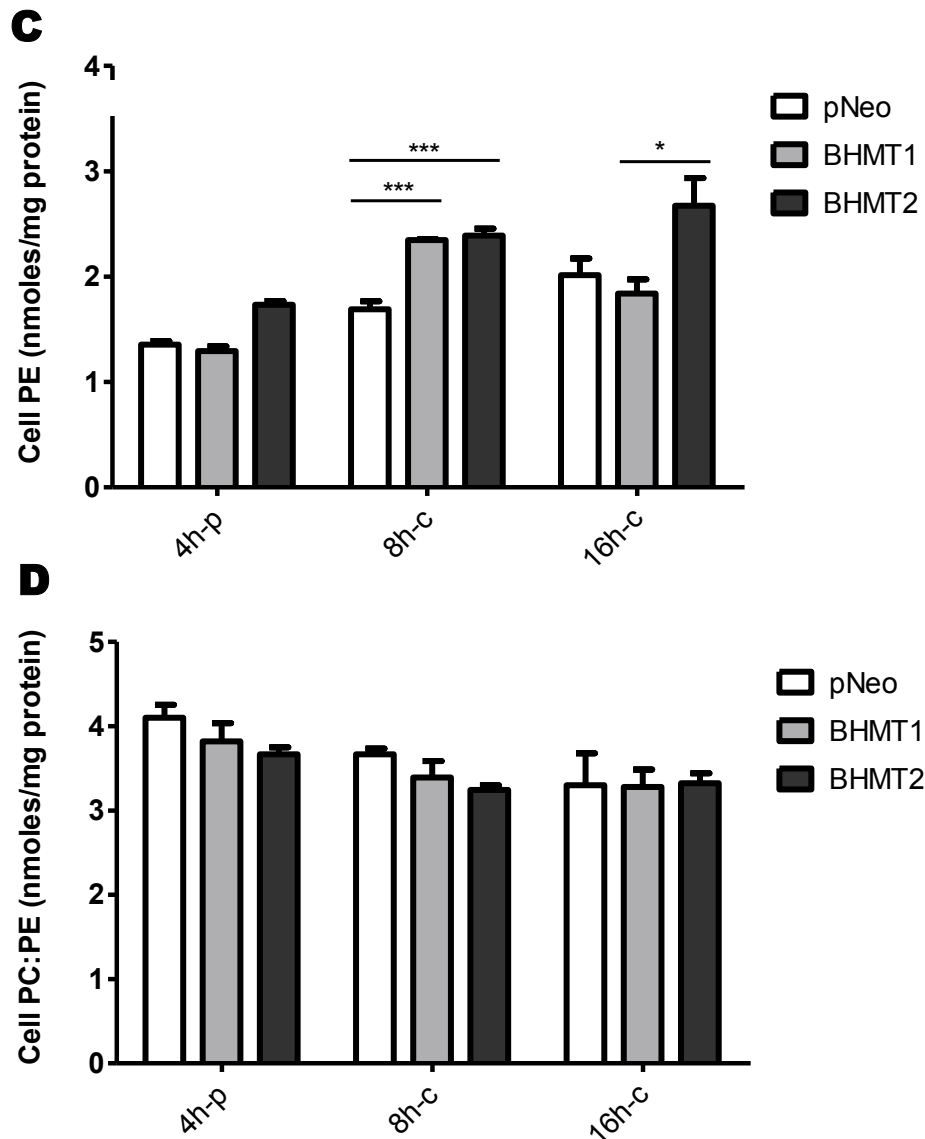


Figure 4-3 [³H]OA pulse–chase experiments in stably transfected McA cells. McA cells stably transfected with empty vector (pNeo), BHMT1 cDNA (BHMT1), and BHMT2 cDNA (BHMT2) were incubated with 0.4 mM [³H]OA/BSA for 4 h (pulse), followed by chase (absence of OA) for 8 and 16 h. Incorporation of [³H]OA into PE (C) and PC/PE ratio (D). Data shown are means ± SD for n=3-4 from 3 different experiments. PC, phosphatidylcholine; PE, phosphatidylethanolamine. **p*<0.05, ***p*<0.01, ****p*<0.001.

TG in the cytosolic LDs. On the other hand, differences were observed in the turnover of TG in BHMT2 expressing cell lines. Relative to controls, BHMT2 turnover was 60% greater during the 8 hour chase period and no further reduction was observed after 16 hour incubation period (**Figure 4-3A**). The incorporation of [³H]OA into glycerophospholipids (PC and PE) were similar among the cell lines during both the chase and pulse period (**Figure 4-3B** and **4-3C**). Consistently, the ratio of PC to PE was not altered (**Figure 4-3D**). To confirm that phospholipid mass was affected in a similar fashion, PC and PE mass was analyzed by phospholipid assay. Data in **Figure 4-4A** and **4-4B** verify that altered TG levels in BHMT1 and BHMT2 cells were not associated with intracellular PC and PE levels, suggesting that altered phospholipid metabolism is unlikely to play an important role in the effect of BHMT1 or BHMT2 on TG metabolism.

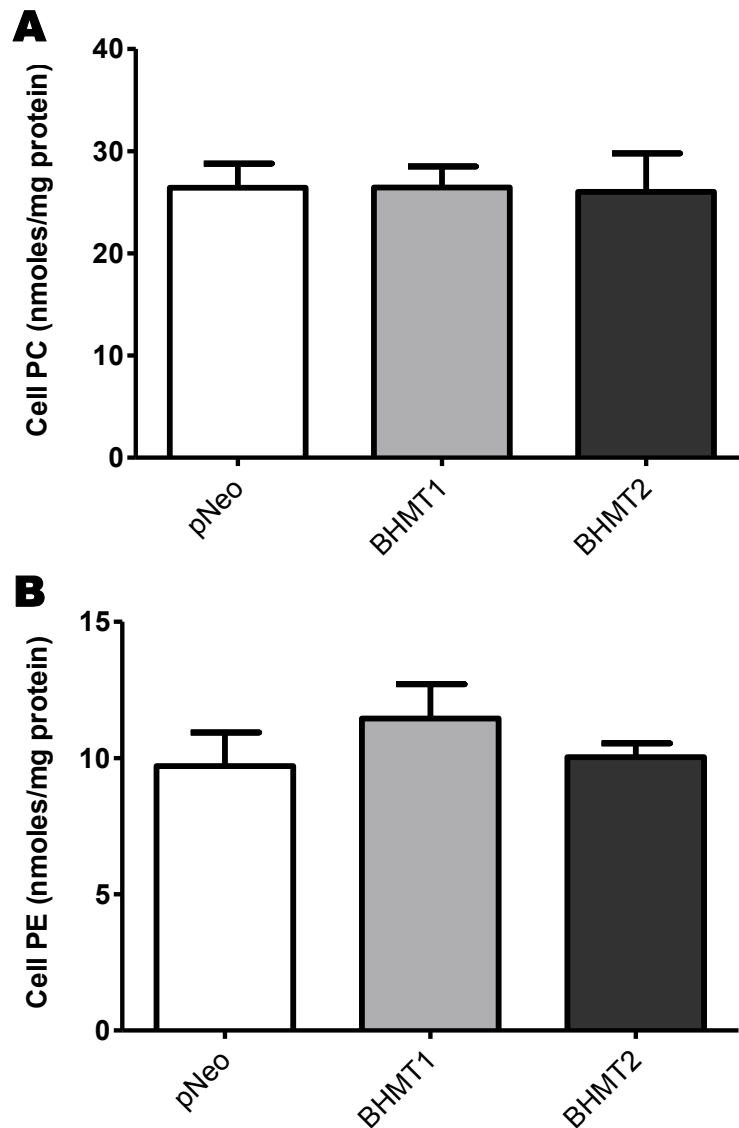


Figure 4-4 Cellular phospholipid mass levels in stably transfected McA cells. McA cells stably transfected with empty vector (pNeo), BHMT1 cDNA (BHMT1), and BHMT2 cDNA (BHMT2) were incubated with 0.4 mM OA/BSA for 4 h. Lipids were extracted and analyzed by thin-layer chromatography as described. The amount of cellular PC (A) and PE (B) was determined by lipid phosphorus assay. Data shown are means \pm SD for n=4.

4.3 Effect of rat BHMT1 and BHMT2 on TG secretion from McA cells

The results from **Figure 4-2A** and **4-3A** suggest that expression of BHMT1 in McA cells reduces the accumulation of intracellular TG levels. To assess whether reduced TG was due to increased secretion, media lipids were analyzed. Surprisingly, analyses of media lipids revealed that after the 4 hour pulse period, TG secretion from both BHMT1 and BHMT2 expressing hepatocytes were comparable to pNeo cell lines (**Figure 4-5A**). Despite accumulating significantly less cellular TG, this data suggest that both BHMT1 and BHMT2 are able to maintain the TG pool destined for secretion, hence other mechanisms are responsible for the reduction. During the chase period, expression of BHMT1 resulted in 47% decrease of TG secretion into the media (**Figure 4-5A**). Since the rate of TG turnover was similar between McA cells expressing BHMT1 and pNeo during both chase periods (8 and 16 hour), it can be speculated that substrate availability was insufficient to maintain TG-containing lipoprotein secretion in BHMT1 cells during the chase period possibly because these substrates were directed towards oxidation.

4.4 Effect of BHMT1 and BHMT2 expression on fatty acid oxidation in McA cells

From the metabolic labeling experiments, it is evident that incorporation of [³H]OA into TG was significantly decreased in McA cells expressing BHMT1. On the other hand, data for BHMT2 expressing cell

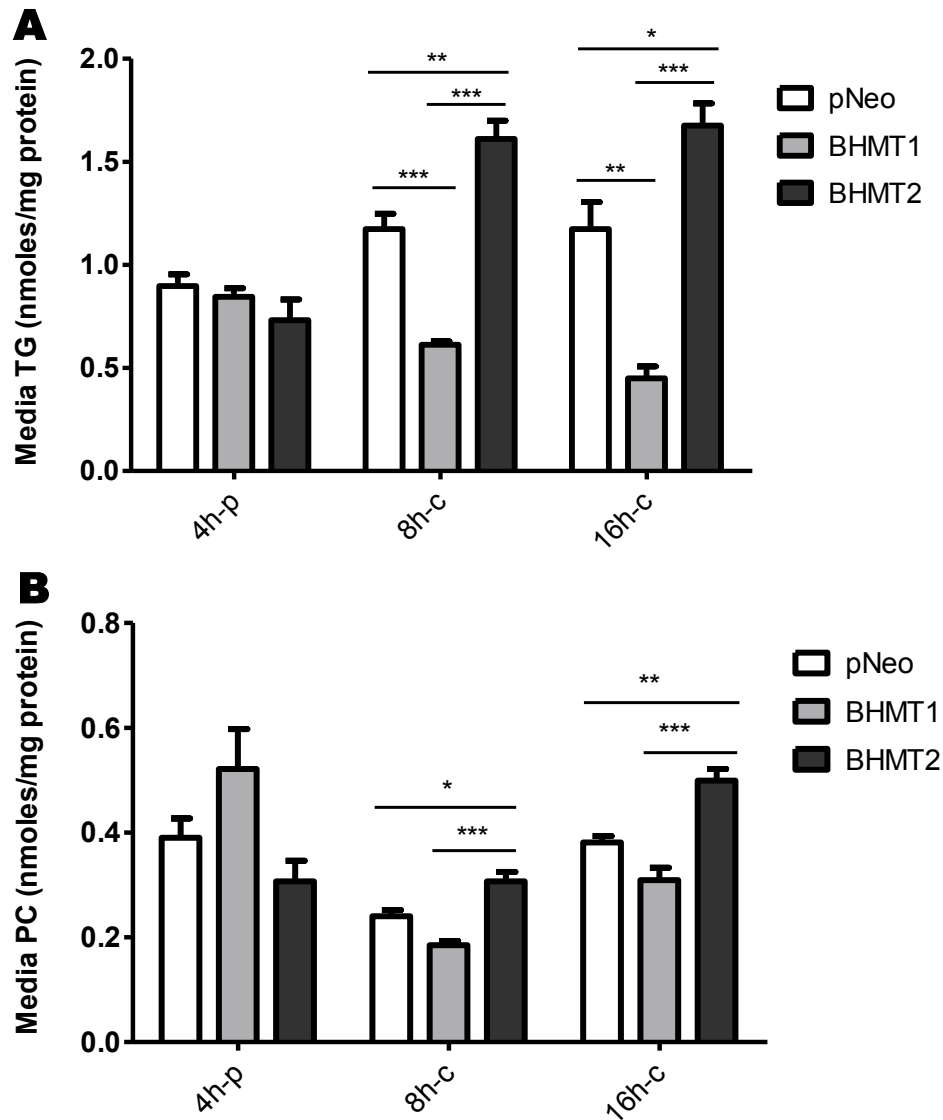


Figure 4-5 [³H]OA pulse-chase experiments in stably transfected McA cells. McA cells stably transfected with empty vector (pNeo), BHMT1 cDNA (BHMT1), and BHMT2 cDNA (BHMT2) were incubated with 0.4 mM [³H]OA/BSA for 4 h (pulse), followed by chase (absence of OA) for 8 and 16 h. Incorporation of [³H]OA into TG (A), PC (B). Data shown are mean ± SD for n=3-4 from 3 different experiments. TG, triacylglycerol; PC, phosphatidylcholine. **p*<0.05, ***p*<0.01, ****p*<0.001.

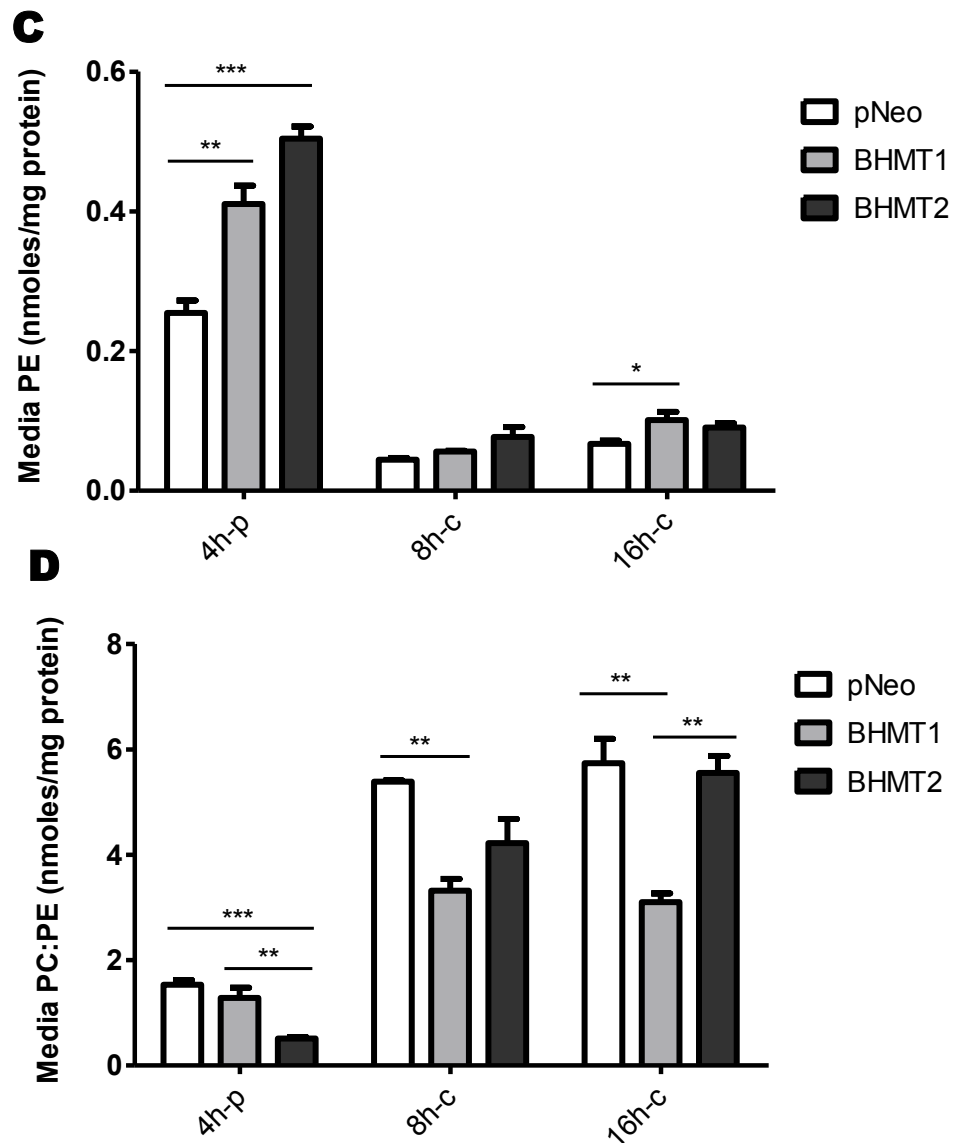


Figure 4-5 [^3H]OA pulse-chase experiments in stably transfected McA cells. McA cells stably transfected with empty vector (pNeo), BHMT1 cDNA (BHMT1), and BHMT2 cDNA (BHMT2) were incubated with 0.4 mM [^3H]OA/BSA for 4 h (pulse), followed by chase (absence of OA) for 8 and 16 h. Incorporation of [^3H]OA into PE (C) and PC/PE ratio (D). Data shown are mean \pm SD for $n=3-4$ from 3 different experiments. PC, phosphatidylcholine; PE, phosphatidylethanolamine. * $p < 0.05$, ** $p < 0.01$, *** $p < 0.001$.

lines produced mixed results. Despite significant reduction in label intracellular TG content in BHMT1 cells, analysis of media lipid revealed that TG secretion was similar in all cell lines, suggesting an involvement of a different pathway. Another possible fate for TG is that it can be hydrolyzed by hepatic lipases and the FAs directed towards the mitochondria or peroxisome for oxidation. To measure FA oxidation in cells, the amount of $^{14}\text{CO}_2$ produced at the end of 4 hour chase experiment with 0.4 mM [^{14}C]OA/BSA was quantified. McA cells expressing BHMT1 exhibit significantly increased FA oxidation rate (1.65 fold) compared to control cells (**Figure 4-6**). This data suggest that BHMT1 decreases intracellular TG levels and increases delivery of FAs for β -oxidation, thus partially explains TG lowering effect of BHMT1. On the other hand, BHMT2 expressing cell lines had a 1.36-fold increase in oxidation rate as compared to controls (**Figure 4-6**). This result is consistent with the reduction in TG levels observed in BHMT2 cells from **Figure 4-2B**, but could not explain the data from the metabolic labeling experiment in which there was increased TG accumulation and secretion (**Figure 4-3A**).

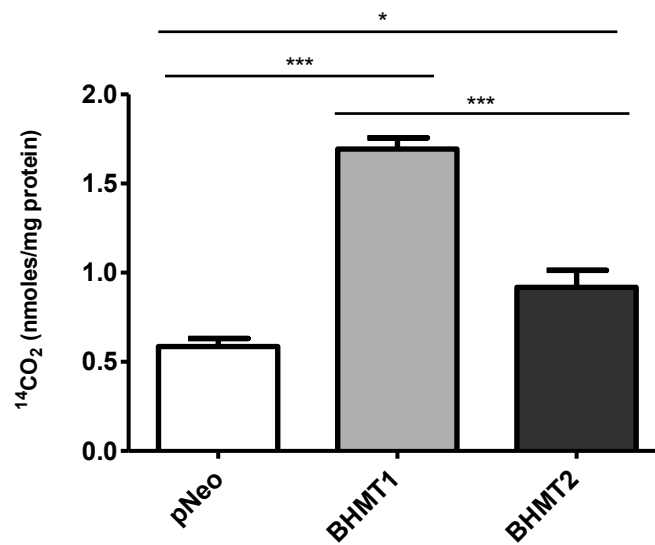


Figure 4-6 β -oxidation in stably transfected McA cells. McA cells stably transfected with empty vector (pNeo), BHMT1 cDNA (BHMT1), and BHMT2 cDNA (BHMT2) were incubated with 0.4 mM [¹⁴C]OA/BSA for 4 h. Radioactivity of ¹⁴CO₂ was measured by scintillation counting. Data shown are means \pm SD for n=4. * p <0.05, ** p <0.01, *** p <0.001.

4.5 Effect of BHMT1 and BHMT2 expression on lipid metabolism related gene-expression

To investigate the role of BHMT1 and BHMT2 in hepatic lipid metabolism in McA cells, total RNA was isolated and the expression of genes involved in lipogenesis, lipid uptake, fatty acid oxidation, phospholipid and glucose metabolism were examined by real-time quantitative PCR assays. The expression of *GPAT1* and *DGAT2* was significantly reduced in both BHMT1 and BHMT2 cells (Table 4-8). The expression of *MGAT1* was downregulated in McA cells expressing BHMT1 but not in BHMT2. This finding suggests that hepatic TG synthesis occurs from both major pathways; the MG and G-3-P pathways were reduced in BHMT1 expressing cell lines whereas only the G-3-P pathway was affected in BHMT2 expressing cells. It is possible that down-regulation of these genes impaired TG synthesis which could lead to reduced TG mass accumulation observed in both BHMT1 and BHMT2 expressing McA cells (Figure 4-2A and 4-2B). It is important to note that no significant changes were observed in the abundance of other TG biosynthesis genes such as *MGAT2*, *AGPAT2* and *LIPIN1* (Table 4-2).

Next, we sought to determine whether genes related to lipoprotein transport were altered by BHMT1 or BHMT2 expression. Previously, Sparks et al. (1999) showed that BHMT1 expression in McA cells increased ApoB mRNA and secretion; however, in this study the opposite was observed. ApoB expression was slightly decreased in both BHMT1 and BHMT2 cells (Table 4-3). Consistent with lower accumulation of intracellular TG, mRNA

levels of *ADRP*, LD associated protein was decreased approximately 2-fold in BHMT1 cells and to a lesser extent in BHMT2 expressing McA cells (Table 4-3). Furthermore, the expression of *ACAT* was almost undetectable in BHMT1 and significantly lower in BHMT2 cells, suggesting reduced cholesterol-ester storage in these cells. Although the mRNA levels of key transcription factor regulating fatty acid oxidation, *PPAR α* , (Table 4-4) was downregulated in BHMT1 cells, the expression of its downstream targets *CD36* and *CPT1* were not affected (Table 4-4). This may suggest that the rate of fatty acid uptake into the cell and the mitochondria was not altered. However, the expression of *VLCAD* and *ACOX* were upregulated in these cells suggesting increased oxidation of long chain fatty acid. The mRNA levels for other dehydrogenases including *MCAD* and *LCAD* were not affected by BHMT1 expression (Table 4-4). Augmented expression of several FA oxidative genes is consistent with the increased production of $^{14}\text{CO}_2$ in the BHMT1 transfected cells (**Figure 4-6**) and potentially provide another explanation to the lack of TG accumulation observed in this cells as compared to pNeo controls. BHMT2 expressing cells had reduced *CD36* expression, an indication of lower FA uptake into the cell but similar to BHMT1, they showed greater expression of *VLCAD* and *ACOX* relative to controls (Table 4-4). In this study, altered TG metabolism in both McA cells expressing BHMT1 and BHMT2 may not be associated with altered FA synthesis as most of the important genes involved in this process including *ACC*, *MCD* and *FAS* were not changed (Table 4-5).

According to the mass and metabolic labeling studies discussed previously, phospholipid levels including PC and PE were not altered in all groups. Consistently, measurement of key genes involved in phospholipid synthesis revealed no significant change in *CKa*, *CKb*, and *CTa* (Table 4-6). This finding further supports the notion that phospholipid levels may not play an important role in the TG lowering effect of BHMTs. A very noticeable change in genes encoding for *PEPCK* and G6Pase was observed primarily in BHMT1 cells and to a lesser extent in BHMT2 cell lines (Table 4-7), suggesting altered glucose metabolism. It is important to note that no significant changes were detected for several other key transcription factors including *SREBP1*, *SREBP2*, and *LXR α* (Table 4-8).

Table 4-2 mRNA levels of genes involved in TG synthesis in pNeo, BHMT1, and BHMT2 cell lines

mRNA	pNeo	BHMT1	BHMT2
<i>MGAT1</i>	1.00 ± 0.03 ^a	0.61 ± 0.06 ^b	1.00 ± 0.21 ^a
<i>MGAT2</i>	1.00 ± 0.15	0.74 ± 0.09 ^a	1.36 ± 0.31 ^b
<i>DGAT1</i>	1.00 ± 0.10 ^a	1.36 ± 0.09 ^b	1.90 ± 0.21 ^c
<i>DGAT2</i>	1.00 ± 0.06 ^a	0.59 ± 0.04 ^b	0.59 ± 0.14 ^b
<i>GPAT1</i>	1.00 ± 0.09 ^a	0.46 ± 0.08 ^b	0.66 ± 0.13 ^b
<i>AGPAT2</i>	1.00 ± 0.02	1.14 ± 0.11	1.12 ± 0.30
<i>LIPIN1</i>	1.01 ± 0.12	1.04 ± 0.21	0.74 ± 0.11

* Values are relative mRNA expression, standardized to cyclophilin, given as means ± SD, n = 6. Different superscripts within a horizontal row represent significant difference, $P < 0.05$. Abbreviations: MGAT1, monoacylglycerol O-acyltransferase 1; MGAT2, monoacylglycerol O-acyltransferase 2; DGAT1, diacylglycerol O-acyltransferase 1; DGAT2, diacylglycerol O-acyltransferase 2; GPAT1, glycerol-3-phosphate acyltransferase 1; AGPAT2, 1-acyl-sn-glycerol-3-phosphate acyltransferase 2; LIPIN1, phosphatidate phosphatase 1.

Table 4-3 mRNA levels of genes involved in cholesterol and lipoprotein metabolism in pNeo, BHMT1, and BHMT2 cell lines

mRNA	pNeo	BHMT1	BHMT2
<i>ApoB</i>	1.11 ± 0.19 ^a	0.73 ± 0.10 ^b	0.72 ± 0.11 ^b
<i>MTTP</i>	1.00 ± 0.09	1.28 ± 0.11	1.69 ± 0.56
<i>ACAT</i>	1.00 ± 0.09 ^a	0.04 ± 0.02 ^b	0.17 ± 0.11 ^b
<i>LDLR</i>	1.01 ± 0.20	1.31 ± 0.20 ^a	0.75 ± 0.19 ^b
<i>ADRP</i>	1.08 ± 0.19 ^a	0.55 ± 0.08 ^b	0.61 ± 0.14 ^b

* Values are relative mRNA expression, standardized to cyclophilin, given as means ± SD, n = 6. Different superscripts within a horizontal row represent significant difference, $P < 0.05$. Abbreviations: ApoB, apolipoprotein B; MTTP, microsomal triacylglycerol transfer protein; ACAT, acyl-CoA:cholesterol acyltransferase; LDLR, low-density lipoprotein receptor; ADRP, adipose differentiation-related protein.

Table 4-4 mRNA levels of genes involved in fatty acid oxidation in pNeo, BHMT1, and BHMT2 cell lines

mRNA	pNeo	BHMT1	BHMT2
CD36	1.00 ± 0.09 ^a	0.95 ± 0.08 ^a	0.51 ± 0.20 ^b
CPT1a	1.01 ± 0.19	1.01 ± 0.11	0.91 ± 0.25
MCAD	1.00 ± 0.09	1.27 ± 0.08	1.73 ± 0.77
LCAD	1.00 ± 0.04	1.17 ± 0.05	1.31 ± 0.35
VLCAD	1.00 ± 0.12 ^a	1.63 ± 0.15 ^b	1.76 ± 0.39 ^b
ACOX	1.00 ± 0.15 ^a	1.62 ± 0.15 ^b	1.36 ± 0.33 ^b
FATP4	1.00 ± 0.04 ^a	0.80 ± 0.11	0.72 ± 0.18 ^b

* Values are relative mRNA expression, standardized to cyclophilin, given as means ± SD, n = 6. Different superscripts within a horizontal row represent significant difference, $P < 0.05$. Abbreviations: CD36, fatty acid transport protein; CPT1a, liver carnitine palmitoyltransferase1; MCAD, medium chain acyl-coA dehydrogenase; LCAD, long chain acyl-coA dehydrogenase; VLCAD, very long chain acyl-coA dehydrogenase; ACOX, peroxisomal acyl-coenzyme A oxidase; FATP4, fatty acid transport protein 4.

Table 4-5 mRNA levels of genes involved in fatty acid synthesis in pNeo, BHMT1, and BHMT2 cell lines

mRNA	pNeo	BHMT1	BHMT2
<i>ACC</i>	1.01 ± 0.17	0.85 ± 0.19	1.10 ± 0.14
<i>MCD</i>	1.00 ± 0.08	0.82 ± 0.06 ^a	1.22 ± 0.19 ^b
<i>FAS</i>	1.31 ± 0.85	0.93 ± 0.72 ^a	2.79 ± 0.82 ^b
<i>SCD1</i>	1.00 ± 0.13 ^a	0.69 ± 0.11 ^b	0.66 ± 0.11 ^b

* Values are relative mRNA expression, standardized to cyclophilin, given as means ± SD, n = 6. Different superscripts within a horizontal row represent significant difference, $P < 0.05$. Abbreviations: ACC, acetyl-coA carboxylase; MCD, malonyl-coA decarboxylase; FAS, fatty acid synthase; SCD1, stearoyl-coenzyme A desaturase 1.

Table 4-6 mRNA levels of genes involved in phospholipid metabolism in pNeo, BHMT1, and BHMT2 cell lines

mRNA	pNeo	BHMT1	BHMT2
CKa	1.01 ± 0.16	1.21 ± 0.09	2.92 ± 0.43
CKb	1.00 ± 0.09	0.10 ± 0.06	1.25 ± 0.57
CTa	1.01 ± 0.16	0.76 ± 0.16	1.04 ± 0.21

* Values are relative mRNA expression, standardized to cyclophilin, given as means ± SD, n = 6. Different superscripts within a horizontal row represent significant difference, $P < 0.05$. Abbreviations: CKa, choline kinase alpha; CKb, choline kinase beta; CTa, CTP:phosphocholine cytidyltransferase alpha.

Table 4-7 mRNA levels of genes involved in glucose metabolism in pNeo, BHMT1, and BHMT2 cell lines

mRNA	pNeo	BHMT1	BHMT2
<i>PEPCK</i>	1.01 ± 0.19 ^a	4.98 ± 0.50 ^b	2.75 ± 0.72 ^c
<i>G6PASE</i>	1.00 ± 0.05 ^a	5.47 ± 1.08 ^b	4.33 ± 0.94 ^b
<i>PK</i>	1.01 ± 0.18 ^a	1.12 ± 0.18 ^a	1.88 ± 0.34 ^b

* Values are relative mRNA expression, standardized to cyclophilin, given as means ± SD, n = 6. Different superscripts within a horizontal row represent significant difference, $P < 0.05$. Abbreviations: PEPCK, phosphoenolpyruvate-carboxykinase; G6Pase, glucose-6-phosphatase; PK, pyruvate kinase.

Table 4-8 mRNA levels of key transcription factors involved in lipid metabolism in pNeo, BHMT1, and BHMT2 cell lines

mRNA	pNeo	BHMT1	BHMT2
<i>PPARa</i>	1.03 ± 0.30 ^a	0.61 ± 0.08 ^b	1.03 ± 0.16 ^a
<i>LXRa</i>	1.00 ± 0.06	1.25 ± 0.13 ^a	1.40 ± 0.24 ^b
<i>SREBP1</i>	1.025 ± 0.26	1.01 ± 0.25	0.92 ± 0.16
<i>SREBP2</i>	1.04 ± 0.35	0.92 ± 0.40	2.29 ± 0.94

* Values are relative mRNA expression, standardized to cyclophilin, given as means ± SD, n = 6. Different superscripts within a horizontal row represent significant difference, $P < 0.05$. Abbreviations: PPARa, peroxisome proliferator-activated receptor alpha; LXRa, liver X receptor alpha; SREBP1, sterol regulatory element binding protein 1; SREBP2, sterol regulatory element binding protein 2.

4-6 Co-localization of BHMT1 or BHMT2 with Lipid droplets

Recent evidence from a shotgun proteomic analysis of the cytosolic LDs fraction further demonstrated the enrichment of enzymes associated with one-carbon metabolism pathway specifically BHMT on the purified LDs (Crunk et al., 2013). To address whether BHMT1 or BHMT2 associated with LDs, we examined intracellular localization of tagged BHMT by immunofluorescence. Although McA cells are capable of forming LD from serum that is present in the medium, the number may be insufficient. To enhance LD formation and facilitate detection, we supplemented the cells with 0.4 μ M oleate. LD size and number is substantially increased following supplementation with additional lipids. Images of McA cells expressing BHMT1 or BHMT2 immunostained using primary antibody against HA-protein and against ADRP, a LD specific marker and secondary antibody conjugated with red or green fluorophore were captured by confocal microscopy. The merge box revealed white signals surrounding LDs as the result of co-localization with ADRP (**Figure 4-7 and 4-8**). The formation of ring-like patterns enveloping LDs of various sizes further suggests that these proteins also associate with LDs (**Figure 4-9**). Our data thus suggest a significant co-localization of BHMT proteins with LDs, with a greater percentage of BHMT1 co-localizes to the LDs more so than BHMT2. Whether this association serves as an important regulatory role for BHMT in hepatocytes metabolic processes warrants further studies.

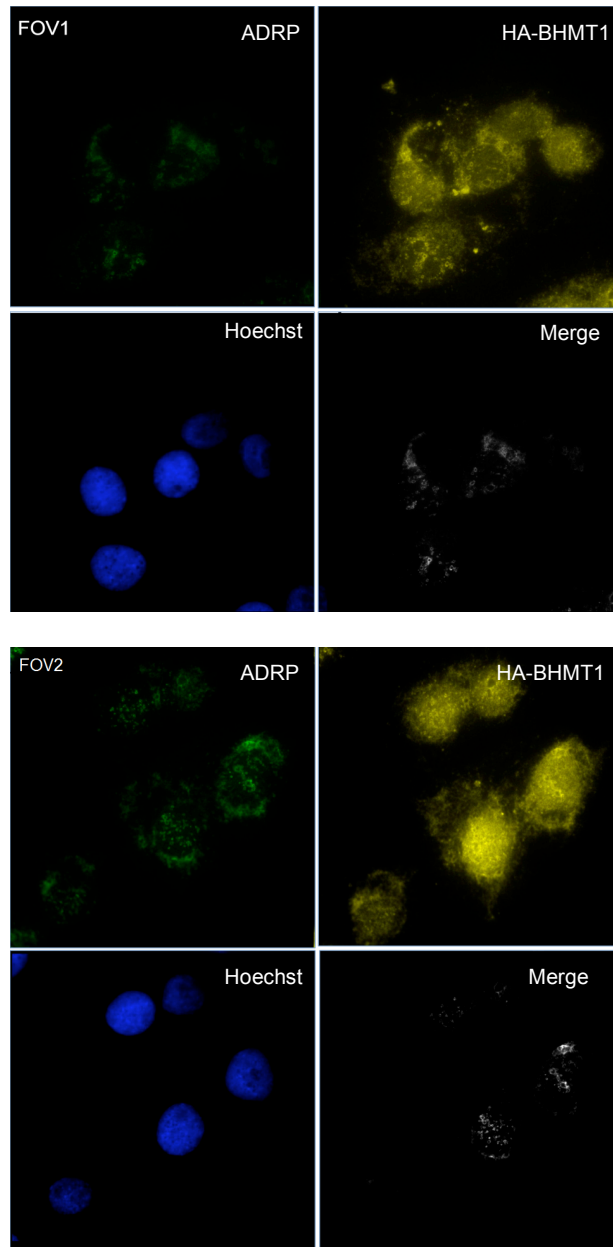


Figure 4-7 BHMT1 is localized to LDs. McA cells transfected with pNeo empty vector or HA-BHMT1 were grown in DMEM containing 0.4 mM OA/BSA overnight to enhance the formation of LDs. Association of HA-BHMT1 with LDs was determined by co-localization with ADRP immunostained with anti-ADRP antibodies. The nucleus was stained with Hoechst. FOV, field of view; ADRP, adipose-differentiation-related protein; HA, hemagglutinin, BHMT, betaine homocysteine S-methyltransferase.

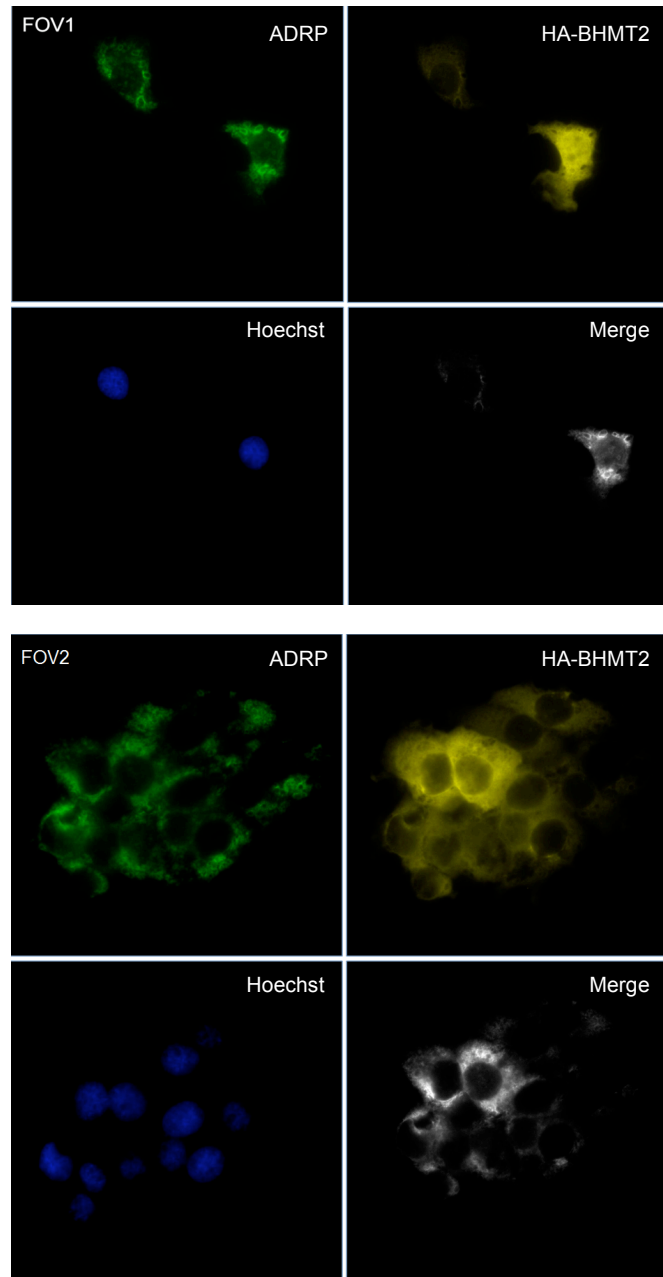


Figure 4-8 BHMT2 is localized to LDs. McA cells transfected with HA-BHMT2 were grown in DMEM containing 0.4 mM OA/BSA overnight to enhance the formation of LDs. Figure shows multiple field of views. Association of HA-BHMT2 with LDs was determined by co-localization with ADRP immunostained with anti-ADRP antibodies. The nucleus was stained with Hoechst. FOV, field of view; ADRP, adipose-differentiation-related protein; HA, hemagglutinin; BHMT, betaine homocysteine S-methyltransferase.

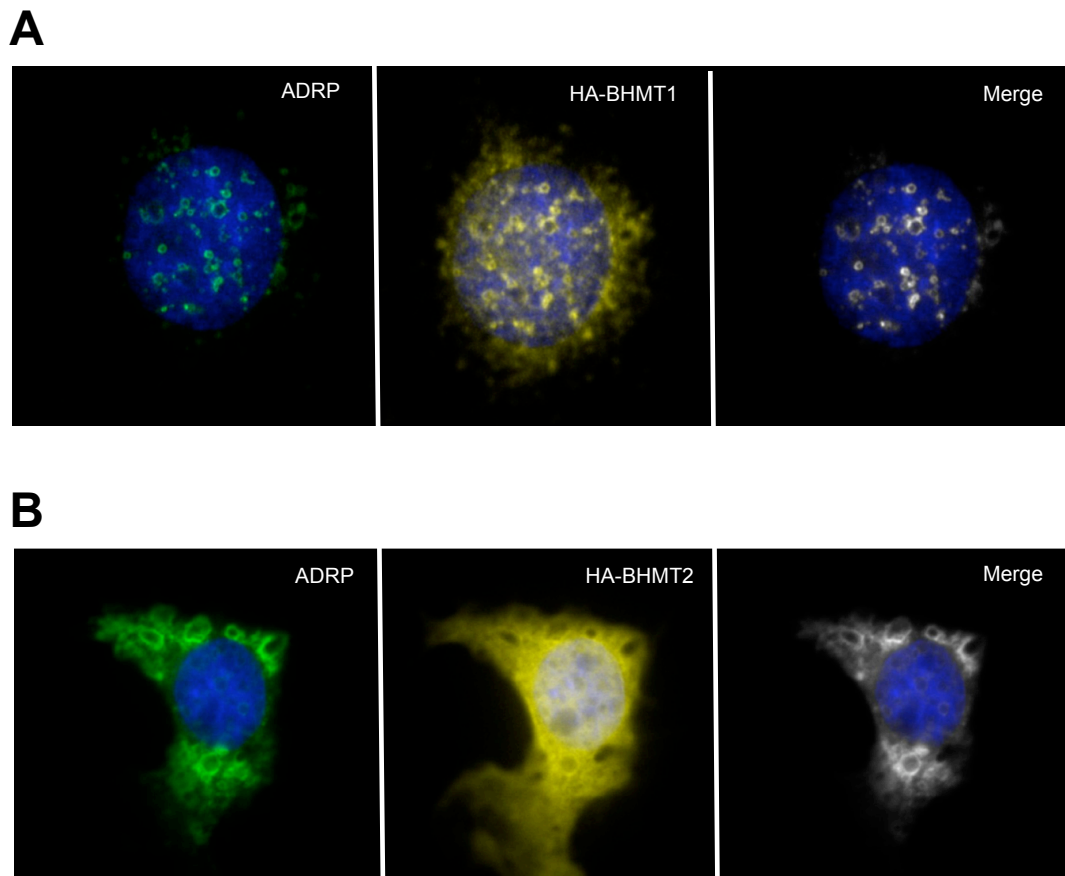


Figure 4-9 Co-localization of BHMT in single cells. McA cells transfected with HA-BHMT1 or HA-BHMT2 were grown in DMEM containing 0.4 mM OA/BSA overnight to enhance the formation of LDs. Association of HA-BHMT1 or HA-BHMT2 with LDs was determined by co-localization with ADRP immunostained with anti-ADRP antibodies. The nucleus was stained with Hoechst. FOV, field of view; ADRP, adipose-differentiation-related protein; HA, hemagglutinin; BHMT, betaine homocysteine S-methyltransferase.

CHAPTER 5

**DISCUSSION, LIMITATIONS AND
FUTURE DIRECTIONS**

5.1 Discussion

Excessive TG storage within hepatocytes is the hallmark of NAFLD. As described in Chapter 2, TG homeostasis is maintained through a balance between TG synthesis and TG removal from the liver. Hepatic free FAs originating from plasma non-esterified FA pool, the diet or *de novo* lipogenesis are utilized for β -oxidation, stored as TG or secreted into the plasma in the form of VLDL. Therefore, alteration in any of these processes could influence TG accumulation in cells (Fujita et al., 2009; Ip et al., 2003; Rinella et al., 2008; Shimomura et al., 1999).

Several lines of evidence showed that increased BHMT1 activity as a result of betaine supplementation protects the liver from TG accumulation (Kwon et al., 2009; Kharbanda et al., 2007). Imbalance in SAM concentration, the universal cellular methyl donor, is highly associated with increased hepatic TG levels. It is well documented that the ability of BHMT1/betaine to regulate hepatic lipid metabolism is possibly mediated by SAM (Barak et al., 1997; Barak et al., 1993; Kharbanda et al., 2007). BHMT1 and BHMT2 catalyze the transfer of a methyl group from betaine and S-methylmethionine, respectively, to Hcy to form methionine, the precursor of SAM (**Figure 1-3**). Although BHMT1 knock-out mice have been characterized and BHMT1 has been shown to be crucial in maintaining hepatic lipid metabolism (Teng et al., 2011), the underlying mechanisms remain speculative. Furthermore, the function of BHMT2 in hepatic lipid metabolism is virtually unknown. Given its high sequence

homology to BHMT1, we postulated that BHMT2 may also have a role in hepatic lipid metabolism. In the present study, we stably expressed rat BHMT1 and BHMT2 cDNA in McA cells and evaluated the effects on lipid metabolism. Indeed, our data suggest that both BHMT1 and BHMT2 alter TG metabolism in McA cells. The cells expressing BHMT1 cDNA have decreased intracellular TG, approximately half of controls. Similarly, BHMT2 expressing cells also have lower hepatic TG than controls, though not as prominent as BHMT1 (**Figure 4-2**). In agreement with the mass analysis data, these cells have lower mRNA levels of ADRP, suggesting lower accumulation of LDs (**Table 4-3**). Prior studies have linked hepatic TG accumulation with altered hepatic PC biosynthesis (Yao & Vance, 1988). A choline-deficient diet induces hepatic steatosis in both human and animal studies (Lombardi et al., 1968; Yao & Vance, 1990; Zeisel et al., 1991). Furthermore, mouse models with deletion of genes needed for PC biosynthesis (CT α , PEMT and BHMT1) have impaired VLDL secretion and increased accumulation of hepatic TG (Jacobs et al., 2004; Teng et al., 2011; Zhu et al., 2003). PC synthesized from the PEMT pathway utilizes methyl groups derived from betaine. It is postulated that BHMT1/betaine exerts its hepatoprotective effects by enhancing PC availability for VLDL secretion. It has been reported that animals supplemented with betaine have enhanced PC levels and are protected from the development of hepatic steatosis (Kharbanda et al., 2007; Kharbanda et al., 2009); however, we did not observe any changes in PC and PE levels in our McA

cells expressing BHMT1 or BHMT2 (**Figure 4-4**). It is important to note that, McArdle cells lack endogenous PEMT activity (Cui et al., 1995). Therefore, our findings suggest that altered phospholipid metabolism may not play a role in the TG-lowering effect of BHMT1/BHMT2. Such contrasting results strengthen our notion that pathway mechanism independent of PC is plausible.

Interestingly, while BHMT1 lowered intracellular TG levels, the secretion of TG was similar between controls and BHMT1-expressing cells during the OA supplementation period (**Figure 4-5**). Furthermore, ApoB mRNA levels were slightly decreased in these cells (**Table 4-3**). This observation is in contrast to previous studies that showed a positive correlation between the expression of BHMT1 in McA cells and the expression of ApoB mRNA and secretion (Sowden et al., 1999). The present finding seems to be in agreement with other research, which found that betaine given to mice with severe hepatic steatosis have decreased hepatic TG mass without normalizing impaired TG secretion nor increased the amount of hepatic PC (Niebergall et al., 2011). Interestingly, we observed a 50% reduction in TG secretion from BHMT1 cells during the subsequent chase period in the absence of exogenous OA. Since the turnover rate of the preformed lipids was similar between BHMT1 expressing and control cells but TG secretion was reduced in BHMT1 cells, we speculated that in the absence of exogenous OA, there was insufficient preformed TG to provide substrates for VLDL assembly and secretion. This

may be due to reduced TG synthesis and/or an increased in FAs being directed towards β -oxidation. Taken together, it did not appear that increased TG export play a role in reducing hepatic TG accumulation in our BHMT1 expressing cells.

Since lower hepatic TG storage was not due to enhanced secretion, another possible pathway is increased delivery of fatty acids for mitochondrial β -oxidation. Indeed, BHMT1 expressing cells displayed significantly higher levels of fatty acid oxidation than control cells, while BHMT2 expression resulted in a small yet significant increase in fatty acid oxidation (**Figure 4-6**). mRNA levels of oxidative genes further supports this observation. Although no differences were observed in the mRNA levels of LCAD, we found significant upregulation of VLCAD and ACOX expression in both BHMT1 and BHMT2 cell lines, suggestive of increased oxidation of long-chain fatty acids (**Table 4-4**). VLCAD is a mitochondrial enzyme specific for long-chain acyl-CoAs, whereas LCAD has a broader substrates specificity from long-chain to medium-chain acyl-CoAs (Houten & Wanders, 2010). In a cell culture model, silencing of VLCAD resulted in a 50% decrease in the rate of OA oxidation (Nouws et al., 2010). Thus, in the presence of exogenous OA, it is not surprising that we see increased VLCAD expression. Furthermore, increased FA oxidation in BHMT1 and BHMT2 expressing cells may not be due to enhanced rate of fatty acid uptake, as both CD36 (transports FA into cell) and CPT1 (transports FA into mitochondria) were not altered. Concurrently, a recent study by Teng et

al. (2012) showed that mice with deletion of BHMT1 gene have impaired fatty acid oxidation by almost 60% compared to controls (Teng et al., 2012). It is clear, therefore, that both BHMT1 and BHMT2 play a critical role in the modulation of fatty acid oxidation and partially explains lower hepatic TG mass accumulation.

Other possibilities through which BHMT1 and BHMT2 expression could lead to decreased hepatic TG levels is reduced *de novo* lipogenesis and TG synthesis. To test this hypothesis, we examined the abundance of several key TG biosynthesis and lipogenic genes. Along with reduced hepatic TG, McA cells expressing BHMT1 or BHMT2 showed significant downregulation of GPAT1 and DGAT2 mRNA levels (**Table 4-2**). GPAT1 catalyzed the first and committed step in the G-3-P pathway; whereas, DGAT2 catalyzed the final and rate-limiting step in TG synthesis, which is the formation of TG from DG. Under normal physiological conditions, it is proposed that most of hepatic TG in the liver originate from this route (Declercq et al., 1984). Lewin et al., showed that overexpression of GPAT1 in rat primary hepatocytes directs fatty acyl-CoA towards TG synthesis and consequently channels it away from FA oxidation (Lewin et al., 2005). On the other hand, mice deficient in GPAT1 have reduced hepatic TG but increased in β -oxidation as reflected by increased hepatic ketogenesis (Neschen et al., 2005). Similarly, regulation of DGAT2 has been reported to be closely associated with the development of hepatic steatosis, whereby overexpression leads to increased accumulation of hepatic TG (Monetti et

al., 2007) and suppression reverses such phenotype (Choi et al., 2007; Jin et al., 2013). Therefore, it is possible that downregulation of GPAT1 and DGAT2 in both BHMT1 and BHMT2 cells impairs FA incorporation into TG and, as a result, increases substrate availability for mitochondrial β -oxidation. Additionally, the abundance of genes encoding for MGAT1, an enzyme that regulates the second major pathway for hepatic TG biosynthesis was also significantly reduced in BHMT1 cells but not in BHMT2. This might account for somewhat more prominent decrease in cellular TG of BHMT1 expressing cells.

There is some evidence that betaine/BHMT1 effects on *de novo* lipogenesis is controlled at the level of sterol regulatory element binding protein 1c (SREBP-1c) expression. Increased level of SREBP-1c has been associated with hepatic steatosis, which was stipulated to be the outcomes of elevated rates of fatty acid synthesis by subsequent increased in SREBP-1c target lipogenic genes (Shimomura et al., 1999). In another study, Ji et al., showed that betaine supplementation to BHMT1 expressing HepG2 cell lines attenuated Hcy-induced SREBP-1c mRNA expression, thereby reducing hepatic TG accumulation (Ji et al., 2007). The author suggested that ER stress induced by elevated Hcy causes the activation of SREBP-1c, and betaine by virtue of being a methyl donor reduces Hcy and subsequently suppresses SREBP-1 induced lipogenesis. However, this is not likely to be the mechanism for our BHMT1 or BHMT2 expressing cells, as we did not find any significant differences in SREBP-1c gene expression

between the three groups (**Table 4-8**). Furthermore, neither of SREBP-1c target genes including ACC and FAS was altered (**Table 4-5**), suggesting that BHMTs regulation of TG metabolism does not act through *de novo* synthesis of fatty acids.

In the present study, we also demonstrated that BHMT1 and BHMT2 expression did not only alter TG metabolism but possibly alter hepatic glucose production. There was an approximately 4 to 5-fold increase in PEPCK and G6Pase mRNA levels in both BHMT1 and BHMT2 cells (**Table 4-7**). These are key genes encoding for gluconeogenic enzymes and our results suggest that both BHMTs expressing cells may have elevated glucose production. Theoretically, the period when oleic acid was supplemented to McA cells mimics the fasted condition *in vivo* where substantial FAs are mobilized from the adipose tissue to the liver. In the fasted state, a normal response to increased FA oxidation is reduced glycolysis for energy production and enhanced glucose synthesis from pyruvate, a process regulated by PEPCK and G6Pase among others. With regards to our BHMT1/BHMT2 cell lines, we have shown earlier that there was an increased in β -oxidation in BHMT1 and BHMT2 cells, thus it is expected to see a prominent upregulation of key gluconeogenic genes. However, we did not measure glucose production in this study.

It is still unclear how betaine/BHMT1 reduces TG content in the hepatocytes. While we have provided evidence that lower hepatic TG accumulation correlates with increase oxidation and decrease expression of

genes involved in TG synthesis, the precise mechanisms by which this is accomplished remain incompletely defined. One report attributes activation of the extracellular signal-regulated kinases 1 and 2 (ERK1/2) pathway with reduced expression and activity of DGAT2 (Wang et al., 2010). The same study showed that activation of ERK1/2 by DGAT2 siRNA in HepG2 cells results in decreased intracellular TG content. The ERK1/2 signaling cascade can be activated by GTPase Ras protein, whose activity requires posttranslational modification that involves carboxyl methylation (Chiu et al., 2004). The activation of ERK1/2 pathway is indirectly influenced by methionine metabolism, as the methylation of Ras requires a methyl group from SAM. It was reported that betaine supplementation of the diet given to alcohol-induced fatty liver mice prevented steatosis as assessed by lower TG accumulation and this hepatoprotective effect was associated with alleviated ERK1/2 inhibition and DGAT2 suppression (Wang et al., 2010). This combination of findings from others provides a potential mechanism by which BHMT1/BHMT2 expression in our McA cells can downregulate DGAT2. It is possible that, by enhancing the synthesis of SAM, BHMT1 and BHMT2 expression in McA cells activates ERK1/2 signaling pathway, reduces DGAT2 expression and subsequently lower hepatic TG content. The precise regulatory mechanism as to how ERK1/2 impacts DGAT2 remains to be determined. It could be that ERK1/2 affected lipid metabolism via short-term regulation of specific enzymes or regulation of genes at transcriptional levels. Additionally, DNA methylation is essential for the reg-

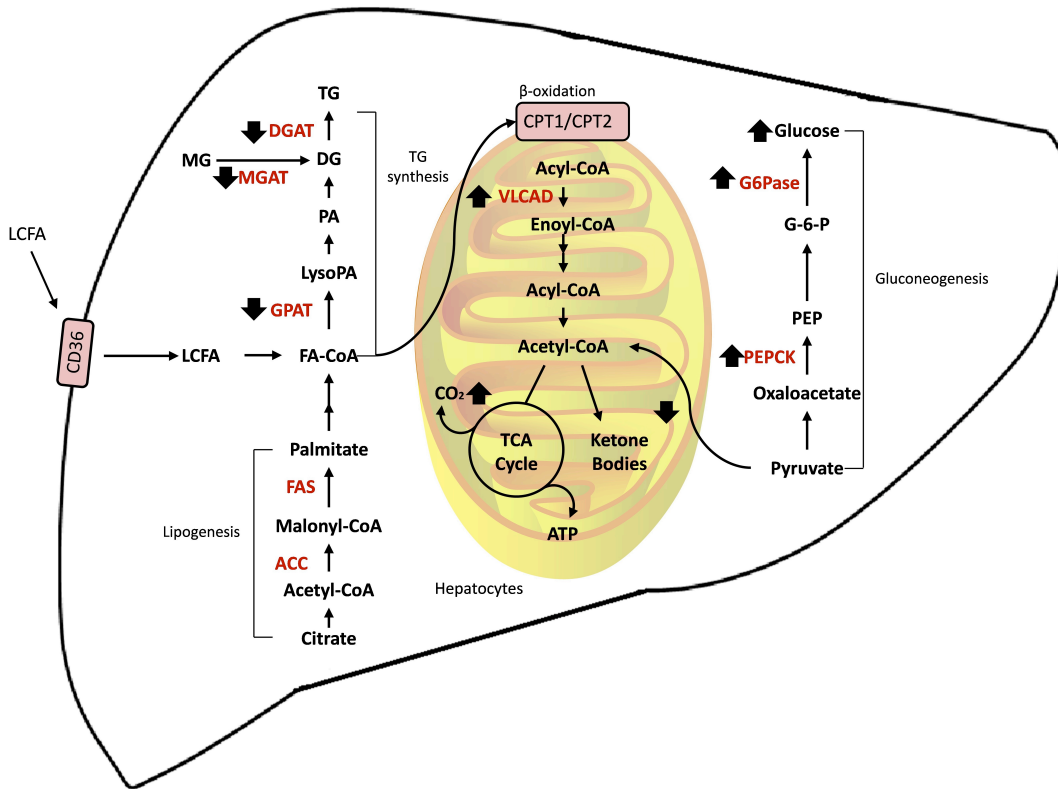


Figure 5-1 Proposed model of BHMT action. BHMT1 and BHMT2 may reduce hepatic content of cellular TG via downregulation of key genes involved in *de novo* biosynthesis of TG. Impaired fatty acids incorporation into TG results in increased substrates availability for mitochondrial β -oxidation. Reduced expression of MGAT in BHMT1 but not BHMT2 may account for somewhat more prominent decrease in cellular TG of BHMT1 cells. In response to increased fatty acid oxidation, pyruvate oxidation to acetyl-CoA is diminished leading to increased gluconeogenesis as indicated by the upregulation of PEPCK and G6Pase. Abbreviation: LCFA, long-chain FA; ACC, acetyl-coA carboxylase; FAS, fatty acid synthase; MGAT, monoacylglycerol O-acyltransferase; DGAT, diacylglycerol O-acyltransferase; GPAT, glycerol-3-phosphate acyltransferase; PEPCK, phosphoenolpyruvate-carboxykinase; G6Pase, glucose-6-phosphatase; CD36, fatty acid transport protein; CPT1, liver carnitine palmitoyltransferase1.

ulation of gene expression. Because SAM is an important methyl donor for DNA methylation, its enrichment by BHMT1 or BHMT2 via enhancement of methionine production may indirectly influence genetic stability and epigenetic modification that could result in the alteration of the expression of genes involved in lipid metabolism (Anderson et al., 2012).

Lipid droplets (LD) are organelles that are involved in lipid storage, metabolism and mobilization of TG through lipolysis/reesterification (Beller et al., 2010). The hydrolysis of TG stored in intracellular LD provides the majority of substrates for reesterification for VLDL assembly and secretion (Gibbons et al., 2000). One of our initial hypotheses was that BHMT1 or BHMT2 prevents lipid accumulation in liver cells by influencing the mobilization of TG-containing lipoprotein. Recent work using a shotgun proteomic approach that analyzed proteome composition of cytosolic LDs fraction revealed an enrichment of enzymes associated with one-carbon metabolism pathway (Crunk et al., 2013). Interestingly, BHMT was among the most abundant proteins found to be associated with cytosolic LDs fractions. However, the study did not provide information on how much of BHMT is in the cytosol or on LDs. Furthermore, a proteomic analysis from Dr. Richard Lehner's lab (personal communication) also reported the presence of BHMT in the isolated LD fractions, which provide further support for the role of BHMT in regulating cellular lipid metabolism. Based on these observations, we hypothesized that BHMT1 and BHMT2 co-localize with LDs, and by doing so, it may be involved in lipid storage and

mobilization. Indeed, we now have supporting evidence that BHMT1 and BHMT2 are co-localized to LDs (**Figure 4-9**). Our data demonstrated that the majority of these proteins associated with ADRP, a LD associated marker, suggesting LD co-localization, with a greater percentage of BHMT1 co-localizes to the LDs more so than BHMT2. This observation may suggest the presence of *bona fide* interactions between BHMTs and the LD, possibly implying that BHMTs are lipid-droplet binding proteins. A number of proteins targeted to LD including but not limited to perilipin, ADRP, and TIP7 have been studied (Brasaemle et al., 2004). These proteins were shown to play a significant regulatory role in lipid metabolism specifically in the storage of neutral lipid and lipolysis (Bickel et al. 2009; Imamura et al., 2002). However, some proteins that are associated to LD were found to only temporarily localize with no apparent role in lipid metabolism. As discussed by Welte in a review, LD may also serve as sequestration sites for proteins that are seemingly unrelated to lipid metabolism, speculatively to either keep proteins inactive or to store proteins for later use (Welte, 2007). Therefore, whether the role BHMT in droplet localization is significance to lipid metabolism or simply another 'refugee' protein remains to be articulately studied. Furthermore, in the present study, the co-localization experiments were performed individually for each protein. It would be interesting to know if co-transfection of BHMT1 and BHMT2 in the same McA cell culture would result in synergistic co-localization with the same LDs and whether they interact with each other.

In conclusion, this study demonstrated that expression of rat BHMT1 and BHMT2 cDNA in McA cells reduces intracellular TG mass accumulation. The downregulation of genes involved in TG synthesis may contribute to the lower incorporation of fatty acids into TG. As a result, more fatty acids are directed to the mitochondria causing an increase in β -oxidation. In addition, our data suggest that increased secretion of hepatic TG may not play a role in the TG-lowering effects of BHMT1/BHMT2. Thus, the present study affirms the critical role of BHMT in regulating hepatic lipid metabolism and provides proposed mechanisms by which BHMT prevents hepatic TG accumulation and to our knowledge, this is the first report to show a potential metabolic role for BHMT2 with respect to lipid metabolism specifically hepatic TG mass accumulation and FA oxidation.

5.2 Limitations and Future directions

Our data suggest that BHMT1 and BHMT2 cDNA expression influences FA esterification into TG and FA oxidation. While we demonstrated reduction in the expression of key enzymes in the pathway of *de novo* TG synthesis, the current study does not address intracellular net TG synthesis *per se*. To demonstrate that lower mRNA levels of lipogenic genes parallel with a reduction in TG synthesis, the use of lipase inhibitor could be employed. The purpose of using lipase/esterase inhibitor E600 is to inhibit or abolish lipolysis or the mobilization of preformed TG. Therefore, accretion of TG in the presence of exogenous OA and E600 should reflect the total rate of TG synthesis. Similarly, follow-up studies are required to understand how BHMT1 and BHMT2 increase FA oxidation.

A pulse-chase analysis using metabolic labeling of lipid was employed to examine lipid turnover and secretion over time. While data from the metabolic labeling studies for BHMT1 supports the mass study, results for BHMT2 seem difficult to reconcile. As compared to the mass data, where we saw lower accumulation of TG mass in BHMT2 cells than pNeo controls, label TG was higher in BHMT2 cells. A possible explanation for the apparent discrepancy could be issues with the sampling of tissues, for example, the different days for performing the experiment, the number of cell density for plating, and the use of different batch of cells. Post-sampling issue including a potential inconsistency of oleic acid concentration from different preparation used to supplement the cells could

also contribute to data discrepancy. Although the tracer study suggests a compensatory role for BHMT2, evidences from FA oxidation and gene expressions experiment best fit the reduction in TG mass in BHMT2 expressing cells. Further work is required to resolve these differences and to determine if the discrepancy is beyond experimental errors.

Gene expression data provide us with useful information in predicting the pattern of a specific protein expression or activity for a better understanding of how a complex regulatory pathway works. However, the quantification of mRNA levels may not always be reflective of the abundance of protein levels, let alone proteins activity. Therefore, future studies could use Western blotting or immunoassays to quantify the expression at protein levels. Enzyme activity assay is also necessary to ascertain whether the activity of GPAT1 and DGAT2 reflects the mRNA data and negatively correlates with the expression of BHMT1 and BHMT2. Furthermore, this research has presented us with several questions in need of further investigation. One of the most important and obvious questions raised from this study is just how does BHMT1/BHMT2 downregulate the expression of two of the most important genes (GPAT1 and DGAT2) in *de novo* TG synthesis? It is therefore highly recommended that detailed mechanism be examined in future studies.

The use of *in vitro* cell lines has been the standard for similar research because of its relative ease of manipulation and consistency of the results generated when handled correctly. However, the use of *in vitro*

cell lines is not without limitations. The protocol requires a routine passaging of the cells, which overtime renders it more susceptible for characteristic alteration. This in itself increases the chance of selecting a sub-population particularly when cells were grown to a very high confluency. Furthermore, cell lines have undergone genetic modification and exhibit behavior that does not precisely represent *in vivo* condition. As with any medical research the purpose is to translate the knowledge into health benefits. The use of *in vitro* rat hepatoma cells in this thesis allows us to gain insight into the role of BHMT1 and BHMT2 in hepatic lipid metabolism; however, future works should consider confirming the physiological function of BHMT1/BHMT2 expressions with primary human hepatocytes as they better resemble the *in vivo* pathophysiology and provides relevant connection to human disease. Furthermore, *in vivo* studies linking BHMT1 and *de novo* TG synthesis are limited. One way to induce hepatic BHMT1 mRNA *in vivo* would be to use methionine-deficient animal models supplemented with betaine. Analyses of gene and protein expression as well as enzyme activity showed approximately 10-fold increase in hepatic BHMT1 mRNA levels in this model (Park & Garrow, 1999). Another possibility would be the use of adenoviral DNA vector containing human or mouse BHMT1/BHMT2 cDNA. Recombinant adenoviruses can be delivered to mice and systematically targeted to the liver for an efficient transduction of BHMT1 and BHMT2 expression.

One of the more interesting findings to emerge from this study is the direct association between BHMT1 and BHMT2 proteins with LDs as observed by co-localization using confocal microscopy. LDs are crucial in regulating cellular lipid metabolism and mobilization. It is possible that BHMT1/BHMT2 co-localization with LDs involves lipid mobilization. If so, this may suggest a new role for BHMT1/BHMT2 in the regulation of hepatic lipid metabolism other than Hcy methylation. Future research should include analyses of the secondary structure of BHMT1/BHMT2 to identify any LD binding motifs. Infection with adenoviruses containing BHMT1/BHMT2 with various truncated regions into hepatocytes, followed by sub-cellular localization, may allow identification (if any) of a unique region that is necessary for association with LDs. Obviously, more work is needed to clearly understand the significance of the association between BHMT1/BHMT2 and the LDs, and to determine if the co-localizations have any metabolic function. Taken together, this thesis describes a role and potential mechanisms for both BHMT1 and BHMT2 in the regulation of hepatic lipid metabolism and as such, could be a promising target for the treatment of fatty liver disease.

References

- Abbas, Z., Anania, F., Ferenci, P., Khan, A., Goh, K. L., ... Lemair, A. (2012). Nonalcoholic Fatty Liver Disease and Nonalcoholic Steatohepatitis. *World Gastroenterology Organisation Guidelines*, 70(10), 1827–34.
- Ahmed, M., Abu, E., & Byrne, C. (2010). Non-Alcoholic Fatty Liver Disease (NAFLD): new challenge for general practitioners and important burden for health authorities? *Primary care diabetes*, 4(3), 129-37.
- Anderson, O. S., Sant, K. E., & Dolinoy, D. C. (2012). Nutrition and epigenetics: an interplay of dietary methyl donors, one-carbon metabolism and DNA methylation. *The Journal of nutritional biochemistry*, 23(8), 853–9.
- Barak, A. J., Beckenhauer, H. C., Badakhsh, S., & Tuma, D. J. (1997). The effect of betaine in reversing alcoholic steatosis. *Alcoholism, clinical and experimental research*, 21(6), 1100–2.
- Barak, A. J., Beckenhauer, H. C., & Tuma, D. J. (1996). Betaine, ethanol, and the liver: a review. *Alcohol (Fayetteville, N.Y.)*, 13(4), 395–8.
- Barak, A. J., Beckenhauer, H. C., Tuma, D. J., & Badakhsh, S. (1987). Effects of prolonged ethanol feeding on methionine metabolism in rat liver. *Biochemistry and cell biology = Biochimie et biologie cellulaire*, 65(3), 230–3.
- Barak, A. J., Beckenhauer, H. C., Junnila, M., & Tuma, D. J. (1993). Dietary Betaine Promotes Generation of Hepatic, 17(3), 552–555.
- Beller, M., Thiel, K., Thul, P. J., & Jäckle, H. (2010). Lipid droplets: a dynamic organelle moves into focus. *FEBS letters*, 584(11), 2176–82.
- Bellia, C., Bivona, G., Scazzone, C., & Ciaccio, M. (2007). Association between homocysteinemia and metabolic syndrome in patients with cardiovascular disease. *Therapeutics and clinical risk management*, 3(6), 999–1001.
- Best, C. H., Ridout, J. H., & Lucas, C. C. (1969). Alleviation of dietary cirrhosis with betaine and other lipotropic agents. *Canadian Journal of Physiology and Pharmacology*, 47(1), 73–79.

- Bickel, P. E., Tansey, J. T., & Welte, M. A. (2009). PAT proteins, an ancient family of lipid droplet proteins that regulate cellular lipid stores. *Biochimica et biophysica acta*, 1791(6), 419–40.
- Borén, J., Rustaeus, S., & Olofsson, S. O. (1994). Studies on the assembly of apolipoprotein B-100- and B-48-containing very low density lipoproteins in McA-RH7777 cells. *The Journal of biological chemistry*, 269(41), 25879–88.
- Brasaemle, D. L., Dolios, G., Shapiro, L., & Wang, R. (2004). Proteomic analysis of proteins associated with lipid droplets of basal and lipolytically stimulated 3T3-L1 adipocytes. *The Journal of biological chemistry*, 279(45), 46835–42.
- Browning, J. D., Szczepaniak, L. S., Dobbins, R., Nuremberg, P., Horton, J. D., Cohen, J. C., ... Hobbs, H. H. (2004). Prevalence of hepatic steatosis in an urban population in the United States: impact of ethnicity. *Hepatology (Baltimore, Md.)*, 40(6), 1387–95.
- Cano, A., Buqué, X., Martínez-Uña, M., Aurrekoetxea, I., Menor, A., García-Rodríguez, J. L., ... Aspichueta, P. (2011). Methionine adenosyltransferase 1A gene deletion disrupts hepatic very low-density lipoprotein assembly in mice. *Hepatology (Baltimore, Md.)*, 54(6), 1975–86.
- Carey, E., & Carey, W. D. (2010). Noninvasive tests for liver disease, fibrosis, and cirrhosis: Is liver biopsy obsolete? *Cleveland Clinic journal of medicine*, 77(8), 519–27.
- Cederbaum, A. I., Wu, D., Mari, M., & Bai, J. (2001). CYP2E1-dependent toxicity and oxidative stress in HepG2 cells. *Free radical biology & medicine*, 31(12), 1539–43.
- Chadwick, L. H., McCandless, S. E., Silverman, G. L., Schwartz, S., Westaway, D., & Nadeau, J. H. (2000). Betaine-homocysteine methyltransferase-2: cDNA cloning, gene sequence, physical mapping, and expression of the human and mouse genes. *Genomics*, 70(1), 66–73.
- Charlton, M., Kasparova, P., Weston, S., Lindor, K., Maor-Kendler, Y., Wiesner, R. H., ... Batts, K. P. (2001). Frequency of nonalcoholic steatohepatitis as a cause of advanced liver disease. *Liver transplantation: official publication of the American Association for the Study of Liver Diseases and the International Liver Transplantation Society*, 7(7), 608–14.

- Chen, S. H., Habib, G., Yang, C. Y., Gu, Z. W., Lee, B. R., Weng, S. A., ... Rosseneu, M. (1987). Apolipoprotein B-48 is the product of a messenger RNA with an organ-specific in-frame stop codon. *Science (New York, N.Y.)*, 238(4825), 363–6.
- Chiu, V. K., Silletti, J., Dinsell, V., Wiener, H., Loukeris, K., Ou, G., ... Pillinger, M. H. (2004). Carboxyl methylation of Ras regulates membrane targeting and effector engagement. *The Journal of biological chemistry*, 279(8), 7346–52.
- Choi, C. S., Savage, D. B., Kulkarni, A., Yu, X. X., Liu, Z.-X., Morino, K., ... Shulman, G. I. (2007). Suppression of diacylglycerol acyltransferase-2 (DGAT2), but not DGAT1, with antisense oligonucleotides reverses diet-induced hepatic steatosis and insulin resistance. *The Journal of biological chemistry*, 282(31), 22678–88.
- Crunk, A. E., Monks, J., Murakami, A., Jackman, M., MacLean, P. S., Ladinsky, M., ... McManaman, J. L. (2013). Dynamic Regulation of Hepatic Lipid Droplet Properties by Diet. (J. Davis, Ed.) *PLoS ONE*, 8(7), e67631.
- Cui, Z., Houweling, M., & Vance, D. E. (1995). Expression of phosphatidylethanolamine N-methyltransferase-2 in McArdle-RH7777 hepatoma cells inhibits the CDP-choline pathway for phosphatidylcholine biosynthesis via decreased gene expression of CTP:phosphocholine cytidyltransferase. *The Biochemical journal*, 312 (Pt 3, 939–45.
- Day, C. P. (2002). Pathogenesis of steatohepatitis. *Best Practice & Research Clinical Gastroenterology*, 16(5), 663–678.
- Declercq, P. E., Haagsman, H. P., Van Veldhoven, P., Debeer, L. J., Van Golde, L. M., & Mannaerts, G. P. (1984). Rat liver dihydroxyacetone-phosphate acyltransferases and their contribution to glycerolipid synthesis. *The Journal of biological chemistry*, 259(14), 9064–75.
- DeLong, C. J., Shen, Y. J., Thomas, M. J., & Cui, Z. (1999). Molecular distinction of phosphatidylcholine synthesis between the CDP-choline pathway and phosphatidylethanolamine methylation pathway. *The Journal of biological chemistry*, 274(42), 29683–8.
- Dixon, J.L. and Ginsberg, H.N (1993). Regulation of hepatic secretion of apolipoprotein B-containing lipoproteins: information obtained from cultured liver cells. *J Lipid Res.* 34:167-79

- Dowman, J. K., Tomlinson, J. W., & Newsome, P. N. (2010). Pathogenesis of non-alcoholic fatty liver disease. *QJM: monthly journal of the Association of Physicians*, 103(2), 71–83.
- Duvnjak, M., Lerotić, I., Barsić, N., Tomasić, V., Virović Jukić, L., & Velagić, V. (2007). Pathogenesis and management issues for non-alcoholic fatty liver disease. *World journal of gastroenterology: WJG*, 13(34), 4539–50.
- Esfandiari, F., Villanueva, J. A., Wong, D. H., French, S. W., & Halsted, C. H. (2005). Chronic ethanol feeding and folate deficiency activate hepatic endoplasmic reticulum stress pathway in micropigs. *American journal of physiology. Gastrointestinal and liver physiology*, 289(1), G54–63.
- Farrell, G. C., Wong, V. W.-S., & Chitturi, S. (2013). NAFLD in Asia-as common and important as in the West. *Nature reviews. Gastroenterology & hepatology*.
- Feng, Q., Kalari, K., Fridley, B. L., Jenkins, G., Ji, Y., Abo, R., ... Weinshilboum, R. M. (2011). Betaine-homocysteine methyltransferase: human liver genotype-phenotype correlation. *Molecular genetics and metabolism*, 102(2), 126–33.
- Finkelstein, J. D. (1990). Methionine metabolism in mammals. *The Journal of nutritional biochemistry*, 1(5), 228–37.
- Finkelstein, J. D., & Martin, J. J. (2000). Homocysteine. *The international journal of biochemistry & cell biology*, 32(4), 385–9.
- Frosst, P., Blom, H. J., Milos, R., Goyette, P., Sheppard, C. A., Matthews, R. G., ... van den Heuvel, L. P. (1995). A candidate genetic risk factor for vascular disease: a common mutation in methylenetetrahydrofolate reductase. *Nature genetics*, 10(1), 111–3.
- Fujita, K., Nozaki, Y., Wada, K., Yoneda, M., Fujimoto, Y., Fujitake, M., ... Nakajima, A. (2009). Dysfunctional very-low-density lipoprotein synthesis and release is a key factor in nonalcoholic steatohepatitis pathogenesis. *Hepatology (Baltimore, Md.)*, 50(3), 772–80.
- Garrow, T. A. (1996). Purification, kinetic properties, and cDNA cloning of mammalian betaine-homocysteine methyltransferase. *The Journal of biological chemistry*, 271(37), 22831–8.

- Gibbons, G. F., Islam, K., & Pease, R. J. (2000). Mobilisation of triacylglycerol stores. *Biochimica et Biophysica Acta (BBA) - Molecular and Cell Biology of Lipids*, 1483(1), 37–57.
- Halsted, C H, Villanueva, J., Chandler, C. J., Stabler, S. P., Allen, R. H., Muskhelishvili, L., ... Poirier, L. (1996). Ethanol feeding of micropigs alters methionine metabolism and increases hepatocellular apoptosis and proliferation. *Hepatology (Baltimore, Md.)*, 23(3), 497–505.
- Halsted, Charles H, Villanueva, J. A., Devlin, A. M., Niemelä, O., Parkkila, S., Garrow, T. A., ... James, S. J. (2002). Folate deficiency disturbs hepatic methionine metabolism and promotes liver injury in the ethanol-fed micropig. *Proceedings of the National Academy of Sciences of the United States of America*, 99(15), 10072–7.
- Hirsch, S., Poniachick, J., Avendaño, M., Csendes, A., Burdiles, P., Smok, G., ... de la Maza, M. P. (2005). Serum folate and homocysteine levels in obese females with non-alcoholic fatty liver. *Nutrition (Burbank, Los Angeles County, Calif.)*, 21(2), 137–41.
- Houten, S. M., & Wanders, R. J. A. (2010). A general introduction to the biochemistry of mitochondrial fatty acid β -oxidation. *Journal of inherited metabolic disease*, 33(5), 469–77.
- Imamura, M., Inoguchi, T., Ikuyama, S., Taniguchi, S., Kobayashi, K., Nakashima, N., & Nawata, H. (2002). ADRP stimulates lipid accumulation and lipid droplet formation in murine fibroblasts. *American journal of physiology. Endocrinology and metabolism*, 283(4), E775–83.
- Ip, E., Farrell, G. C., Robertson, G., Hall, P., Kirsch, R., & Leclercq, I. (2003). Central role of PPAR α -dependent hepatic lipid turnover in dietary steatohepatitis in mice. *Hepatology (Baltimore, Md.)*, 38(1), 123–32.
- Jacobs, R. L., Devlin, C., Tabas, I., & Vance, D. E. (2004). Targeted deletion of hepatic CTP:phosphocholine cytidyltransferase α in mice decreases plasma high density and very low density lipoproteins. *The Journal of biological chemistry*, 279(45), 47402–10.
- Jacobs, R. L., Lingrell, S., Zhao, Y., Francis, G. A., & Vance, D. E. (2008). Hepatic CTP:phosphocholine cytidyltransferase- α is a critical predictor of plasma high density lipoprotein and very low density lipoprotein. *The Journal of biological chemistry*, 283(4), 2147–55.

- Jacobs, R. L., Zhao, Y., Koonen, D. P. Y., Sletten, T., Su, B., Lingrell, S., ... Vance, D. E. (2010). Impaired de novo choline synthesis explains why phosphatidylethanolamine N-methyltransferase-deficient mice are protected from diet-induced obesity. *The Journal of biological chemistry*, 285(29), 22403–13.
- Ji, C., Shinohara, M., Kuhlenkamp, J., Chan, C., & Kaplowitz, N. (2007). Mechanisms of protection by the betaine-homocysteine methyltransferase/betaine system in HepG2 cells and primary mouse hepatocytes. *Hepatology (Baltimore, Md.)*, 46(5), 1586–96.
- Jin, J., Iakova, P., Breaux, M., Sullivan, E., Jawanmardi, N., Chen, D., ... Timchenko, N. A. (2013). Increased expression of enzymes of triglyceride synthesis is essential for the development of hepatic steatosis. *Cell reports*, 3(3), 831–43.
- Kalhan, S. C., Edmison, J., Marczewski, S., Dasarathy, S., Gruca, L. L., Bennett, C., ... Lopez, R. (2011). Methionine and protein metabolism in non-alcoholic steatohepatitis: evidence for lower rate of transmethylation of methionine. *Clinical science (London, England: 1979)*, 121(4), 179–89.
- Kathirvel, E., Morgan, K., Nandgiri, G., Sandoval, B. C., Caudill, M. a, Bottiglieri, T., ... Morgan, T. R. (2010). Betaine improves nonalcoholic fatty liver and associated hepatic insulin resistance: a potential mechanism for hepatoprotection by betaine. *American journal of physiology. Gastrointestinal and liver physiology*, 299(5), G1068–77. d
- Kharbanda, K. K., Mailliard, M. E., Baldwin, C. R., Beckenhauer, H. C., Sorrell, M. F., & Tuma, D. J. (2007a). Betaine attenuates alcoholic steatosis by restoring phosphatidylcholine generation via the phosphatidylethanolamine methyltransferase pathway. *Journal of hepatology*, 46(2), 314–21.
- Kharbanda, K. K., Mailliard, M. E., Baldwin, C. R., Beckenhauer, H. C., Sorrell, M. F., & Tuma, D. J. (2007b). Betaine attenuates alcoholic steatosis by restoring phosphatidylcholine generation via the phosphatidylethanolamine methyltransferase pathway. *Journal of hepatology*, 46(2), 314–21.
- Kharbanda, K. K., Todero, S. L., Ward, B. W., Cannella, J. J., & Tuma, D. J. (2009). Betaine administration corrects ethanol-induced defective VLDL secretion. *Molecular and cellular biochemistry*, 327(1-2), 75–8.

- Kim, C. H., & Younossi, Z. M. (2008). Nonalcoholic fatty liver disease: A manifestation of the metabolic syndrome. *Cleveland Clinic Journal of Medicine*, 75(10), 721–728.
- Kotronen, A., Yki-Järvinen, H., Männistö, S., Saarikoski, L., Korpi-Hyövälti, E., Oksa, H., ... Peltonen, M. (2010). Non-alcoholic and alcoholic fatty liver disease - two diseases of affluence associated with the metabolic syndrome and type 2 diabetes: the FIN-D2D survey. *BMC public health*, 10, 237.
- Kurose, I., Higuchi, H., Kato, S., Miura, S., Watanabe, N., Kamegaya, Y., ... Ishii, H. (1997). Oxidative stress on mitochondria and cell membrane of cultured rat hepatocytes and perfused liver exposed to ethanol. *Gastroenterology*, 112(4), 1331–43.
- Kwon, D. Y., Jung, Y. S., Park, H. K., & Kim, Y. C. (2009). Impaired sulfur-amino acid metabolism and oxidative stress in nonalcoholic fatty liver are alleviated by betaine supplementation in rats. *The Journal of nutrition*, 139(1), 63-3.
- Lever, M., & Slow, S. (2010). The clinical significance of betaine, an osmolyte with a key role in methyl group metabolism. *Clinical biochemistry*, 43(9), 732–44.
- Lewin, T. M., Wang, S., Nagle, C. A., Van Horn, C. G., & Coleman, R. A. (2005). Mitochondrial glycerol-3-phosphate acyltransferase-1 directs the metabolic fate of exogenous fatty acids in hepatocytes. *American journal of physiology. Endocrinology and metabolism*, 288(5), E835–44.
- Liu, Y., Millar, J. S., Cromley, D. A., Graham, M., Crooke, R., Billheimer, J. T., & Rader, D. J. (2008). Knockdown of acyl-CoA:diacylglycerol acyltransferase 2 with antisense oligonucleotide reduces VLDL TG and ApoB secretion in mice. *Biochimica et biophysica acta*, 1781(3), 97–104.
- Lombardi, B., Pani, P., & Schlunk, F. F. (1968). Choline-deficiency fatty liver: impaired release of hepatic triglycerides. *Journal of lipid research*, 9(4), 437–46.
- Lu, S. C., Alvarez, L., Huang, Z. Z., Chen, L., An, W., Corrales, F. J., ... Mato, J. M. (2001). Methionine adenosyltransferase 1A knockout mice are predisposed to liver injury and exhibit increased expression of genes involved in proliferation. *Proceedings of the National Academy of Sciences of the United States of America*, 98(10), 5560–5.

- Marí, M., Morales, A., Colell, A., García-Ruiz, C., & Fernández-Checa, J. C. (2009). Mitochondrial glutathione, a key survival antioxidant. *Antioxidants & redox signaling*, *11*(11), 2685–700.
- Martínez-Chantar, M. L., Corrales, F. J., Martínez-Cruz, L. A., García-Trevijano, E. R., Huang, Z.-Z., Chen, L., ... Lu, S. C. (2002). Spontaneous oxidative stress and liver tumors in mice lacking methionine adenosyltransferase 1A. *FASEB journal: official publication of the Federation of American Societies for Experimental Biology*, *16*(10), 1292–4.
- Mason, T. M. (1998). The role of factors that regulate the synthesis and secretion of very-low-density lipoprotein by hepatocytes. *Critical reviews in clinical laboratory sciences*, *35*(6), 461–87.
- Matteoni, C. A., Younossi, Z. M., Gramlich, T., Boparai, N., Liu, Y. C., & McCullough, A. J. (1999). Nonalcoholic fatty liver disease: a spectrum of clinical and pathological severity. *Gastroenterology*, *116*(6), 1413–9.
- Mazza, A., Fruci, B., Garinis, G. A., Giuliano, S., Malaguarnera, R., & Belfiore, A. (2012). The role of metformin in the management of NAFLD. *Experimental diabetes research*, *2012*, 716404.
- Millian, N. S., & Garrow, T. A. (1998). Human betaine-homocysteine methyltransferase is a zinc metalloenzyme. *Archives of biochemistry and biophysics*, *356*(1), 93–8.
- Monetti, M., Levin, M. C., Watt, M. J., Sajan, M. P., Marmor, S., Hubbard, B. K., Hevener, A. L. (2007). Dissociation of hepatic steatosis and insulin resistance in mice overexpressing DGAT in the liver. *Cell metabolism*, *6*(1), 69–78.
- Mudd, S. H., & Poole, J. R. (1975). Labile methyl balances for normal humans on various dietary regimens. *Metabolism: clinical and experimental*, *24*(6), 721–35.
- Musso, G., Gambino, R., & Cassader, M. (2009). Recent insights into hepatic lipid metabolism in non-alcoholic fatty liver disease (NAFLD). *Progress in lipid research*, *48*(1), 1–26.
- Neschen, S., Morino, K., Hammond, L. E., Zhang, D., Liu, Z.-X., Romanelli, A. J., ... Shulman, G. I. (2005). Prevention of hepatic steatosis and hepatic insulin resistance in mitochondrial acyl-CoA:glycerol-sn-3-phosphate acyltransferase 1 knockout mice. *Cell metabolism*, *2*(1), 55–65.

- Niebergall, L. J., Jacobs, R. L., Chaba, T., & Vance, D. E. (2011). Phosphatidylcholine protects against steatosis in mice but not non-alcoholic steatohepatitis. *Biochimica et biophysica acta*, 1811(12), 1177–85.
- Noga, A. A., Zhao, Y., & Vance, D. E. (2002). An unexpected requirement for phosphatidylethanolamine N-methyltransferase in the secretion of very low density lipoproteins. *The Journal of biological chemistry*, 277(44), 42358–65.
- Nordmann, R. (1994). Alcohol and antioxidant systems. *Alcohol and alcoholism (Oxford, Oxfordshire)*, 29(5), 513–22.
- Nouws, J., Nijtmans, L., Houten, S. M., van den Brand, M., Huynen, M., Venselaar, H., ... Vogel, R. O. (2010). Acyl-CoA dehydrogenase 9 is required for the biogenesis of oxidative phosphorylation complex I. *Cell metabolism*, 12(3), 283–94.
- Page, J. M., & Harrison, S. A. (2009). NASH and HCC. *Clinics in liver disease*, 13(4), 631–47.
- Pajares, M. A., Corrales, F., Durán, C., Mato, J. M., & Alvarez, L. (1992). How is rat liver S-adenosylmethionine synthetase regulated? *FEBS letters*, 309(1), 1–4.
- Park, E. I., & Garrow, T. A. (1999). Interaction between dietary methionine and methyl donor intake on rat liver betaine-homocysteine methyltransferase gene expression and organization of the human gene. *The Journal of biological chemistry*, 274(12), 7816–24.
- Park, E. I., Renduchintala, M. S., & Garrow, T. A. (1997). Diet-Induced Changes in Hepatic Betaine-Homocysteine Methyltransferase Activity Are Mediated By Changes in the Steady-State Level of Its mRNA. *The Journal of Nutritional Biochemistry*, 8(9), 541–545.
- Rinella, M. E., Elias, M. S., Smolak, R. R., Fu, T., Borensztajn, J., & Green, R. M. (2008). Mechanisms of hepatic steatosis in mice fed a lipogenic methionine choline-deficient diet. *Journal of lipid research*, 49(5), 1068–76.
- Schreuder, T. C. M. A., Verwer, B. J., van Nieuwkerk, C. M. J., & Mulder, C. J. J. (2008). Nonalcoholic fatty liver disease: an overview of current insights in pathogenesis, diagnosis and treatment. *World journal of gastroenterology: WJG*, 14(16), 2474–86.

- Schwahn, B. C., Chen, Z., Laryea, M. D., Wendel, U., Lussier-Cacan, S., Genest, J., ... Rozen, R. (2003). Homocysteine-betaine interactions in a murine model of 5,10-methylenetetrahydrofolate reductase deficiency. *FASEB journal: official publication of the Federation of American Societies for Experimental Biology*, 17(3), 512–4.
- Shelness, G. S., & Sellers, J. a. (2001). Very-low-density lipoprotein assembly and secretion. *Current opinion in lipidology*, 12(2), 151–7.
- Shimomura, I., Bashmakov, Y., & Horton, J. D. (1999). Increased levels of nuclear SREBP-1c associated with fatty livers in two mouse models of diabetes mellitus. *The Journal of biological chemistry*, 274(42), 30028–32.
- Song, J., Ann, K., Fischer, L. M., Kohlmeier, M., Wang, S., & Zeisel, S. H. (2005). Polymorphism of the PEMT gene and susceptibility to nonalcoholic fatty liver disease (NAFLD), 19(10), 1266–1271.
- Song, Z., Zhou, Z., Chen, T., Hill, D., Kang, J., Barve, S., & McClain, C. (2003). S-adenosylmethionine (SAME) protects against acute alcohol induced hepatotoxicity in mice small star, filled. *The Journal of nutritional biochemistry*, 14(10), 591–7.
- Sowden, M. P., Collins, H. L., Smith, H. C., Garrow, T. A., Sparks, J. D., & Sparks, C. E. (1999). Apolipoprotein B mRNA and lipoprotein secretion are increased in McArdle RH-7777 cells by expression of betaine-homocysteine S-methyltransferase. *The Biochemical journal*, 341 (Pt 3, 639–45.
- Sparks, J. D., Collins, H. L., Chirieac, D. V, Cianci, J., Jokinen, J., Sowden, M. P., ... Sparks, C. E. (2006). Hepatic very-low-density lipoprotein and apolipoprotein B production are increased following in vivo induction of betaine-homocysteine S-methyltransferase. *The Biochemical journal*, 395(2), 363–71.
- Suzuki, T., Matsuo, K., Sawaki, A., Mizuno, N., Hiraki, A., Kawase, T., ... Tanaka, H. (2008). Alcohol drinking and one-carbon metabolism-related gene polymorphisms on pancreatic cancer risk. *Cancer epidemiology, biomarkers & prevention: a publication of the American Association for Cancer Research, cosponsored by the American Society of Preventive Oncology*, 17(10), 2742–7.
- Szegedi, S. S., Castro, C. C., Koutmos, M., & Garrow, T. A. (2008). Betaine-homocysteine S-methyltransferase-2 is an S-methylmethionine-homocysteine methyltransferase. *The Journal of biological chemistry*, 283(14), 8939–45.

- Teng, Y.-W., Ellis, J. M., Coleman, R. A., & Zeisel, S. H. (2012). Mouse betaine-homocysteine S-methyltransferase deficiency reduces body fat via increasing energy expenditure and impairing lipid synthesis and enhancing glucose oxidation in white adipose tissue. *The Journal of biological chemistry*, 287(20), 16187–98.
- Teng, Y.-W., Mehedint, M. G., Garrow, T. A., & Zeisel, S. H. (2011). Deletion of betaine-homocysteine S-methyltransferase in mice perturbs choline and 1-carbon metabolism, resulting in fatty liver and hepatocellular carcinomas. *The Journal of biological chemistry*, 286(42), 36258–67.
- Vance, D. E. (1990). Boehringer Mannheim Award lecture. Phosphatidylcholine metabolism: masochistic enzymology, metabolic regulation, and lipoprotein assembly. *Biochemistry and cell biology = Biochimie et biologie cellulaire*, 68(10), 1151–65.
- Vance, J. E. (2002). Assembly and secretion of lipoproteins. In *Biochemistry of lipids, lipoproteins and membranes*. D. E Vance and J. E Vance, editors. Elsevier Science, Amsterdam. 513p.
- Wang, Z., Yao, T., & Song, Z. (2010). Involvement and mechanism of DGAT2 upregulation in the pathogenesis of alcoholic fatty liver disease. *Journal of lipid research*, 51(11), 3158–65.
- Welte, M. A. (2007). Proteins under new management: lipid droplets deliver. *Trends in cell biology*, 17(8), 363–9.
- Wieland, P., & Lauterburg, B. H. (1995). Oxidation of mitochondrial proteins and DNA following administration of ethanol. *Biochemical and biophysical research communications*, 213(3), 815–9.
- Yao, Z. M., & Vance, D. E. (1988). The active synthesis of phosphatidylcholine is required for very low density lipoprotein secretion from rat hepatocytes. *The Journal of biological chemistry*, 263(6), 2998–3004.
- Yao, Z. M., & Vance, D. E. (1990). Reduction in VLDL, but not HDL, in plasma of rats deficient in choline. *Biochemistry and cell biology = Biochimie et biologie cellulaire*, 68(2), 552–8.
- Yen, C. L., Stone, S. J., Cases, S., Zhou, P., & Farese, R. V. (2002). Identification of a gene encoding MGAT1, a monoacylglycerol acyltransferase. *Proceedings of the National Academy of Sciences of the United States of America*, 99(13), 8512–7.

- Younossi, Z., Stepanova, M., Afendy, M., Fang, Y., Younossi, Y., Mir H., & Srishord, M. (2011). The changing face of chronic liver disease (CLD) in the United States: The rising epidemic of Non-Alcoholic Fatty Liver Disease (NAFLD). *Presented at The International Liver Congress TM*.
- Zeisel, S. H., Da Costa, K. A., Franklin, P. D., Alexander, E. A., Lamont, J. T., Sheard, N. F., & Beiser, A. (1991). Choline, an essential nutrient for humans. *FASEB journal: official publication of the Federation of American Societies for Experimental Biology*, 5(7), 2093–8.
- Zhu, X., Song, J., Mar, M.-H., Edwards, L. J., & Zeisel, S. H. (2003). Phosphatidylethanolamine N-methyltransferase (PEMT) knockout mice have hepatic steatosis and abnormal hepatic choline metabolite concentrations despite ingesting a recommended dietary intake of choline. *The Biochemical journal*, 370(Pt 3), 987–93.